Regulation and Dynamics of the Plasma Membrane of *Toxoplasma gondii*

Julia von Knoerzer-Suckow

Dissertation zur Erlangung des Doktorgrades
der Fakultät für Biologie
der Ludwig-Maximilians-Universität
München 2025

Diese Dissertation wurde angefertigt unter der Leitung von Prof. Dr. Michael Boshart an der Fakultät für Biologie der Ludwig-Maximilians-Universität München

Erster Gutachter: Prof. Dr. Michael Boshart

Zweiter Gutachter: Prof. Dr. Markus Meißner

Datum der Abgabe: 30.01.2025

Datum der mündlichen Prüfung: 23.05.2025

Statutory Declaration

I hereby declare under oath that the submitted dissertation was written independently and without unauthorized aids. This dissertation was not submitted in whole or in part to any other examination board. I have never previously attempted to submit a dissertation or take a doctoral exam.

Eidesstattliche Erklärung

Ich versichere hiermit an Eides statt, dass die vorgelegte Dissertation selbständig und ohne unerlaubte Hilfsmittel angefertigt worden ist. Die vorliegende Dissertation wurde weder ganz noch teilweise bei einer anderen Prüfungskommission vorgelegt. Ich habe noch zu keinem früheren Zeitpunkt versucht, eine Dissertation einzureichen oder an einer Doktorprüfung teilzunehmen.

Julia Felicitas von Knoerzer-Suckow

München, 12.08.2025

Parts of this thesis have been under revision in PLOS Biology:

Toxoplasma gondii micropore is required for regulating the membrane reservoir during parasite replication.

Julia von Knoerzer-Suckow, Eva-Helena Aden, Romuald Haase, Andreas Klingl, Ignasi Forné, Simon Gras

Table of contents

List of Figures

List of Tables

List of Abbreviations

Abbreviation	Meaning
3D	3-dimensional
AP	Adaptor protein
AAP	apical annuli protein
ADP	Adenosine di-phosphate
AID	Auxin-inducible degron
Arf6	ADP-ribosylation factor 6
ART	Artemisinin
ATP	Adenosine Triphosphate
AV	Apical Vesicle
BAR	BIN-amphiphysin-Rvs
BSA	Bovine serum albumin
CbEm	Chromobody-Emerald Fluorescents Protein
CCP	Clathrin coated pits
CCV	Clathrin coated vesicles
cFRAPc	Fluorescence Recovery after Photoconversion
CGN	Cis-Golgi network
CIE	Clathrin independent endocytosis
CLEM	Correlative light and electron microscopy
CLIC	Clathrin-Independent Carriers
CME	Clathrin-mediated endocytosis
COPI	Coat protein complex I
COPII	Coat protein complex II
CRISPR/Cas9	Clustered Regularly Interspaced Short Palindromic Repeats / Crisper Associated protein 9
Cyto-D	Cytochalasin D
DIC	Differential Interference Contrast
DiCre	Dimerisable Cre recombinase

DMEM	Dulbecco's modified Eagle medium
DMSO	Dimethyl Sulfoxide
DNA	Deoxyribonucleic Acid
dNTP	Deoxynucleotide triphosphate
DrpB	Dynamin B
DrpC	Dynamin C
dsDNA	Double stranded DNA
ELC	Endosome-Like Compartment
Endo-SAG1	Internalised (endocytosed) plasma membrane SAG1 vesicles
ER	Endoplasmic Reticulum
EtOH	Ethanol
EuPaGDT	Eukaryotic pathogen sgRNA design tool
EX	Expansion microscopy
FACS	Fluorescence-Activated Cell Sorting
F-actin	Filamentous actin
FBS	Foetal bovine serum
FIJI	FIJI is just ImageJ
FLIP	Fluorescents loss in photobleaching
FRAP	Fluorescence recovery after photobleaching
G-actin	Globular actin
gDNA	Genomic DNA
GAP-45	Glidosome associated protein
GEEC	GPI-Enriched Early Endocytic Compartments
GFP	Green Fluorescent Protein
GPI	Glycosylphosphatidylinositol
GRA	Dense Granule protein
HA	Haemagglutinin
HCC	Haemoglobin-containing cytostome
HDAC	Histone deacetylase
HEPES	4-(2-hydroxyethyl)-1-piperazineethanesulfonic acid

HF	FITC-labelled heparin
HFF	Human foreskin fibroblast
His	Histidine
IFA	Immunofluorescence assay
IMC	Inner Membrane Complex
Int-SAG1	Internal SAG1
IRG	immunity-related GTPases
IRM	Interference Reflection Microscopy
IVN	Intravacuolar network
KD	Knockdown
KO	Knockout
K13	Kelch-domain protein 13
LIC	Ligation-independent cloning
mAID	Minimal AID domain
MeOH	Methanol
MFI	Mean fluorescence intensity
MIC	Microneme proteins
MLC	Myosin Light Chain
MP	Membrane-permeable dyes
M-SAG1	Mother SAG1
MNP	Membrane-non-permeable dyes
MTOC	Microtubule organisation centre
Myo	Myosin
mRNA	Messenger RNA
NCBI	National Centre for Biotechnology Information
NEB	New England Biolabs Inc.
NHEJ	Non-Homologous End-Joining
n-SAG1	New SAG1
NIH	National Institutes of Health
OG	Oregon Green

PAM	Protospacer adjacent motif
PALM	Photoactivated Localisation Microscopy
P. falciparum	Plasmodium falciparum
PBS	Phosphate buffered saline
PCR	Polymerase Chain Reaction
PFA	Paraformaldehyde
PLV	Plant-Like Vacuole or Vacuolar Compartment
PLVAC	Plant-like vacuole Compartment
PM	Plasma membrane
PMR	Plasma membrane reservoir
PS	Phosphatidylserine
PM-SAG1	SAG1 at the plasma membrane
ProM2AP	M2AP pro-peptide
PV	parasitophorous Vacuole
Rab	Ras related in brain
Rapa	Rapamycin
RFP	Red Fluorescent Protein
RNA	Ribonucleic Acid
RON	Rhoptry neck protein
ROP	Rhoptry bulb protein
RPM	Revolutions per minute
RSA	Rhoptry secretory apparatus
SAG	Surface Antigen
sCas9	Split Cas9
sgRNA	Single Guide RNA
SortLR	Sortilin-Like Receptor
SPT	Single-particle tracking
STED	Stimulated Emission Depletion
STORM	Stochastic Optical Reconstruction Microscopy
TEM	Transmission electronic microscope

Tg	Toxoplasma gondii
TGN	Trans-Golgi Network
Tir	Transport inhibitor response
TIRF	Total internal reflection fluorescence
t-SNARE	target Snap-Receptor
UPRT	Uracil Phosphoribosyl Transferase
VAC	Vacuolar Compartment
VSG	Variant surface glycoproteins
WHO	World Health Organisation
WT	Wildtype
YFP	Yellow Fluorescent Protein

Abstract:

Apicomplexan parasites residing in a parasitophorous vacuole are separated from their host environment but can take up nutrients from the host cell via endocytosis. Part of this endocytic process occurs in a structure called the micropore. The micropore has been shown to form a ring inside the inner membrane complex (IMC) of the parasite. It is composed of numerous proteins, including a kelch-domain protein, K13, which is central to malarial drug resistance. In the absence of K13, the micropore collapses, leading to plasma membrane accumulation on the surface of the parasite, suggesting that the micropore plays a critical role in plasma membrane homeostasis.

In this thesis, I characterized the plasma membrane dynamics and the recycling during parasite replication. It was proved that the plasma membrane of the mother tachyzoite is inherited by the daughter cells, and that the delivery of newly generated surface antigen 1 (SAG1) to the PM occurs during this process. Furthermore, during this inheritance, the plasma membrane undergoes a cycle of endocytosis and exocytosis. The endocytic vesicles follow a distinct pathway from the de novo vesicles and appear to depend on the small GTPase Rab5b, with which significant colocalisation has been demonstrated. Myosin F (MyoF) was also investigated as a potential molecular motor involved in uptake. In parallel, the function of the P4ATPase FLP2 was studied. Knockdown experiments revealed a phenotype in transmission electronic microscope (TEM) similar to that of micropore-depleted parasites. Analysis of the effects of FLP2 depletion on vesicle formation and transportation highlights its influence on Golgi fragmentation and vesicle accumulation at the plasma membrane.

Additionally, a new membranous structure was identified and described: the establishment of an extracellular plasma membrane reservoir (PMR) during parasite replication. This PMR forms prior to the generation and budding of daughter cells and is reabsorbed at the end of replication. Upon deletion of K13, parasites are unable to reabsorb the PMR, leading to membrane accumulation and the complete disruption of membrane homoeostasis and the death of the parasites.

Zusammenfassung:

Apikomplexan Parasiten, die in einer parasitophoren Vakuole leben, sind von ihrer Wirtsumgebung getrennt, können aber Nährstoffe aus der Wirtszelle durch Endozytose aufnehmen. Ein Teil dieser endozytotischen Prozesse findet an der Mikropore statt. Es wurde gezeigt, dass die Mikropore einen Ring innerhalb des inneren Membrankomplexes (IMC) des Parasiten bildet. Sie besteht aus zahlreichen Proteinen, darunter insbesondere einem Kelch-Domänen-Protein, K13, das eine zentrale Rolle bei der Resistenz gegen Malaria-Medikamente spielt. In Abwesenheit von K13 kollabiert die Mikropore, was zu einer Akkumulation der Plasmamembran an der Oberfläche des Parasiten führt, das deutet darauf hin, dass die Mikropore eine entscheidende Rolle in der Homöostase der Plasmamembran spielt.

In dieser Arbeit wurden die Dynamik und das Recycling der Plasmamembran während der Parasitenreplikation charakterisiert. Es wurde gezeigt, dass die Plasmamembran des Mutter-Tachyzoiten von den Tochterzellen geerbt wird, und dass neu gebildetes Oberflächen antigen 1 (SAG1) während dieses Prozesses in die Plasmamembrane integriert wird. Darüber hinaus durchläuft die Plasmamembran während dieser Vererbung einen Zyklus aus Endozytose und Exozytose. Dabei kann beobachtet werden, dass die endozytotischen Vesikel einem anderen Weg folgen, als die de-novo-Vesikel. Diese endozytotischen Vesikel kolokalisieren signifikant mit Rab5b, welches für ihren Transport wichtig zu sein scheint. Myosin F (MyoF) wurde ebenfalls als potentieller molekularer Motor für die Endozytose und den Transport der Vesikel untersucht.

Parallel dazu wurde die Funktion der P4ATPase FLP2 untersucht. Knockdown-Experimente zeigten einen Phänotyp der in der Transmissionselektronenmikroskopie (TEM), ähnlich dem des Mikropore Nullmutanten-Parasiten war. Die Analyse der Auswirkungen der FLP2 Abbaus auf die Vesikelbildung und deren Transport hebt ihren Einfluss auf die Fragmentierung des Golgi-Apparates und die Vesikel Ansammlung an der Plasmamembran hervor.

Zusätzlich wurde eine neue membranöse Struktur beschrieben: die Bildung eines extrazellulären Plasmamembranreservoirs (PMR) während der Replikation des Parasiten. Dieses PMR entsteht vor der Bildung und der vollständigen Ausbildung der Tochterzellen und wird am Ende der Replikation wieder resorbiert. Bei einer Deletion von K13 sind die Parasiten

nicht in der Lage, das PMR wieder aufzunehmen, was zu einer Akkumulation der Membran und letztlich zur vollständigen Störung der Membranhomöostase und zum Sterben der Parasiten führt.

1 Introduction

1.1 Apicomplexan

Apicomplexan parasites are protozoans with unique life cycles and specialised organelles. They represent the only phylum composed predominantly of parasitic species, though some exist symbiotically with corals (1). Apicomplexans are known to cause various human and veterinary diseases (2). Together with dinoflagellates, they form the group Alveolates (3,4). The name Apicomplexa is derived from their characteristic apical organelle complex, which includes the conoid (a structure composed of spiral microtubules), the apicoplast, rhoptries, and micronemes (5,6). These organelles are critical for host-parasite interactions and tissue invasion (5,7).

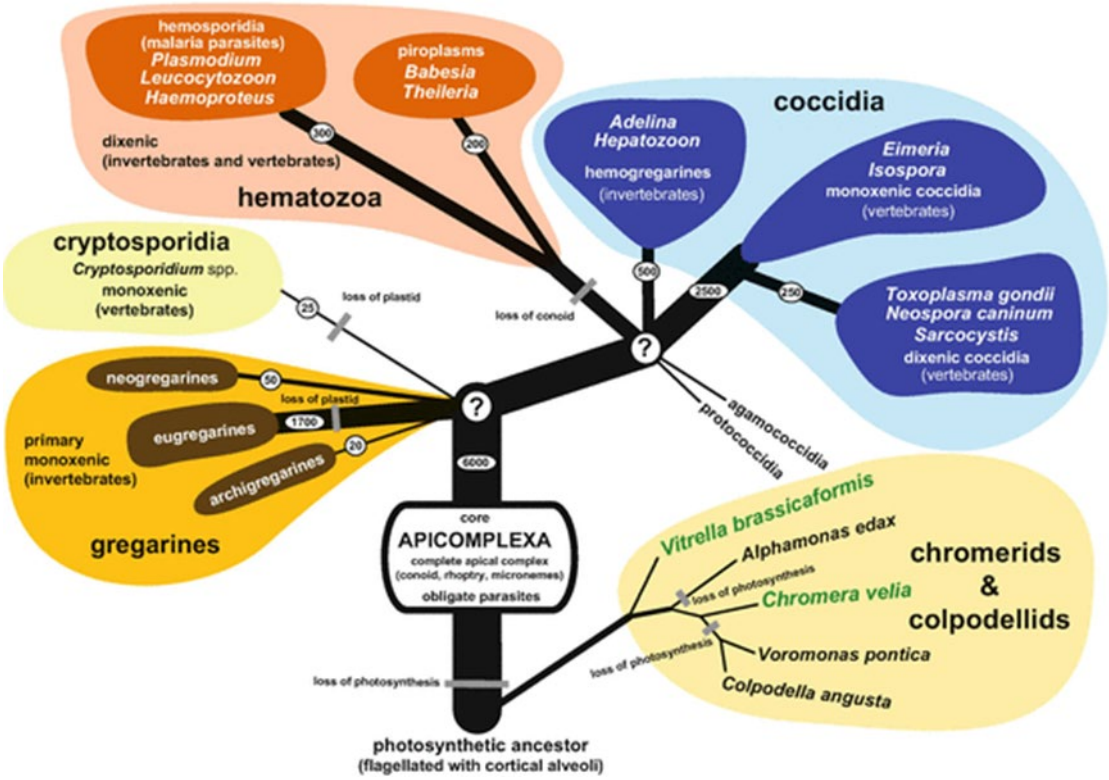

Figure 1: ***Apicomplexa can be divided into four subgroups based on phylogenetic analyses*** *(8). These subgroups are gregarines, cryptosporidia, haematozoa, and cyst-forming coccidia. All apicomplexan subgroups include parasites of veterinary and human medical relevance. Unlike their ancestors, apicomplexans have lost the ability to photosynthesise. Their closest known relatives that retain photosynthetic capabilities are the chromerids and colpodellids. Image from Votýpka et al. 2017.*

Apicomplexans are divided into four groups based on phenotypic characteristics: gregarines, cryptosporidia, haematozoa, and coccidia. These groups include important human pathogens

such as *Plasmodium*, the causative agent of malaria, and *Toxoplasma gondii* (9–13). The Cryptosporidia family consists of only one genus, *Cryptosporidium* spp., which can cause severe gastrointestinal disorders (14,15). All apicomplexans successfully occupy specific ecological niches and pose a significant threat to humans, farm animals, and wildlife (16,17). Despite some differences, these groups share substantial similarities, including a calcium-dependent gliding motility powered by an actin-myosin motor and the secretion of microneme proteins (MIC), which bind to host cell ligands on the membrane (5,6,18). All apicomplexans are obligate intracellular parasites, requiring one or more hosts to complete their sexual and asexual reproduction (18). Their complex life cycle alternates between asexual schizogony, sexual gametogony, and asexual sporogony (19). Following ingestion, the oocyst of Coccidia parasite releases sporozoites, the first invasive stage, which invade nearby host cells mostly the intestinal villi (20). Inside the host cell, sporozoites transform into trophozoites, the replicative stage (19). During asexual reproduction, a process known as schizogony produces schizonts, which develop into merozoites (21). These merozoites possess a single mitochondrion and an apical organelle (22). Merozoites can subsequently undergo gametocytogenesis, differentiating into female macrogametes and male microgametes (22,23). The fusion of gametes forms a zygote, which undergoes mitosis to produce a sporont. The sporont develops into a sporoblast, which ultimately gives rise to sporozoites (6,19).

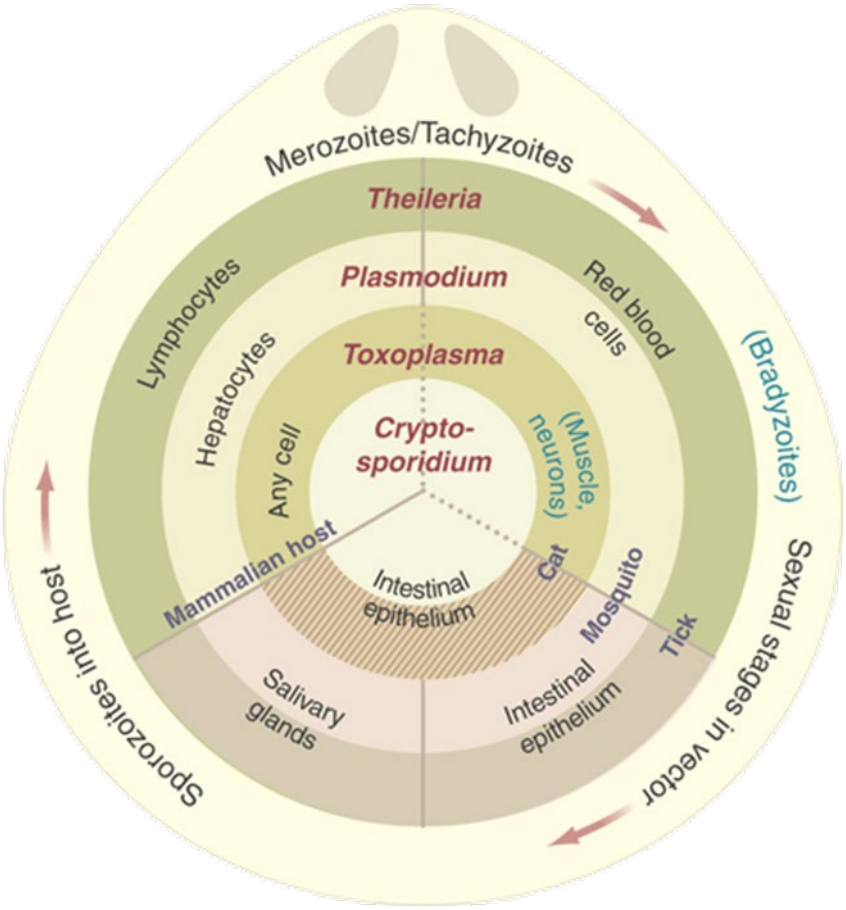

Figure 2: ***A circular diagram depicting the traversing stages of the apicomplexan life cycle*** *(24). Radial lines represent distinct invasion events. Sporozoites enter host cells, initiating the cycle, as shown in the upper left corner. Merozoites invade new cells, where they can propagate indefinitely under favourable conditions. Image from Roos 2005.*

Despite shared life cycle features and sexual stage transitions, apicomplexans exhibit significant differences. Their life cycles often involve alternating between different host species, commonly referred to as primary and secondary hosts. Many apicomplexans pose a considerable threat to humans and livestock (5,22). The ability to infect multiple hosts complicates both treatment and eradication of these pathogens, highlighting the need for extensive research to better understand their biology and life cycles (16).

1.1.1 *Toxoplasma gondii*

Toxoplasma is a protozoan parasite belonging to the phylum Apicomplexa and the group of cyst-forming coccidia (23). It possesses the unique ability to invade any nucleated cell of warm-blooded animals, exhibiting no specificity for a particular species as a secondary or intermediate host. The global infection rate of *Toxoplasma* is estimated to range between 30% and 60% of the human population (25,26). In immunocompetent individuals, infection is typically asymptomatic and self-limiting due to a functional immune system. However, recent findings suggest that ocular diseases associated with *Toxoplasma* infection are more common

than previously recognised (26–29). The most vulnerable populations include immunocompromised individuals, such as those with HIV infection or patients who have undergone organ transplantation (28). In these cases, *Toxoplasma* infection can lead to severe health consequences, including encephalitis, which may be fatal (9,30,31). Additionally, congenital transmission of the parasite during pregnancy can result in miscarriages, severe health complications, or malformations in the unborn child, making pregnant women particularly vulnerable to infection (10).

1.1.2 Life Cycle

Toxoplasma possesses the typical alternation of asexual and sexual stages, a hallmark of the apicomplexan life cycle. Sexual replication occurs exclusively in the definitive hosts, which belong to the family Felidae (32). Mice are considered the most significant intermediate hosts, as asexual replication takes place in them. This is supported by findings that certain strains of *Toxoplasma gondii* exhibit adaptations to specific mouse populations (33). As part of these adaption Mice produce a specific family of immunity-related GTPases (IRGs), which are interferon-γ (IFNγ)-inducible proteins that accumulate at the parasitophorous vacuole membrane (PVM) following infection. These proteins disrupt the PVM and kill the parasite (34). Furthermore, mice are both abundant and accessible prey for cats, making them a critical reservoir for sustaining the infection cycle (35,36). However, all other warm-blooded mammals can act as intermediate hosts where the parasite replicates asexually (22).

In cats, infection primarily occurs through the ingestion of sporozoite-containing oocysts or bradyzoite-containing tissue cysts from infected prey. The tissue cysts formed in intermediate hosts are approximately 300 µm in size. Once ingested, these cysts rupture, releasing the parasites, which infect intestinal cells in the gut. Here, they multiply asexually through schizogony, producing four generations of schizonts. In the final generation, merozoites differentiate into macrogametocytes (female) or microgametocytes (male) (22,33). Microgametocytes produce microgametes, which fuse with macrogametes to form oocysts. These oocysts are shed in the faeces (22,30,37). *Toxoplasma* oocysts are approximately 12.5 µm × 11 µm in size and contain a 350 nm micropyle (38,39). Mature oocysts house two sporocysts, each containing four sporozoites (21,22,36).

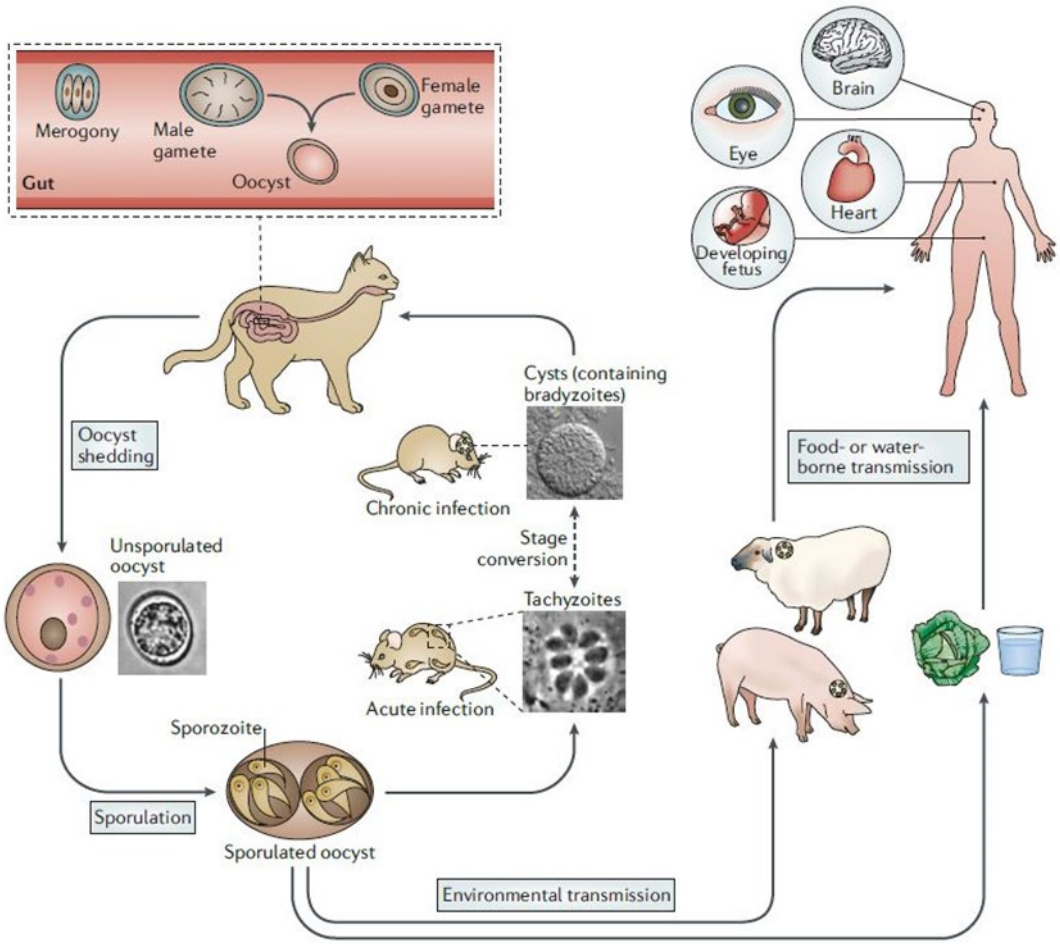

Figure 3: ***Overview of the Toxoplasma life cycle. Cats serve as definitive hosts where sexual reproduction occurs****, leading to the formation of oocysts that are shed in faeces. Ingestion of these oocysts through contaminated food or water results in the infection of humans and other animals, which act as intermediate hosts and can develop severe diseases (12).Image from Hunter and Sibley 2012.*

Oocysts and tissue cysts can both be ingested by intermediate hosts. Within the small intestine, proteolytic enzymes and bile salts trigger the release of sporozoites from oocysts and the excystation of bradyzoites from tissue cysts (40). The parasite then infects the lamina propria, either by passing between or through epithelial cells in the intestine (41). After invading host cells, the parasites undergo asexual multiplication through endodyogeny, a process of rapid replication that produces tachyzoites. Tachyzoites are crescent-shaped and measure approximately 6 µm × 2 µm (37). These stages quickly lyse host cells, releasing free tachyzoites that invade neighbouring cells, including immune cells. Tachyzoites can also spread via the bloodstream, facilitating vertical transmission (42–44). However, after a few days, the host immune system limits replication, and tachyzoites differentiate into bradyzoites, forming dormant tissue cysts. These cysts can persist for many years, particularly in brain and muscle cells, where they remain quiescent (22,26,29,37).

1.1.3 *Toxoplasma gondii*: Cellular Organisation

T. gondii possess the typical cellular composition found in all apicomplexan parasites.

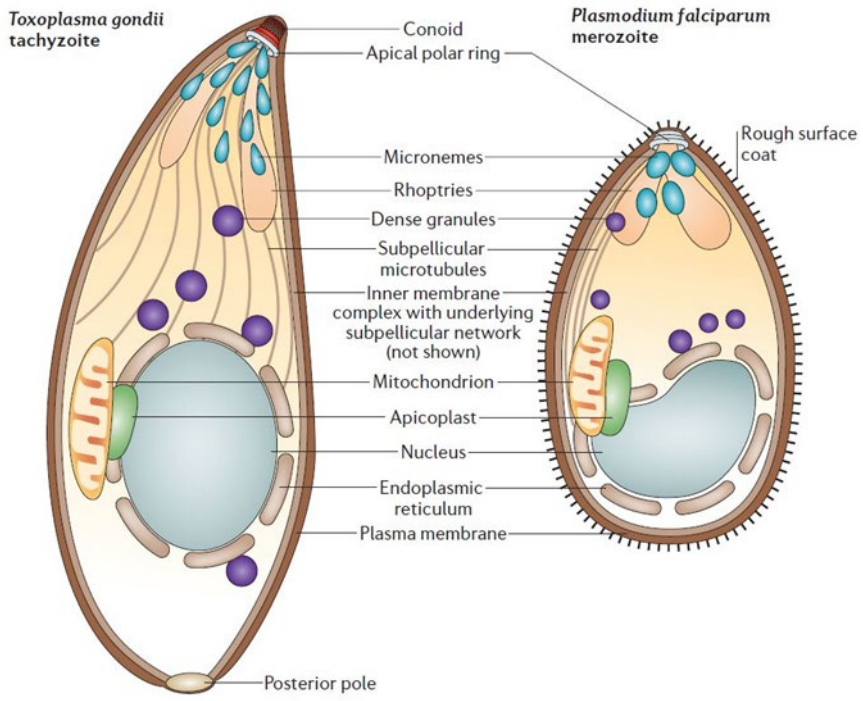

Figure 4: ***Toxoplasma gondii tachyzoites and Plasmodium merozoites****. Showing similarities in cell organelles and inner structures (45) .Image from Baum et al. 2006.*

In general, tachyzoites of *Toxoplasma gondii* exhibit the characteristic organelle organisation of apicomplexan parasites. At their apical end, tachyzoites possess the conoid, a tubular structure composed of spirally arranged microtubules organised in a helical configuration (46). The extension at the apical end is actin-myosin-based (47). The conoid resides between the two apical polar rings (ARP1 and ARP2) (48). ARP1 defines the margin of the inner membrane complex (IMC), while ARP2 functions as a microtubule organising centre (MTOC), which is essential for host cell invasion (27,49–52). Directly below the conoid are the unique secretory organelles, the micronemes and rhoptries. These organelles play a crucial role in host cell invasion and are secreted during or immediately after the invasion process. In addition, dense granules secrete GRA proteins that are involved in modifying the parasitophorous vacuole (53). While micronemes are secreted at the conoid with the assistance of the apical polar ring protein TgRNG2 (54), rhoptry proteins are discharged through the rhoptry secretory apparatus (RSA), a specialised structure unique to apicomplexans (55). Once the parasite has fully invaded the host cell, dense granule proteins (GRAs) are secreted at the apical annuli, which form small pore-like structures at the parasite's apical end (53,55–57). Another distinctive

feature of apicomplexans is the apicoplast, a four-membrane-bound organelle thought to have originated either from a green alga or a red alga during secondary endosymbiosis (58). The apicoplast is essential for specific lipid synthesis and other metabolic functions (58).

Toxoplasma gondii also possesses a plant-like vacuole (PLV), which has functions analogous to the plant vacuole. In *Toxoplasma*, the PLV is associated with roles similar to those of the lysosome in eukaryotic cells, including endocytotic and exocytotic trafficking, protein maturation, and calcium and salt homeostasis (59). Unlike most eukaryotic cells, *Toxoplasma* possesses an inner membrane complex (IMC) directly underlying the plasma membrane. This IMC serves as a barrier between the plasma membrane and the intracellular environment (60). The recently characterised micropore is a structure embedded in the IMC that connects the plasma membrane to the cytoplasm (61,62). The micropore consists of a K13 ring integrated into the IMC, through which runs a funnel of adaptor proteins (AP-2μ, AP-1, AP-2α). At the base of the funnel, dynamin (DrpC), a protein known for its role in vesicle cleavage, is localised (61,63,64). This structure is involved in membrane endocytosis in *Toxoplasma gondii* parasites.

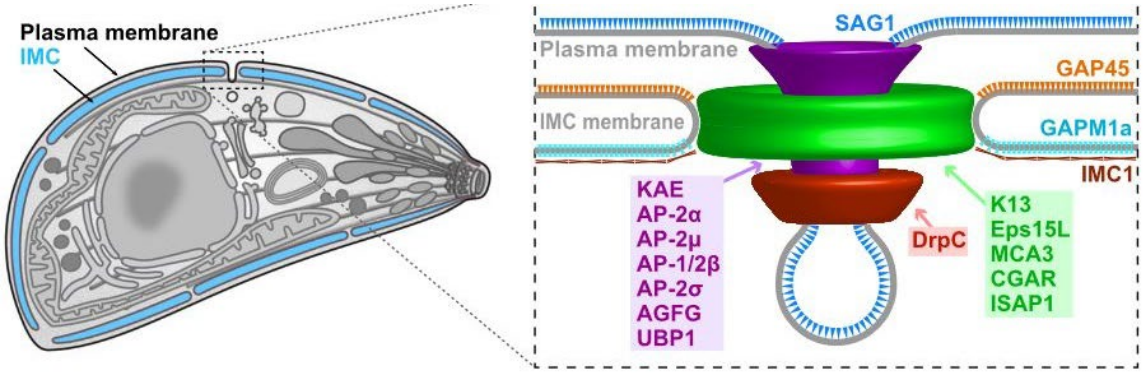

Figure 5: ***Micropores form a pore through the IMC, facilitating membrane uptake from the plasma membrane****. The micropore has a unique composition consisting of a ring made of K13 and Eps15L proteins, along with a funnel containing adaptor proteins (AP) and Dynamin (DrpC) for vesicle cleavage (61). Image adapted from Koreny et al. 2023a.*

As in all eukaryotic cells, *Toxoplasma* contains a mitochondrion. However, unlike most eukaryotes, it has only one mitochondrion, which is enclosed by a double membrane. The mitochondrion originated from an ancient endosymbiotic event and is essential for ATP energy generation (5). The parasite's nucleus is surrounded by both a rough and smooth endoplasmic reticulum (ER), similar to other eukaryotic cells. The secretory system includes a Golgi apparatus, which is typically divided into cis and trans-Golgi for protein modifications and the

generation and transport of vesicles. These processes are crucial for the function of the endosomal-like compartments (ELCs) (65–70).

1.1.4 Lytic Cycle

In cell culture, the most studied stage of *Toxoplasma gondii* is the fast-replicating tachyzoite stage. For invasion, *Toxoplasma* tachyzoites detect host cell surfaces, likely by interacting with common cell surface receptors, such as lectins present on the host membrane (23,71). After attachment, the parasites initiate the invasion process (51,72–74). Gliding motility and host cell invasion are complex processes involving the release of micronemal proteins at the apical end, triggered by Ca^{2+} signalling (75). Micronemal transmembrane proteins (MICs) attach to host cell receptors at the plasma membrane, while their cytosolic domains interact with the parasite's actomyosin system (76). The apical-to-basal translocation of actin filaments, powered by the myosin motor, transports MICs to the basal pole of the parasite, resulting in forward gliding and host cell invasion (50,51,77–82).

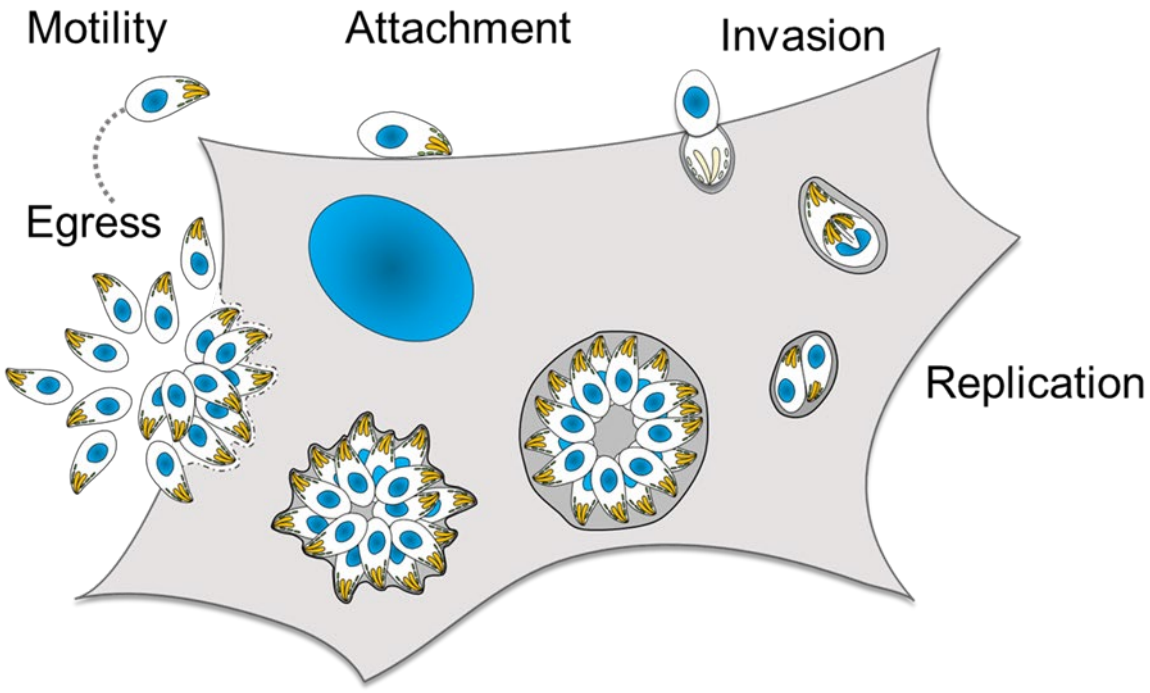

Figure 6: ***Schematic representation of the lytic cycle of T. gondii****. Following host cell lysis, tachyzoites are released (egress) and become motile, enabling them to search for and invade new host cells. This is followed by attachment, invasion, and a new round of replication (51). Image from Jamie A. Whitelaw et al. 2017.*

During invasion, the coordinated action of micronemal and rhoptry proteins leads to the formation of the moving junction (MJ), a ring-like structure integrated into the host cell

membrane through which the parasite invades (83). This process involves the invagination of the host cell membrane, forming the parasitophorous vacuole membrane (PVM) (84) around the parasite. Within the PVM, the parasite begins asexual replication (19,85,86). After completing replication, parasite egress is triggered by multiple stimuli originating from the PVM, initiating a new lytic cycle. This cycle involves host cell lysis, tachyzoite egress, and subsequent invasion of new host cells, perpetuating the infection.

1.2 Eucaryotic Phospholipid Membranes

Like all eukaryotic cells, *Toxoplasma gondii* possesses a cell membrane, which is fundamental to the evolution of life in complex environments. Among the most significant cellular components to evolve were semipermeable membranes, which protect the delicate cellular interior while enabling the formation of membrane-enclosed compartments, each capable of carrying out specialised functions (87). Semipermeable membranes act as both barriers and gatekeepers, segregating distinct cellular compartments and maintaining critical pH and electron gradients within and around the cell (88). These gradients are essential for processes such as the controlled breakdown of nutrients, waste management, and cellular repair (89). The development of internal membrane systems, such as the endoplasmic reticulum, mitochondria, and Golgi apparatus, enabled further functional specialisation within cells (90,91). These organelles are enclosed by membranes that separate their specific functions from the cytosol: the endoplasmic reticulum supports protein and lipid synthesis, mitochondria generate ATP, and the Golgi apparatus modifies and sorts proteins for transport (90,91). Additionally, the nuclear membrane plays a crucial role in protecting the DNA from external stresses while enabling regulated communication with the cytoplasm (88,92).

1.2.1 Functions of Eucaryotic Membranes

Biological membranes are phospholipid bilayers that separate intracellular compartments from the external environment. These membranes are composed of lipids, membrane proteins, and channels, which collectively ensure specialised functions (88,93). Essential tasks such as immune recognition, cell communication, molecular uptake. And movement depend, on the composition and integrity of these membranes. The lipid composition of the outer and

inner leaflets of the bilayer is asymmetrical, generating functional gradients (94,95). The outer leaflet is primarily responsible for cell-environment interactions, while the inner leaflet regulates intracellular signalling pathways. The dynamic nature of membranes facilitates cell signalling, mediated by transmembrane proteins and receptors, which enable communication with neighbouring cells, the immune system, and pathogens (96). Additionally, specialised structures like tight junctions play a critical role in sensing the cellular environment within clusters and contribute to intercellular communication and ion channel regulation (97).

1.2.2 Composition of Membrane, Lipids Proteins and More

This project aims, among other objectives, to characterise FLP2, a flippase suggested to be involved in *Toxoplasma gondii* endocytosis. As membrane lipid regulators, flippases are essential for membrane fluidity and endocytosis. Therefore, the following sections provide an overview of lipid and protein composition in eukaryotic membranes.

Eukaryotic membranes consist of lipids and proteins embedded within the bilayer, while their composition varying depending on the organism, the membrane's function, its location within the cell, and the temperature at which the cell resides. Different membranes contain varying ratios of lipids and proteins, with considerable diversity in lipid headgroups and aliphatic chains. This variation results in the presence of more than 1,000 different lipids in the cell membrane of eukaryotic cells (94). Membrane proteins can be categorised into three main types: transmembrane proteins, GPI-anchored proteins, and channels.

1.2.2.1 Lipids

Lipids are the fundamental components of cellular membranes, primarily in the form of glycerophospholipids. These consist of a glycerol backbone, a phosphate group, and fatty acid chains (94). The cylindrical shape of glycerophospholipids allows them to align side by side, forming sheets held together by non-covalent forces. This unique composition enables lipids to spontaneously form bilayers in an aqueous environment without energy input. In these bilayers, the hydrophilic head groups orient towards the surrounding aqueous environment, while the hydrophobic tails face inwards, creating a stable, water-impermeable core (94,95).

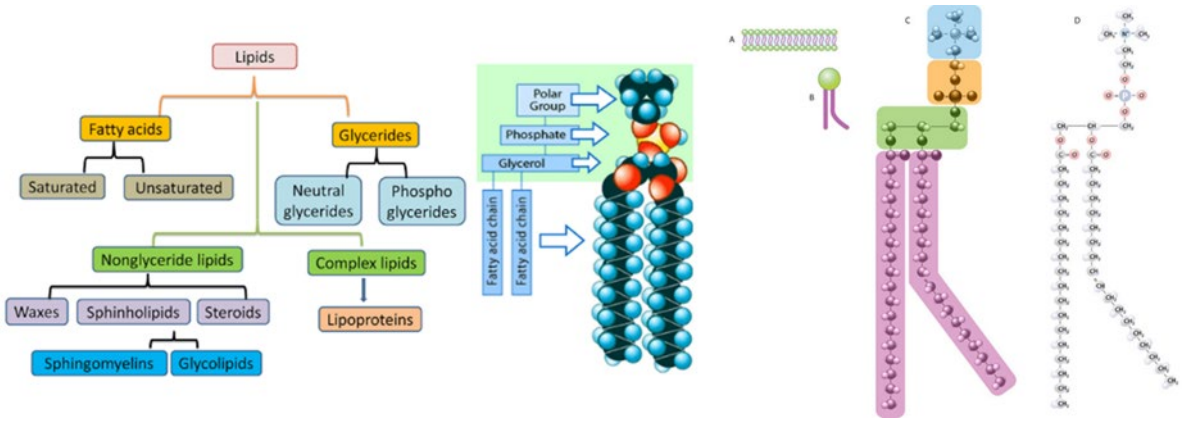

Figure 7: ***Overview of lipid types and their general structure.*** *Showing the different subclasses of lipids and zoom in on the structure.* ***A)*** *Aggregation of lipids in a bilayer.* ***B)*** *Schematic of a glycerolipid structure, highlighting the significant head groups and their associated tails.* ***C)*** *Detailed diagram showing the distinct regions of a glycerophospholipid.* ***D)*** *Atomic structure illustrating the molecular composition of lipids (87,98). Image adapted from Science at Scitable, Nature and Lipids 2021.*

Biological membranes are composed of three major lipid classes: phospholipids, cholesterol, and glycolipids, which together form the lipid bilayer (99). Structural lipids in mammalian cell membranes include glycerophospholipids, sphingolipids, and cholesterol. Lipids remain fluid at room temperature but solidify at lower temperatures due to the properties of their fatty acyl chains. The distinct lipid compositions of the bilayer's outer and inner leaflets contribute to the membrane's unique geometrical structure (93,94,100). Lipids, particularly cholesterol, are primarily synthesised in the endoplasmic reticulum (ER) and subsequently transported to other organelles (90,101). Additional lipid synthesis, particularly of sphingolipids, occurs in the Golgi apparatus, after which these lipids are exported to the plasma membrane (102). The proper distribution of these lipids across the bilayer ensures membrane fluidity, signal transduction, and immune regulation (103–105). For membranes to function effectively, lipids must be able to translocate between the bilayer's leaflets in a process known as flip-flop motion. This asymmetrical distribution of lipids is critical for processes such as signal transduction and membrane bending (106). However, while cholesterol can move between layers freely, most other lipids cannot spontaneously cross the membrane due to their charge, head group size, and hydrophobicity.

The movement of lipids across the bilayer is facilitated by specific phospholipid translocators:

- Flippases: Transport lipids from the outer leaflet to the inner leaflet (107).
- Floppases: Move lipids from the inner leaflet to the outer leaflet (100).
- Scramblases: Facilitate bidirectional lipid movement between the two leaflets (108).

These proteins, particularly flippases from the P4 subfamily of P-type ATPases, play a crucial role in regulating membrane fluidity and enabling the rapid transfer of lipids across the bilayer (107–109). Each of these phospholipid translocators serves a distinct function to maintain membrane homeostasis and support cellular processes such as vesicle formation and membrane repair (107,108).

1.2.2.2 Membrane Proteins

Transmembrane proteins are amphipathic, with their hydrophobic regions spanning the lipid bilayer and interacting with the membrane lipids. These proteins have a unique orientation based on their function, which differs between the cytoplasmic and non-cytoplasmic sides of the membrane (103,110). Transmembrane proteins can be categorised into single-pass and multi-pass proteins. These proteins serve various roles, including forming pores (e.g., porins), acting as enzymes, or assembling into multicomponent complexes embedded within the membrane.

Lipids and proteins exhibit two types of movement within the membrane:

1. Rotational diffusion: Rotation around their axis.
2. Lateral diffusion: Movement across the bilayer plane (108,111,112).

These lateral diffusion rates can be measured by fluorescence recovery after photobleaching (FRAP) (113) and complementary fluorescence loss in photobleaching (FLIP) (114), allowing the calculation of the diffusion coefficient for individual proteins. The cell membrane also contains specialised protein pores that facilitate the transport of small molecules, such as sodium and calcium ions. These pores function as pumps, utilising ATP to transfer molecules against their concentration gradients (115). Maintaining ion balance across membranes is vital for processes such as cellular signalling, particularly in neurons (116). For example, the Na^+/K^+ pump regulates ionic concentrations, enabling depolarisation and rapid signal transduction in neurons through the controlled opening and closing of ion channels (94,116).

1.2.3 Cargo Vesicle

Cargo vesicles are membrane-bound transporters that play a crucial role in intracellular trafficking. These vesicles transport proteins, lipids, and other cargo between cellular compartments, ensuring proper distribution within the cell.

Cargo vesicles are composed of a lipid bilayer membrane with two functionally distinct layers:

1. Inner layer: Responsible for cargo selection through specific adaptor proteins, such as AP complexes and nexins, which ensure cargo specificity (117,118).
2. Outer layer: Involved in coat selection, where coat proteins such as COPII (ER to Golgi), COPI (Golgi to ER), and clathrin (plasma membrane, Golgi, and endosomes) assemble into a coat that directs the vesicle to its destination (119–121).

The formation of cargo vesicles is highly organised at the membrane of origin. Coat proteins are recruited, initiating membrane budding. Cargo proteins contain sorting signals, such as KDEL sequences, which are recognised by adaptor proteins to ensure proper cargo loading (122). The vesicle undergoes scission, facilitated by GTPases, and begins its journey to the target organelle. For short distances, vesicles move along actin filaments, while for longer distances, they utilise microtubules (69,123,124). At the target membrane, vesicles must dock before fusion occurs. This process relies on surface markers expressed on the vesicle and target membrane. Two key protein classes mediate this process:

1. Rab GTPases: Monomeric GTPases that direct vesicles to specific spots on the target membrane (125–127). Each Rab protein is associated with specific organelles, ensuring accurate vesicle targeting (128).
2. SNARE proteins: Mediate membrane fusion. V-SNAREs (vesicle-associated) and t-SNAREs (target membrane-associated) bind together to form a trans-SNARE complex, which overcomes the energetic barrier to lipid mixing and mediates membrane fusion (129,130).

Lipid flow between the vesicle and target membrane is energetically unfavourable and requires fusion proteins to bring the two membranes within 1.5 nm for bidirectional lipid flow to occur.

1.2.4 Vesicle Transport from the Endomembrane System and Back

The endomembrane system regulates both secretory and endocytic pathways and includes the endoplasmic reticulum (ER), Golgi apparatus, lysosomes, endosomes, and the plasma membrane (101,125). Within this system, nutrients, receptors, and molecules are transported between organelles in vesicles, ensuring proper intracellular trafficking.

The fate of a vesicle depends on its cargo, origin, destination, and site of production (125). Molecular markers, such as Rab GTPases, enable vesicles to distinguish between organelles and ensure delivery to the correct location (102,131). Most cargo vesicles originate from specific regions of membranes and share two key characteristics. First, the inner vesicle layer selectively concentrates membrane proteins that recognise and bind the transported molecules. Second, the outer coat layer assembles into a curved, basket-like lattice structure, which shapes and stabilises the vesicle during its formation (121).

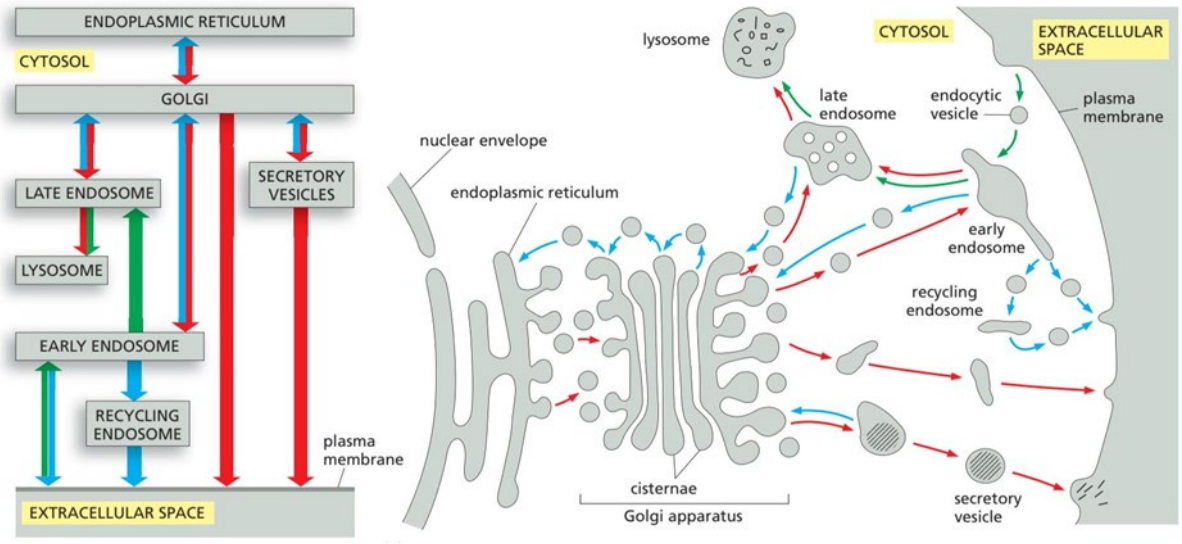

Figure 8: ***Schematics of vesicle transport through various organelles highlighting the dynamic and different routes vesicles can follow in the cell*** *(121). Image from Alberts et al. 2002a.*

Three vesicle classes exist within the transport pathways: clathrin-coated vesicles, COPI vesicles, and COPII vesicles (132,133). These vesicle types differ not only in their coat proteins but also in their trafficking routes. Clathrin-coated vesicles mediate transport between the Golgi apparatus and the plasma membrane, whereas COPI and COPII vesicles facilitate transport between the ER and the Golgi cisternae (134,135).

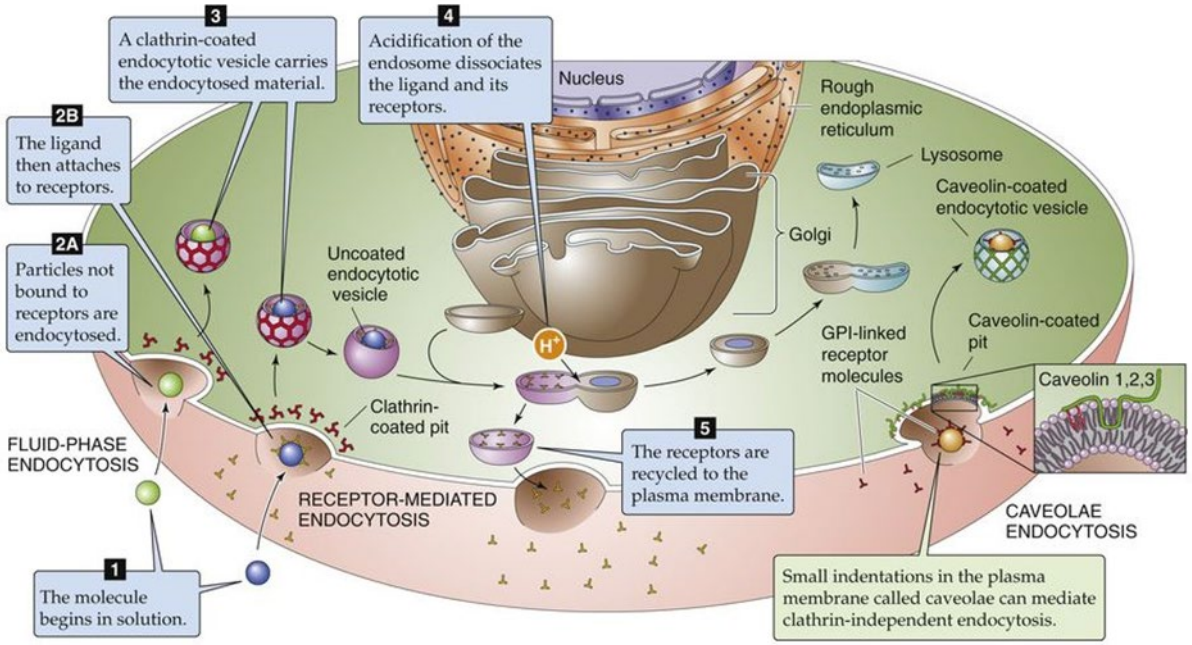

Figure 9: ***An overview of different classes of vesicles transported in the cell****, showing mechanisms and transport ways depending on the uptake vesicle (136). Image adapted from Textbook of Medical Physiology: 14th Edition.*

Clathrin-coated vesicles are specialised transport vesicles covered with a clathrin coat. Clathrin subunits consist of three large and three small polypeptide chains that form a triskelion structure (120). These triskelion's assemble into basket-like lattices of hexagons and pentagons, forming the vesicle coat. Adaptor proteins (AP) localised between the clathrin cage and the membrane selectively trap transmembrane receptors with their cargo (137–139).

Newly synthesised proteins at the ER must enter the secretory pathway for modification and delivery to their target destination (90). This strictly regulated process ensures that proteins are transported from the ER to the Golgi apparatus for carbohydrate synthesis, post-translational modification, and vesicle sorting (102). Proteins destined for transport are packaged into COPII vesicles. In contrast, COPI vesicles mediate retrograde transport, returning misdirected vesicles or resident ER proteins back to the ER (101). Upon arrival at the Golgi, COPII vesicles pass through the cisternae, a series of stacked compartments (4–6 per Golgi apparatus) (91). While passing through the stacks, proteins are covalently modified depending on their function. Each Golgi cisternae has two distinct faces called the interconnected tubular and cisternal structures consisting of the cis-Golgi network (CGN) and the trans-Golgi network (TGN) (91). At the CGN, vesicles either move on in the Golgi or return to the ER. Vesicles reaching the TGN move to their next destination, which can be endosomes, secretory vesicles, or directly to the cell surface, some of which are sent back to an earlier department. The TGN

forms a steady stream of secretory vesicles on the cell surface, where the vesicles fuse to the plasma membrane during exocytosis. However, before the proteins leave the TGN, they must be sorted again into three classes: destined for lysosomes, destined for secretory vesicles, and for immediate delivery to the plasma membrane (102,125). Destined for lysosomes means that the proteins/vesicles will be destroyed, and their building blocks will be reused. Secretory vesicles are stored near the plasma membrane and wait for the signal to release their cargo, which is especially important for depolarisation in neuronal cells (102). Furthermore, these vesicles patch fissions in the membrane, which can occur during mechanical stress. Here, homotypic vesicle-vesicle fusion and exocytosis work together to patch the cell. Secretory membrane vesicles also play an essential role in cellularisation during daughter cell formation (140,141).

1.2.4.1 The Cytoskeletal Network in Vesicle Transport

To ensure vesicles reach their correct organelles, vesicle trafficking is tightly regulated and supported by the cytoskeletal network, which provides tracks and mechanical forces for transport. The cytoskeletal network comprises of actin filaments and microtubules, which work alongside motor proteins to facilitate vesicle movement.

Actin filaments perform a wide range of functions, with their dynamic behaviour primarily occurring in the cell cortex (142). Actin subunits, also known as G-actin, polymerise in a head-to-tail fashion to form flexible, polar filaments, which assemble into a right-handed helical structure called filamentous actin (F-actin) (143). F-actin exhibits polarity, with structurally distinct ends: a slow-growing minus-end and a fast-growing plus-end (143,144). Actin filaments perform unique functions in both cell motility and vesicle transport. Essential are actin filaments for the short-range transport of vesicles especially near the plasma membrane participating in endo and exocytosis (142). Especially in endocytosis actin provides the force for membrane budding and vesicle scission. In intracellular sorting actin is used for direct movement in dense cellular regions (145,146).

Myosin motor proteins interact with actin filaments to facilitate vesicle movement. Myosin consists of two heavy chains and two light chains, with a globular head domain that binds and hydrolyses ATP, enabling movement along actin filaments (123,147). Cargo vesicles are attached to myosin and transported as the protein “walks” along actin filaments carrying

behind cargo vesicles bound to the myosin (123). In endo and exocytosis, this carrier mechanism helps to bring and fuse vesicles with the plasma membrane and stabilise the fusion, especially important here is myosinVI (MyoVI) which moves the cargo from the minus-end of actin filaments. Other sub classes of myosin's are important for different transports (123). MyoI is especially associated with short-range membrane trafficking and endocytosis while MyoV is important for Golgi-plasma membrane transportation (123,148).

Microtubules are another key component of the cytoskeletal network. They are hollow cylindrical filaments composed of α- and β-tubulin dimers. Like actin filaments, microtubules are polarised: the plus-end is the growing end, while the minus-end is anchored at the MTOC (69,149). Especially important are microtubules for long range vesicle transport (150). Microtubules have distinct molecular motors then actin they work together with kinesin which moves vesicle towards the plus-end and dynein's which work the other way around. Microtubules are specifically used for long-range transport like ER to Golgi or for bidirectional movement (69).

The actin and microtubule networks interact to ensure efficient vesicle transport. Transition zones enable vesicles to switch between actin and microtubule tracks, ensuring uninterrupted movement to the plasma membrane (144). Cross-linking proteins such as cortactin (151) and spectraplaktin (152) play a critical role in linking actin filaments and microtubules, facilitating vesicle handover between the two networks. These specialised interactions are particularly crucial for endocytosis and exocytosis at the plasma membrane, where precise vesicle movement and fusion are required.

1.3 Endocytosis

The primary mechanism for the uptake of membrane proteins and nutrients is endocytosis, which can be classified into passive diffusion, active uptake, and diffusion-mediated mechanisms (153). Diffusion occurs only for small molecules capable of passively crossing the cell membrane without energy expenditure. In contrast, active endocytosis is highly specific and can be further divided into distinct uptake mechanisms (153). These mechanisms are categorised based on factors such as: helper or adaptor proteins involved in plasma membrane (PM) uptake, the proteins to be internalized, the processing route, and the goal of uptake (e.g., nutrition, receptor internalization, etc.) (154,155).

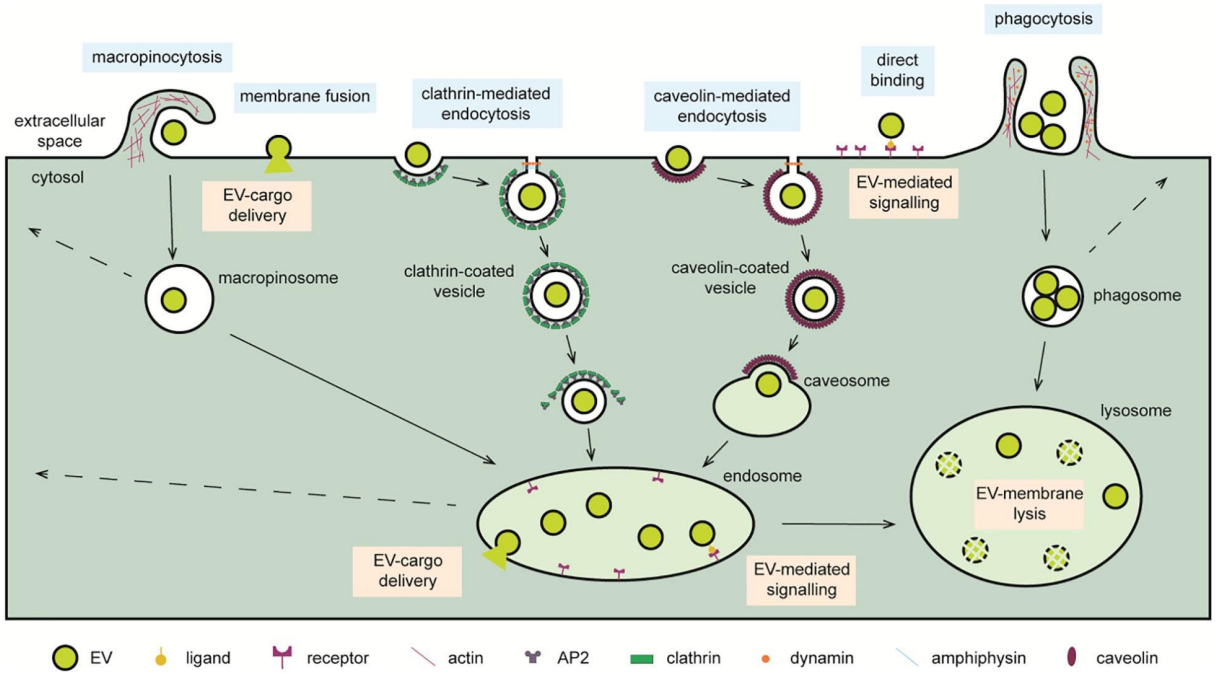

Figure 10: ***The endocytosis schematic shows the uptake and transport in endocytosed vesicles****, especially clathrin-coated vesicles, and other endocytosis mechanisms in the cell (156). Image from Pedrioli and Paganetti 2021.*

Endocytic sites at the plasma membrane are marked by specific phosphoinositides, including PtdIns(4,5)P_2, PtdIns3P, PtdIns(3,5)P_2, and PtdIns4P (96,157). Proteins involved in vesicle trafficking and membrane homeostasis are recruited to these sites. Here, the membrane can be invaginated into vesicles, which are cleaved and trafficked to their specific target point in the cell. These endosomes can either fuse with lysosomes to be destroyed, transported to the Golgi or re-secreted back to the membrane (158).

1.3.1 Clathrin Depending Endocytosis

Clathrin-mediated endocytosis is one of the best-studied endocytic pathways. The vesicles generated in this process are generally small (60–120 nm) and primarily transport transmembrane proteins and extracellular ligands that are essential for nutrient uptake, cell signalling, cell adhesion, and the regulation of development (159). It is considered the canonical pathway for cargo internalisation and plays key roles in nutrient uptake, receptor downregulation, membrane recycling, and signal transduction. Clathrin-mediated endocytosis results in the formation of clathrin-coated vesicles (CCVs) at the plasma membrane, which deliver cargo to early endosomes (120). The process is initiated by the recruitment of adaptor proteins, such as AP2, to pre-selected clathrin-coated pit (CCP) hotspots marked by specific

lipids (160). One of the most critical lipids is phosphatidylinositol 4,5-bisphosphate [PI(4,5)P_2], which serves as a binding site for adaptor proteins (160).

Two main hypotheses describe how the clathrin coat forms:

1. Constant Curvature Model: The clathrin coat polymerises directly into a curved membrane, increasing the curvature as the pit enlarges.
2. Constant Area Model: Clathrin initially assembles on a flat membrane until a critical protein density is reached, at which point the membrane begins to curve (161).

Both membrane tension and rigidity regulate the assembly and curvature of the coat (159,161,162). Clathrin forms a triskelion-shaped structure composed of three heavy chains and three light chains. These triskelia polymerise into a polyhedral lattice, which forms the coat. The process begins with the recruitment of clathrin adaptors, primarily to membrane regions enriched in PI(4,5)P_2 (160). The recruitment of FCHo1 and FCHo2, proteins containing BIN-amphiphysin-Rvs (BAR) domains, generates membrane curvature. BAR domains can be classified based on their curvature (163):

- F-BAR domains: Facilitate shallow curvature.
- N-BAR domains: Support high curvature.

These proteins provide a platform for AP2 adaptor proteins to bind (63,163,164). AP2 recognises sorting signals on cargo, such as tyrosine-based motifs and di-leucine motifs (165). Clathrin then interacts with adaptor proteins, linking to the cytoplasmic tails of transmembrane cargo. As the critical density of adaptor proteins is reached, the coated region begins to invaginate, forming CCPs. The assembly process is further regulated by BAR domain-containing proteins, which stabilise the curvature. Myosin-based contraction can also recruit BAR proteins and influence membrane tension. After membrane curvature is initiated, clathrin triskelia bind to the adaptor proteins and form a cage-like structure. This process recruits EPS15 and EPS15R, which interact with the coat proteins (160,166–169). During the late phase of endocytosis, actin polymerisation begins. Actin preferentially polymerises in regions surrounding the clathrin coat and at the base of the membrane invagination, resulting in the formation of a stabilising actin network at the rim of the clathrin cage (146). This process is regulated by BAR domain-containing proteins, such as amphiphysin, FBP17, sorting nexin, and

others (169). The formation and stabilisation of the actin network are mediated by WASP family proteins, including Pan1 and End2, which are essential for actin filament recruitment(166). These proteins recruit the ARP2/3 complex, which nucleates actin filaments and promotes actin polymerisation (170). Membrane fission and vesicle release are powered by GTPase dynamin, which assembles into a helical collar at the neck of the clathrin-coated pit. Dynamin is recruited to the CCP neck, where it oligomerises and drives vesicle scission through GTP hydrolysis (162,171). Actin filaments provide additional mechanical force to assist in the membrane fission process. Once vesicle scission occurs, the clathrin-coated vesicle is rapidly uncoated to allow further intracellular transport. The uncoating process is facilitated by auxilin, which recruits Hsc70. Hsc70 uses ATP hydrolysis to disassemble the clathrin coat (172). The resulting uncoated vesicles fuse with early endosomes, where cargo sorting takes place (173).

1.3.2 Clathrin-Independent Endocytosis (CIE)

In contrast to clathrin-mediated endocytosis, clathrin-independent pathways exhibit a high capacity for membrane turnover in response to rapid mechanical changes at the plasma membrane (174,175). These processes are independent of clathrin but can further be distinguished by their reliance (or lack thereof) on dynamin. Importantly, these pathways depend on lipid microdomains, such as caveolae and lipid rafts, and are primarily involved in the uptake of GPI-anchored proteins, lipid-bound cargo, and specific receptors. To better understand clathrin-independent mechanisms, the following major pathways will be discussed.

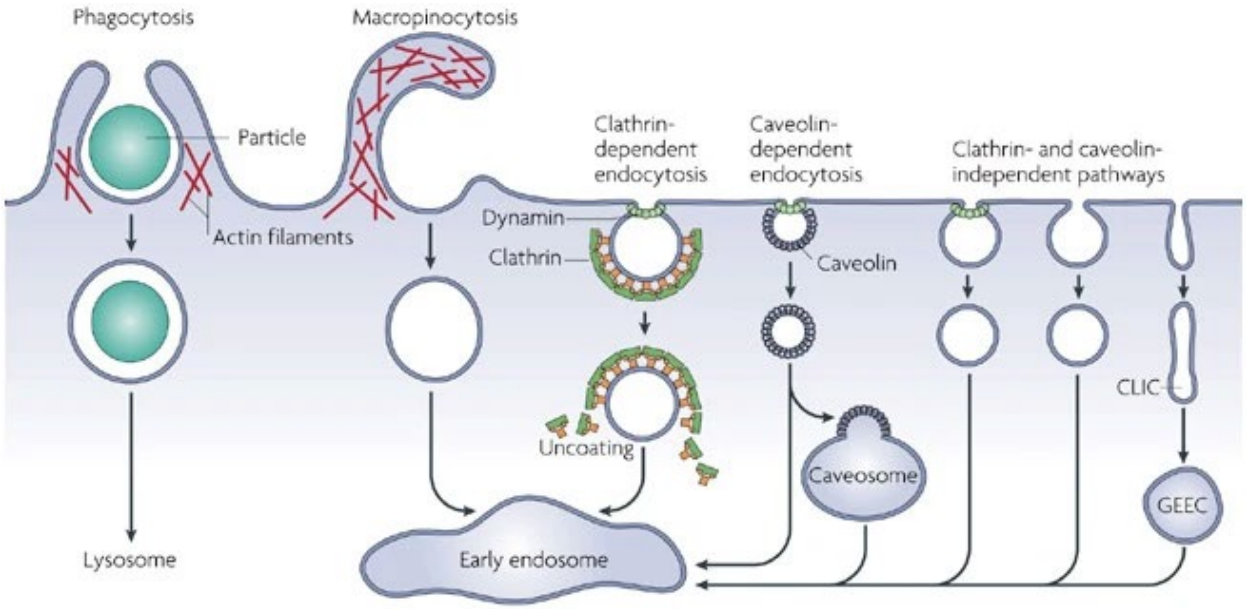

Figure 11: ***Overview endocytosis pathway until they fuse in an early endosome*** *(176)****.*** *Image from Mayor and Pagano 2007.*

1. Caveolae and lipid raft endocytosis

The caveolae-mediated pathway is characterised by flask-shaped invaginations of the plasma membrane. Caveolae are specialised lipid raft domains enriched in cholesterol and sphingolipids, which form stable regions in the plasma membrane (177,178). Caveolae are stabilised by caveolins (integral membrane proteins) that interact with cholesterol and lipid domains, creating a scaffold for the caveolar structure (179). On the cytoplasmic side, cavin proteins bind to caveolins, forming a large complex that stabilises membrane curvature Caveolae play critical roles in mechanotransduction, membrane repair, and transcellular transport (178,180). Under mechanical stress, caveolae can disassemble, increasing the available membrane surface area**.**

The first step in caveolar endocytosis involves cargo selection, mediated by lipid interactions and protein binding**.** Caveolin-1 facilitates membrane curvature, while dynamin mediates vesicle scission. The resulting caveolar vesicles undergo transcytosis or are recycled back to the plasma membrane (177,178).

A similar pathway is flotillin-dependent endocytosis, which originates in lipid rafts and relies on Flotillin-1 and Flotillin-2 (181). Flotillins are lipid-raft-associated proteins anchored to the cytoplasmic leaflet of the plasma membrane via their prohibitin homology (PHB) domain, which interacts with membrane lipids (181,182). Flotillins oligomerise at lipid rafts, and their

stability depends on the cholesterol content of the membrane. Unlike caveolar endocytosis, flotillin-mediated endocytosis is dynamin-independent but driven by actin polymerisation, which generates mechanical force for vesicle budding and scission. This pathway is particularly important for the uptake of GPI-anchored proteins.

Arf6 (ADP-ribosylation factor 6)-dependent endocytosis is crucial for plasma membrane remodelling and specific receptor internalisation (183). Arf6 targets specific receptors and regulates the actin cytoskeleton by activating Rac1 and Cdc42. Actin polarisation drives membrane curvature and vesicle budding. Arf6-positive vesicles can fuse with early endosomes or be recycled back to the plasma membrane through Rab11-dependent pathways (183–185).

2. CLIC/GEEC Pathway (Clathrin-Independent Carriers and GPI-Enriched Early Endocytic Compartments)

The CLIC/GEEC pathway (Clathrin-Independent Carriers and GPI-Enriched Early Endocytic Compartments) is a bulk endocytosis pathway involved in the uptake of GPI-anchored proteins and fluid-phase cargo (176,186). Like Arf6-dependent endocytosis, this pathway originates at cholesterol-rich lipid rafts. The plasma membrane invaginates to form tubulovesicular structures known as CLICs. This process is actin-driven and regulated by Cdc42, a Rho family GTPase, which remodels the actin cytoskeleton (187,188). The ARP2/3 complex facilitates the branching and nucleation of actin filaments. Phosphoinositides provide docking sites for effector proteins at the membrane.

After vesicle scission, CLICs fuse to form GPI-Enriched Early Endocytic Compartments (GEECs). Cargo within these compartments is sorted for either recycling to the plasma membrane via Rab11a or trafficking to endosomal compartment (176,186).

3. Trans endocytosis

Trans-endocytosis is a specialised mechanism in which membrane components are internalised into an adjacent cell, making it essential for intercellular communication and signalling. Direct cell-to-cell contact is required, usually via receptor-ligand interactions or adhesion molecules. Examples include clathrins, immunoreceptors, or Notch-Delta pairs (189). Receptors on the donor cell are recognised by the recipient cell, triggering endocytotic

machinery that internalises the ligand-receptor complex. During vesicle scission, parts of the donor plasma membrane and the receptor-ligand complex are internalised into the recipient cell. The cargo-containing vesicle follows standard endocytotic routes, fusing with early endosomes for sorting or recycling endosomes for further transport (184,190–192).

4. Macropinocytosis

All eukaryotic cells ingest portions of their plasma membranes via pinocytosis. While the process varies among cell types, the rate of ingestion is relatively high. Importantly, the cell surface area and membrane volume remain unchanged during pinocytosis, as endocytosis and exocytosis are balanced. Pinocytic vesicles form through invagination of the plasma membrane, which mediates membrane bending and subsequent vesicle formation (174,175). Pinocytosis is an actin-driven bulk endocytosis process that internalises large amounts of extracellular fluid, solutes, and particles. Unlike other endocytic pathways, pinocytosis does not rely on coat proteins. Instead, it requires the activity of Rho family GTPases**,** PI3K, and actin polymerisation for membrane remodelling. The resulting vesicles are termed macropinosomes (193).

5. Phagocytosis

Phagocytosis is a specialised form of endocytosis that evolved to engulf large particles, such as cell debris, foreign substances, and microorganisms. It is primarily carried out by immune cells known as phagocytes (194). In contrast to other forms of endocytosis, phagocytosis begins with the recognition of specific surface receptors or signals on the target organism (194). These signals include opsonin’s, which coat the particle, or pathogen-associated molecular patterns (PAMPs) on microorganisms. To recognise these foreign signals, cells have evolved specialised receptors, such as the Fc receptor or complement receptors, among others (195). Once the receptors bind to the target, the actin cytoskeleton begins to reorganise, forming pseudopodia that engulf the particle, thereby generating a phagosome. The phagosome undergoes maturation by fusing with early endosomes for sorting, followed by fusion with late endosomes, where degradative enzymes are delivered. Finally, fusion with lysosomes leads to the destruction of the engulfed particle by hydrolytic enzymes. Phagocytosis plays a critical role in tissue homeostasis, nutrient recycling, and the immune response by facilitating the clearance of debris and defence against pathogens (196).

1.4 Endocytosis in Protozoan Parasites

In both intra- and extracellular parasites, endocytic mechanisms are essential for cellular homeostasis and immune evasion. In *Trypanosoma* parasites, endocytic events play a key role in maintaining the fluidity of GPI-anchored variant surface glycoproteins (VSGs). These parasites must display a wide variety of VSGs on their surface; thus, bulk flow and efficient transport of these proteins to the surface are essential (197). This mechanism has been well-investigated in *Trypanosoma*. Endocytosis and exocytosis in these parasites occur exclusively at the flagellar pocket, where CCPs rapidly form and invaginate (197,198). At this site, *Trypanosoma* recruits specific adaptor proteins, such as TbEpsinR, TbCALM, and TbHs70, but notably lacks AP-2, which is typically involved in mammalian endocytosis (197). Additionally, the actin cytoskeleton and TbMyo1 are known to play roles in vesicle endocytosis and translocation through the parasite (197,198). In contrast to the well-characterised endocytic pathways in other eukaryotes and *Trypanosoma* species, endocytosis in apicomplexan parasites remains poorly understood. Most available data come from studies on trophozoites of *Plasmodium* parasites, describing the uptake of haemoglobin from erythrocytes as a nutrient source. This process occurs at the cytostome, a specialised structure involving various proteins, including AP2 adaptor proteins and Kelch13 (K13) (199–203). In the blood stages of *P. falciparum*, host cytosol uptake is the only thoroughly investigated endocytic process in apicomplexans. At this stage, the parasite exclusively internalises haemoglobin (199,204). This bulk uptake process is unrestricted, with the ingested material being transported to and digested within the digestive vacuole (DV). However, the mechanistic details of this process remain unclear. Haemoglobin uptake begins with the invagination of the membrane at the periphery of the parasite's cytostome, which features a small neck (205,206). Two main hypotheses describe this process: the cytostome may detach from the membrane to form vesicles, or it may serve as a hub for further endocytotic events. While the full protein repertoire mediating uptake at the cytostome is unknown, actin, PI(3)P kinases, and SNARE (soluble N-ethylmaleimide-sensitive factor attachment protein receptor) proteins are believed to be involved (200,201,207,208). One key protein, VPS45, has been identified as essential for vesicle transport, as its inactivation causes an accumulation of haemoglobin-containing cytostome (HCC)-filled vesicles in the parasite (202). The involvement of Rab proteins, such as Rab5b and Rab7, in this process remains unclear. Other proteins, including AP2μ, Eps15, KIC7, Kelch13, and UBP1, are also implicated in *Plasmodium* endocytosis (204). Inhibition of these

proteins, referred to as Kelch13 interaction candidates, disrupts the delivery of HCC, highlighting the significance of the endocytosis-initiation complex (209). Interestingly, Kelch13 also plays a key role in artemisinin (ART) resistance. Mutations in Kelch13 reduce haemoglobin uptake, leading to decreased haem production and, consequently, reduced activation of ART (209). In contrast to *Plasmodium*, endocytic processes in other apicomplexan parasites are poorly understood. It remains unclear whether similar mechanisms operate or if these parasites utilise distinct endocytic pathways.

1.4.1 Endocytosis in *T. gondii*

Early studies demonstrated the ability of *Toxoplasma gondii* extracellular tachyzoites to take up FITC-labelled heparin (HF). Additionally, it was shown that mCherry expressed in the host cell cytoplasm could be internalised by parasites (67). *Gras et al.* showed the presence of a flow similar to the retrograde membrane flow and further revealed a flow mechanism similar to retrograde membrane flow through the uptake of lipids and antibodies targeting SAG1 at the parasite's plasma membrane (210).The fountain flow model, or retrograde membrane flow, relies on the uptake of the plasma membrane at the basal pole and its exocytosis at the apical pole of the cell. This dynamic process generates pseudopodia and facilitates parasite movement (211). Notably, this model depends exclusively on the endocytosis and exocytosis of the plasma membrane itself. However, it remains unclear whether the endocytosed SAG1 vesicles participate in retrograde membrane flow or serve the alternative purpose of protein and molecule uptake from parasitophorous vacuoles (PVs) or the host cell. Studies investigating this process were limited because SAG1 antibodies interfered with parasite invasion, preventing the examination of endocytosis during replication (73). Furthermore, the endocytosis of antibody-bound proteins may disrupt their natural trafficking pathways. To overcome these limitations, a new endocytic assay was developed, suitable for both extracellular and replicating intracellular parasites. This assay involved integrating an exogenous Halo tag (212) into the SAG1 gene, upstream of the GPI anchor, enabling the labelling of SAG1 both extracellularly and intracellularly using Halo ligands (61).

Recently, K13 micropores were discovered by two independent research groups. These micropores are composed of a K13 ring, which spans the inner membrane complex (IMC1) and

connects to the plasma membrane via a funnel of adaptor proteins. These micropores have been implicated in the uptake of the plasma membrane, and their absence results in the inhibition of endocytosis and subsequent parasite death (62,213).

1.4.1.1 Flippases in *T. gondii*

Flippases are enzymes known for translocating membrane lipids and proteins from one side of the bilayer to the other (214). Inhibition of flippases can significantly impair or even block endocytosis in eukaryotic cells. Flippases are primarily members of the P4-ATPase family, a group of ATP-dependent phospholipid translocases. These enzymes are responsible for maintaining membrane asymmetry by transporting specific phospholipids, such as phosphatidylserine (PS), from the outer to the inner leaflet of the lipid bilayer (108). This process is critical for membrane integrity, vesicle formation, and intracellular trafficking. In *Toxoplasma gondii*, flippases are believed to play pivotal roles in the parasite's life cycle, particularly in endocytosis, exocytosis, and the maintenance of organelle membranes. Recent studies have identified a heterocomplex of CDC50.4 and ATP2B/ATP2A, which act as PS flippases at the plasma membrane and are involved in microneme exocytosis (215). ATP2 is a highly conserved protein across the Apicomplexa phylum (215). and has been shown to flip phosphatidylethanolamine (PE) and phosphatidylserine (PS) in *Plasmodium chabaudi*.

These lipids are synthesised at the cytosolic leaflet of the endoplasmic reticulum (ER), with the membrane asymmetry maintained at the Golgi apparatus and plasma membrane. This asymmetry is particularly important for exocytotic vesicle sorting (216). Changes in PS concentration may alter plasma membrane tension and curvature, which can, in turn, affect signalling components and membrane dynamics. Disruption of these flippase complexes can impair membrane trafficking, resulting in defective secretion of invasion-associated proteins and significantly reduced virulence (217). Despite these insights, the role of P4-ATPases in apicomplexan parasites remains under investigation. This thesis will focus on FLP2, a specific P4-ATPase, and its role in endocytosis in *T. gondii*.

1.4.2 The Model System *Toxoplasma*

The *Toxoplasma gondii* genome has been sequenced and is approximately 65 Mb in size, organised into 14 chromosomes coding for around 9,000 genes (218). The availability of the *T. gondii* genome has enabled significant advances in the genetic manipulation of parasites. In particular, the introduction of the CRISPR/Cas9 system in *T. gondii* has facilitated rapid and precise genetic alterations (219,220). The CRISPR/Cas9 system relies on the Cas9 endonuclease, which recognises specific RNA sequences. Guided by a single-guide RNA (sgRNA), Cas9 targets specific sites in the genome. These sgRNA sequences include a protospacer adjacent motif (PAM), which is essential for Cas9 activity. Once Cas9 binds to the target sequence, it induces a double-strand break (221,222). Using a ΔKu80 parasite strain, which lacks the ability to repair double strand breaks via non-homologous end joining (NHEJ), repair occurs exclusively through homologous recombination using a supplied repair donor DNA template. This enables the expression of modified proteins or proteins tagged with specific fluorescence tags. Such modifications make it possible to localise proteins and track the movement of soluble and secreted proteins in live-imaging assays. While the straightforward generation of null mutants is efficient with this approach, the analysis of essential genes requires the use of conditional gene expression systems.

Several conditional systems have been established in *T. gondii*, allowing the regulation of gene expression at the transcriptional, translational, or protein levels (219).

Within this thesis, two technologies were employed: DiCre and mAID. For the generation of conditional null mutants, the DiCre system has the advantage of allowing the complete and conditional deletion of the gene of interest. This leads to mutants with no background expression, which can otherwise obscure phenotypes, particularly in the case of weakly expressed genes. This system employs Cre recombinase, which is split into two subunits: one fused to an FKBP domain and the other to an FRB domain. Cre recombinase recognises short DNA sequences called LoxP sites, enabling site-specific DNA recombination. When LoxP sites are integrated at a gene's N- and C-termini, the region between them can be excised in the presence of rapamycin, resulting in a stable knockout (KO) (223). While these KOs are useful for studying gene function, they are irreversible. Another limitation of the DiCre system is its slow kinetics, with phenotypes often becoming apparent 48–72 hours post-induction. To

address the limitations of the DiCre system, fast and reversible knockdown systems have been developed. The auxin-inducible degron (mAID) system (224) requires a parasite strain that expresses the plant-derived Tir1 (Transport Inhibitor Response 1) protein from *Arabidopsis thaliana* (225). Proteins tagged with an auxin-inducible degron (AID) sequence can be selectively degraded upon exposure to the plant hormone auxin, which activates Tir1. By introducing the mAID tag into the protein of interest, usually as a C-terminal tag, researchers can rapidly degrade the protein, facilitating phenotype interpretation.

However, a major disadvantage of this system is that knockdown efficiency may be insufficient to obtain a phenotype. Additionally, the mAID tag can interfere with the protein's natural function (224,225).

1.5 Aims of the study

Recent studies on K13, a key component of the micropore have highlighted its critical role in membrane endocytosis and parasite survival (61,62). Knockdown of K13 has been shown to impair plasma membrane endocytosis during parasite replication, characterised by a reduction in both the number of vacuoles where endocytosis occurs and the average number of endocytic SAG1 vesicles per vacuole. In addition to the inhibition of endocytosis, depletion of K13 leads to membrane accumulation and, ultimately, a complete disruption of membrane homeostasis, resulting in parasite death. These findings underscore the essential role of plasma membrane homeostasis in parasite survival.

This study aimed to characterise plasma membrane dynamics during parasite replication and to investigate the mechanisms involved in endocytic vesicle trafficking. To address these objectives, the potential of SAG1-Halo as a proxy for tracking plasma membrane dynamics was explored and validated. Plasma membrane behaviour in replicating parasites was subsequently analysed, focusing on distinct membrane subpopulations, including the membrane at the surface of the parasites, the internal stock of plasma membrane either inherited or generated de novo, and the trafficking pathways involving motor proteins.

The impact of membrane composition on endocytosis and endocytic vesicles was further examined by analysing the role of FLP2, a P4-ATPase responsible for switching phospholipids critical for membrane curvature. Finally, a novel membranous structure, termed the plasma membrane reservoir (PMR), was characterised, appearing exclusively in replicating parasites.

2 Results

2.1 Studying Membrane Dynamics in Intercellular Parasites Based on the Major Surface Antigen 1 (SAG1)

The plasma membrane (PM) of apicomplexan parasites is essential for efficient gliding motility and host-cell invasion (37,49,51,82). Despite its importance, membrane dynamics remain poorly understood, specifically during intracellular development. Previous studies on extracellular parasites demonstrated the presence of membrane flow using antibodies targeting the surface antigen SRS49/SAG1 and fluorescent beads (210). These studies revealed dynamic changes upon transferring parasites from 4 °C to 37 °C, including the translocation of membrane-bound beads to various positions on the parasite surface and the uptake of antibody-bound SAG1 (210). However, antibody-based assays have certain limitations and can inhibit host cell invasion depending on their concentration (226). New endocytic assays are therefore needed to investigate membrane dynamics during intracellular parasite development.

Live-cell imaging techniques employing yellow fluorescent protein (YFP) (227), mCherry (228), SNAP-Tag (229)and HaloTag (230) enable detailed analysis of fluorescently tagged proteins in eukaryotic cells in real time. Based on these fluorescent tags, novel labelling techniques have been developed that permit live-cell imaging without interfering with critical cellular processes, such as cell division or, in the case of *Toxoplasma gondii*, host-cell invasion and intracellular replication (61,212). In *T. gondii*, fluorescent tagging has facilitated organelle-specific visualisation, which is particularly advantageous for specific labelling of membrane proteins. In contrast, lipid dyes such as Nile Red have been shown to diffuse across all membranes in *T. gondii* and even into host-cell membranes, thereby limiting their utility for specific membrane labelling (231). By implementing the HaloTag method, defined tracking of membranes and micronemes can be achieved in the parasite (61,212). The HaloTag is a modified version of the bacterial *Haloalkane Dehalogenase* that has been mutated to lose its catalytic activity while retaining the ability to bind covalently to chloroalkane ligands (230,232). These ligands can be conjugated to fluorophores, biotin, or affinity tags, depending on the desired application. Ligand binding results in a stable, irreversible covalent bond, making this method highly specific and efficient.

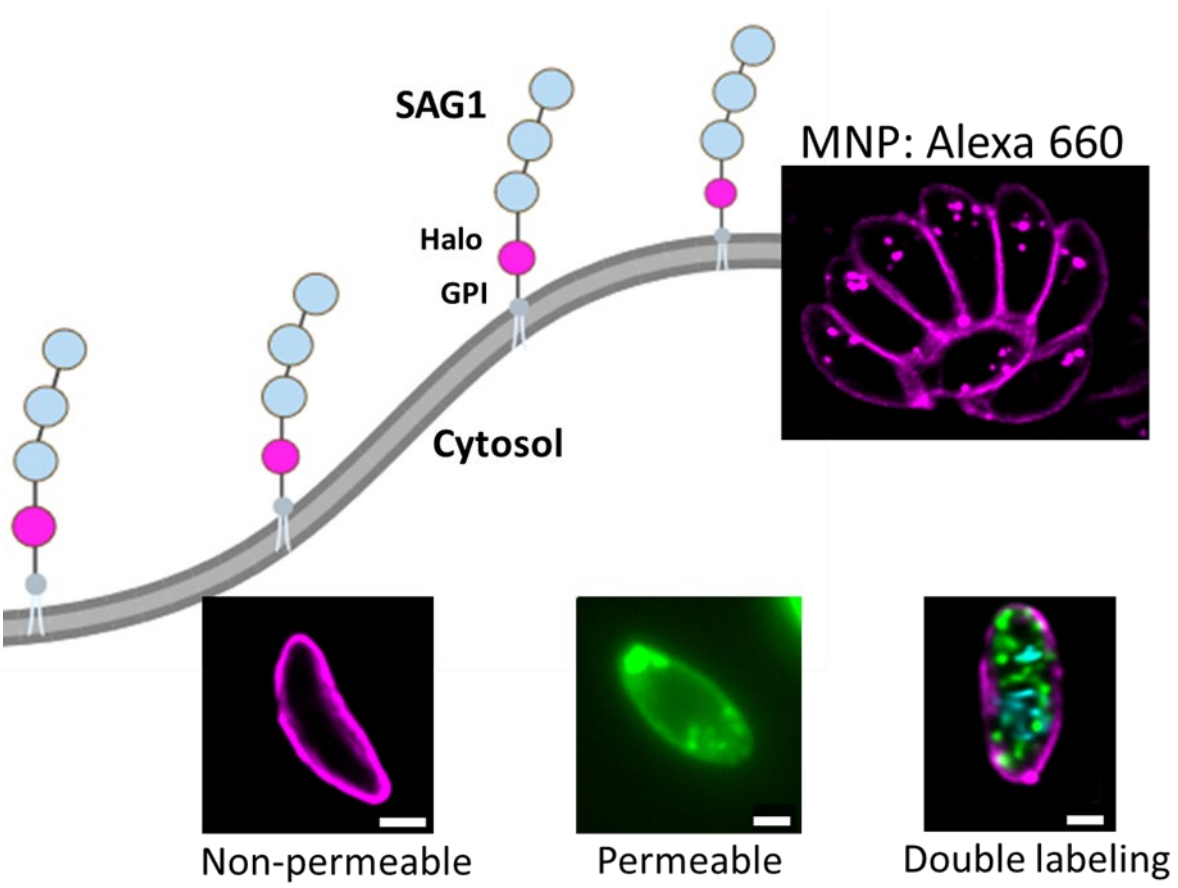

Figure 12: ***Labelling schematic of HaloTag integration.*** *This illustration visualises the integration of the HaloTag after the GPI anchor, enabling the use of both membrane-permeable (MP) and membrane-non-permeable (MNP) Halo dyes on the same parasite. Enabling differentiation of the Halo tagged protein localised at the parasite surface and on intracellular vesicles during replication (MNP: Alexa660, MP:Oregon Green). Created using BioRender. Scale bar: 1 µm.*

Figure 12 shows the adaptation of the HaloTag to label the major surface antigen 1 (SAG1), a GPI-anchored protein localised on the parasite membrane. The HaloTag was inserted before the GPI anchor (61) but after the SRS domains of SAG1, ensuring the extracellular localisation of the tag on the parasite surface. Using this technique, it was possible to demonstrate different SAG1 population and to differentiate between SAG1 localisation on the surface and within the vesicles (61,210).

2.1.1 Fluidity and Dynamics of SAG1-Halo in Intracellular Parasites Showing the Ability of SAG1 as a Proxy

To analyse the dynamics of the parasite PM within a PV, the suitability of SAG1-Halo as a membrane proxy was investigated by FRAP (fluorescence recovery after photobleaching)

(113,233). FRAP involves selectively bleaching a pre-set area for a given duration to deplete the fluorescent signal in the chosen region. After bleaching, the fluorescence recovery of the protein is measured, providing insights into the lateral diffusion of the protein on the membrane. Rapid recovery typically occurs in eukaryotic cells for cytosolic proteins or membrane-anchored lipids that can move freely within the membrane (233). Conversely, if the protein is part of a bound complex, stationary, or not rapidly diffusing, the recovery will be slow or negligible (113,233).

In this study, SAG1-Halo parasites were intracellularly labelled with Oregon Green (OG), a membrane-permeable (MP) dye, and subjected to FRAP to analyse SAG1-Halo signal recovery. Initially, FRAP was performed on a single parasite targeting a small area of the PM (Figure 13A). The signal intensity at the PM was recorded at two positions: the bleached region (A1), representing the region of interest, and the opposite unbleached region (A2), serving as a reference to monitor PM changes.

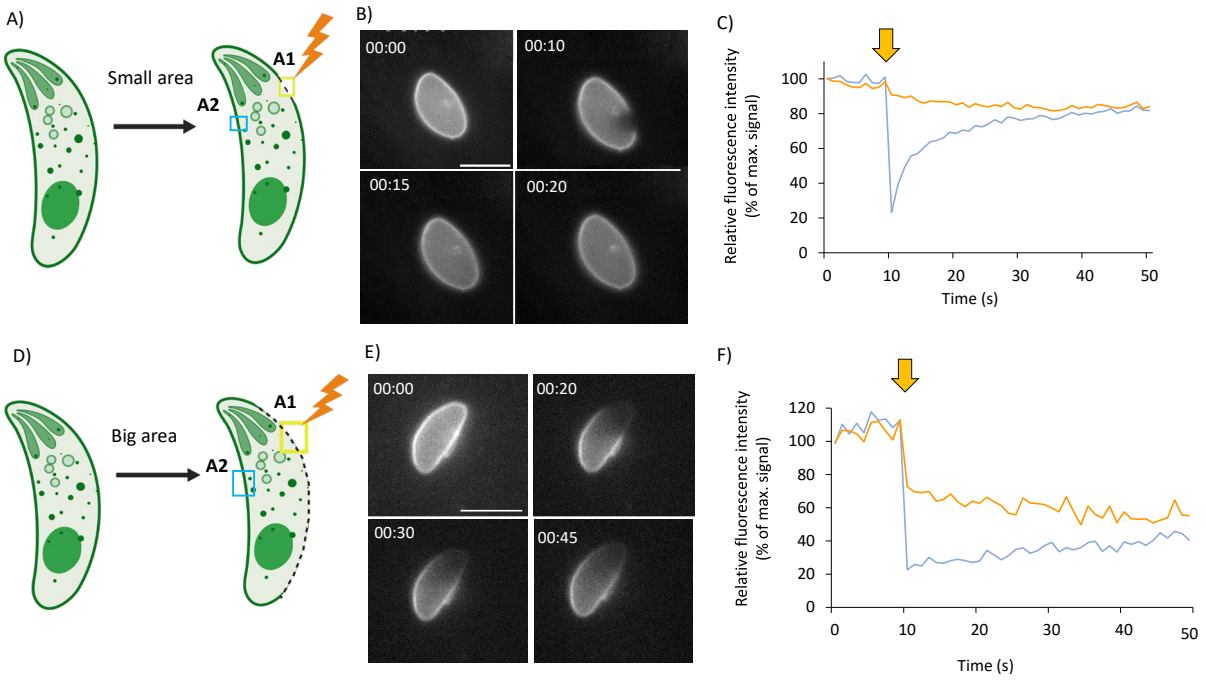

Figure 13: ***Single-Parasite FRAP****.* ***A)*** *Schematic of the FRAP setup, showing the bleached FRAP area (A1) and the opposite non-bleached area (A2) as a control.* ***B)*** *Live parasite images illustrating the FRAP time course in single parasites.* ***C)*** *FRAP and control curves display fluorescence intensity of SAG1-Halo in the FRAP region (A1) over 60 seconds and the unaffected control area (A2), respectively.* ***D)*** *Schematic representation of a large-area FRAP in a single parasite.* ***E)*** *FRAP images showing the parasite before bleaching, immediately after bleaching, and up to 45 seconds post-bleaching****. F)*** *FRAP analysis revealed slower recovery over 50 seconds for the large-area FRAP compared to the small-area FRAP, while the control area remained unaffected. Created with BioRender. Scale bar: 5 µm.*

To normalise the data, the PM signal intensity of another parasite in the field of view (not bleached) was recorded. For FRAP, signal intensity was measured briefly before bleaching and during recovery over 50 seconds. Three experiments were analysed, and all bleached parasites were normalised to the control parasite to account for photobleaching effects during recording.

Bleaching of the small area resulted in a significant decrease in PM signal intensity, dropping to ~30% of the initial fluorescence. Recovery was rapid, with the signal returning to ~80% of the initial intensity within 20 seconds. Interestingly, the signal intensity at the opposite side of the parasite (A2) also decreased, reaching ~80% of the initial intensity, consistent with the bleached region. The FRAP curve indicated an even distribution of fluorescence across the membrane, demonstrating that SAG1-Halo is dynamic and diffuse freely within the PM.

To validate the rapid recovery observed in small-area FRAP and investigate whether diffusion across the entire PM influences recovery dynamics, a large-area FRAP was performed (Figure 13D). After bleaching a large area, the fluorescence recovery was significantly slower than in the small-area FRAP (Figuer13C and F). During the observed 50 seconds, recovery reached ~44% of the initial fluorescence intensity. Notably, the unbleached side of the parasite exhibited a decrease of ~43% to 57%, which was a larger reduction in total membrane fluorescence compared to the decrease to~80% observed in small-area FRAP. As expected, bleaching a larger region eradicated more SAG1 fluorescence signal, resulting in broader diffusion of the remaining SAG1 and slower recovery. This is reflected in the reduced fluorescence in both sides of the parasite (Figure 13F) and prolonged recovery time, underscoring the dynamic behaviour of SAG1 in the membrane and its ability to diffuse across the entire membrane surface.

These findings highlight the potential to use SAG1 as a membrane proxy for analysing plasma membrane dynamics. However, the data also indicate limitations in recovery rates when larger membrane regions are bleached (234).

2.1.2 SAG1 Diffuses Between Connected Daughter Parasites Within the Parasitophorous Vacuole

To determine whether connections to daughter cells and the size of the FRAP area influence membrane flow between parasites within a PV, FRAP experiments were conducted using on intracellular parasites in the 2-cell stage. Parasites in a PV are connected via the residual body (235–237). Previous studies demonstrated that cytosolic GFP can diffuse between parasites in the same vacuole through connections at the basal body (238,239). This connection can be observed using electron microscopy (Figure 14A) and fluorescence microscopy (Figure14B and C). Figure 14 demonstrate that parasites are connected via a PM bridge containing F-actin filaments, which colocalise with SAG1-Halo in 93% of cases. This connection over the residual body is maintained during replication.

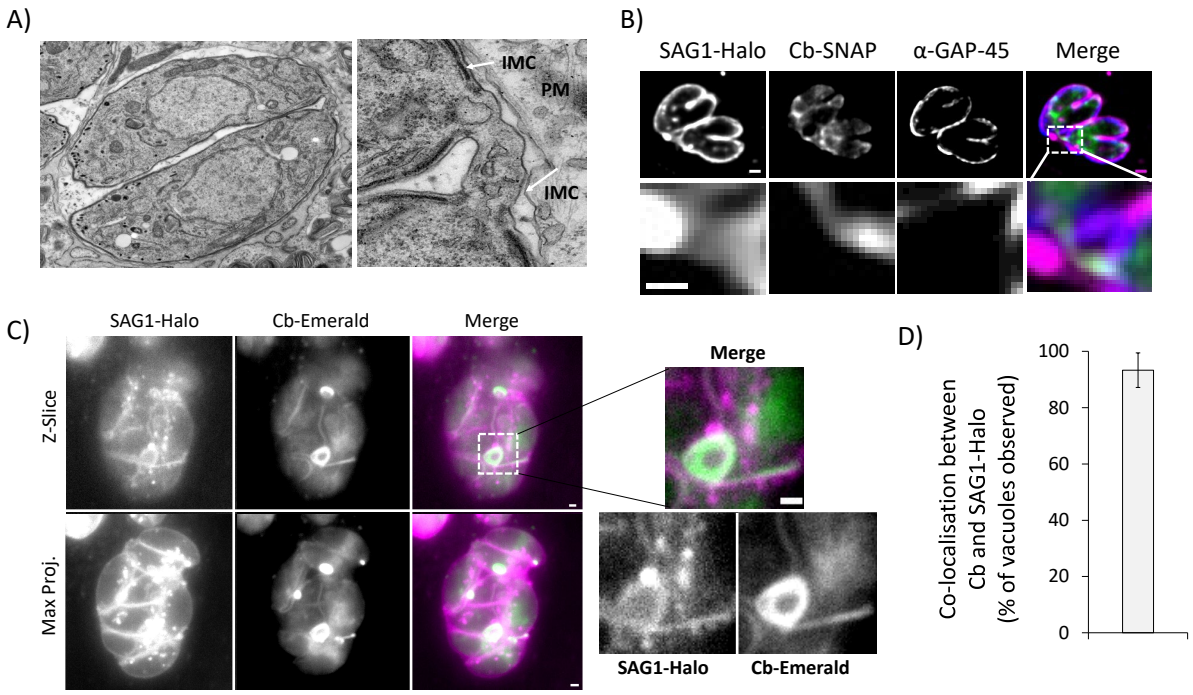

Figure 14: ***Connections in replicating parasites****.* ***A)*** *Electron microscopy image showing parasites in a PV connected via the PM.* ***B)*** *Immunofluorescence images showing SAG1-Halo, actin (CB-SNAP), and the Inner Membrane Complex (anti-GAP-45). GAP45 is shown to be absent in the residual body.* ***C)*** *SAG1 Halo and Cb-Emerald highlight colocalisation of the PM and actin filaments at the residual body* ***D)*** *SAG1-Halo and CB-Emerald colocalises in all parasites (100% colocalisation). Scale bars :1 µm.*

To explore SAG1 membrane dynamics, FRAP was performed on one of two connected parasites, targeting either a small or large area of the plasma membrane. The second parasite served as a control for fluorescence intensity (Figure 15A).

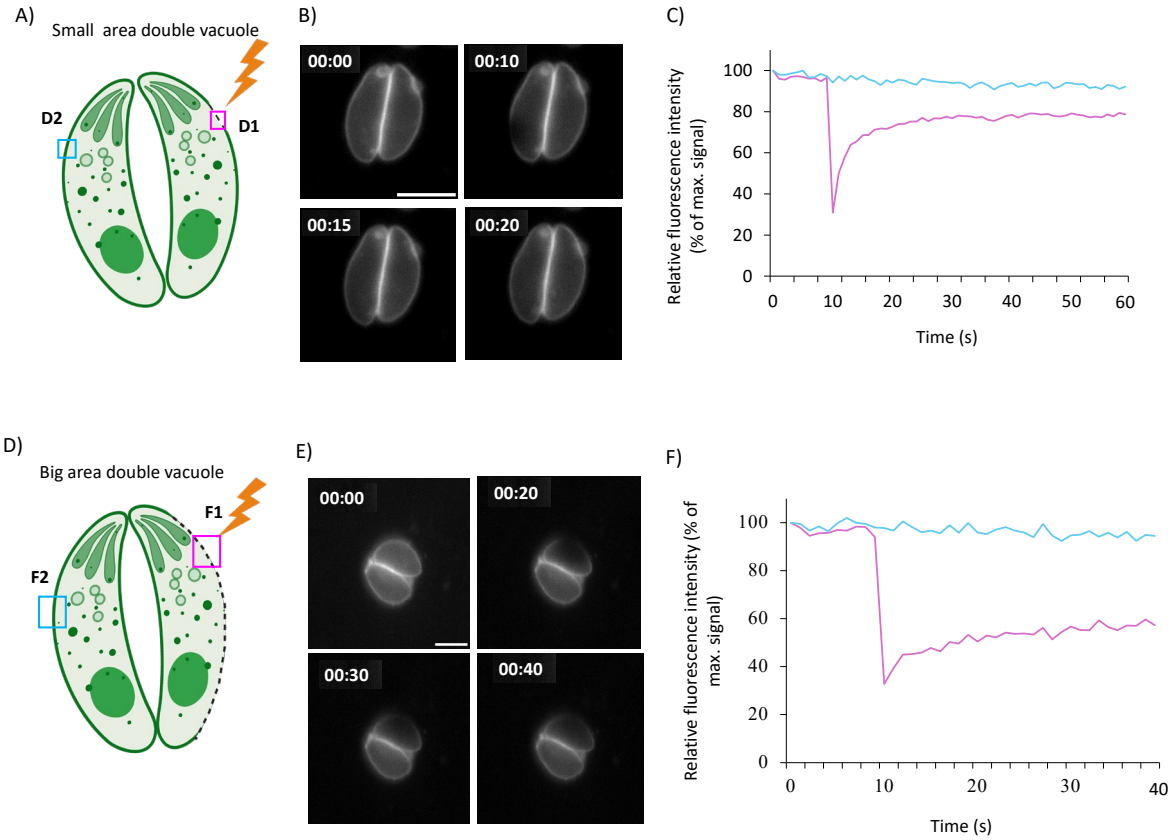

Figure 15: ***Double-stage parasite FRAP. A)*** *Schematic of a double vacuole showing the small FRAP area (D1) and control region (D2).* ***B)*** *Live-cell images of parasites before FRAP, at the FRAP point, and during recovery over 20 seconds .****C)*** *FRAP curves showing 80% recovery of fluorescence, as observed for single parasites in 20 seconds.* ***D)*** *Schematic of a large FRAP area (F1) with a control region (F2).* ***E)*** *Live-cell images of large-area FRAP showing recovery over 40 seconds.* ***F)*** *FRAP curves showing slower recovery of the large-area FRAP (to ~60%) while the control region remained unaffected. Recovery time shows to be elongated until the observed 40 seconds. Created with BioRender Scale bar :5 µm.*

In small-area FRAP, fluorescence recovery reached ~80% within 15–20 seconds, consistent with results from single parasites. The second parasite exhibited no significant decrease in fluorescence intensity. However, the small FRAP area may have been insufficient to impact the second parasite, as unbleached SAG1 could balance the fluorescence signal.

To further assess the effects of larger membrane bleach, a large-area FRAP was performed, targeting half of the parasite's membrane (Figure 15D). Recovery in the bleached parasite occurred more slowly, requiring ~40 seconds to reach ~60% of the initial fluorescence intensity. The control parasite remained unaffected, indicating restricted membrane flow between the two parasites.

To examine whether membrane diffusion time increases with parasite number and connection complexity, FRAP combined with FLIP was performed on parasites within 8-stage

vacuoles and 4-stage vacuole. Using a confocal microscope, half of the vacuole was continuously bleached following an initial FRAP, while the remaining parasites were left untouched (Figure 16A). This illustrates membrane flow between individual parasites interconnected by membrane bridges (Figure 14) and basal body connections.

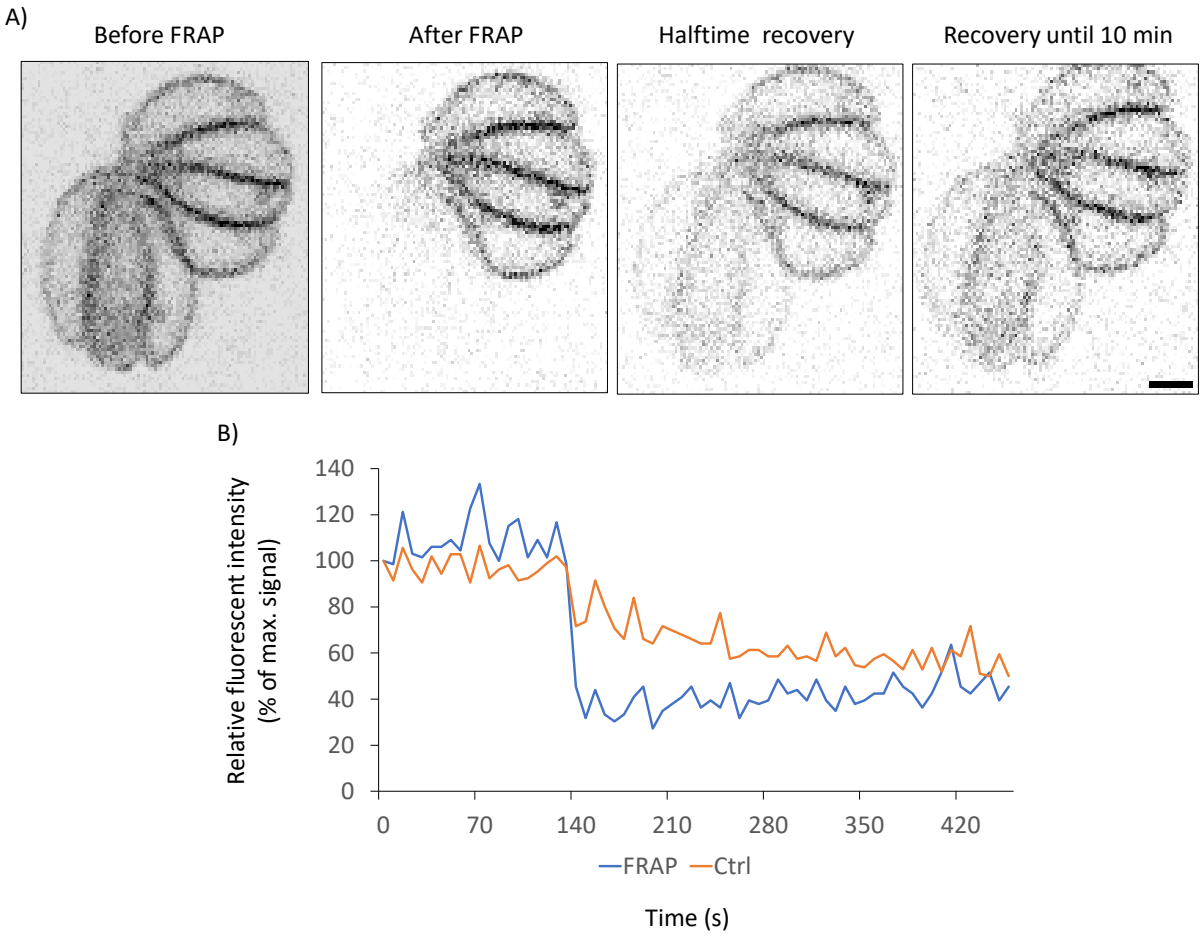

Figure 16: ***Confocal FRAP/FLIP Approach****.* ***A)*** *Eight-stage vacuole before bleaching half of the vacuole. Recovery was recorded immediately after bleaching and monitored over 10 minutes.* ***B)*** *Quantification of FRAP curves for the bleached and control regions in 8-stage vacuoles, showing the recovery of the FRAP area and diminishing fluorescence intensity in the control area over 10 minutes. Scale bar:2 µm. (Single experiment; data not statistically significant. Images were taken every 5 seconds).*

In 8-stage vacuoles, fluorescence recovery in bleached parasites was significantly slower, requiring over 10 minutes to reach measurable levels. Simultaneously, fluorescence in the unbleached regions decreased gradually, suggesting limited diffusion of SAG1 across the vacuole (Figure 16A-B). This observation indicates that as more parasites become connected, membrane flow is increasingly constrained, likely due to elongation and increased resistance within the basal body connections. Further aberrant connections (Figure 17) showed no recovery and distinct FRAP curves then parasites with an organised connection.

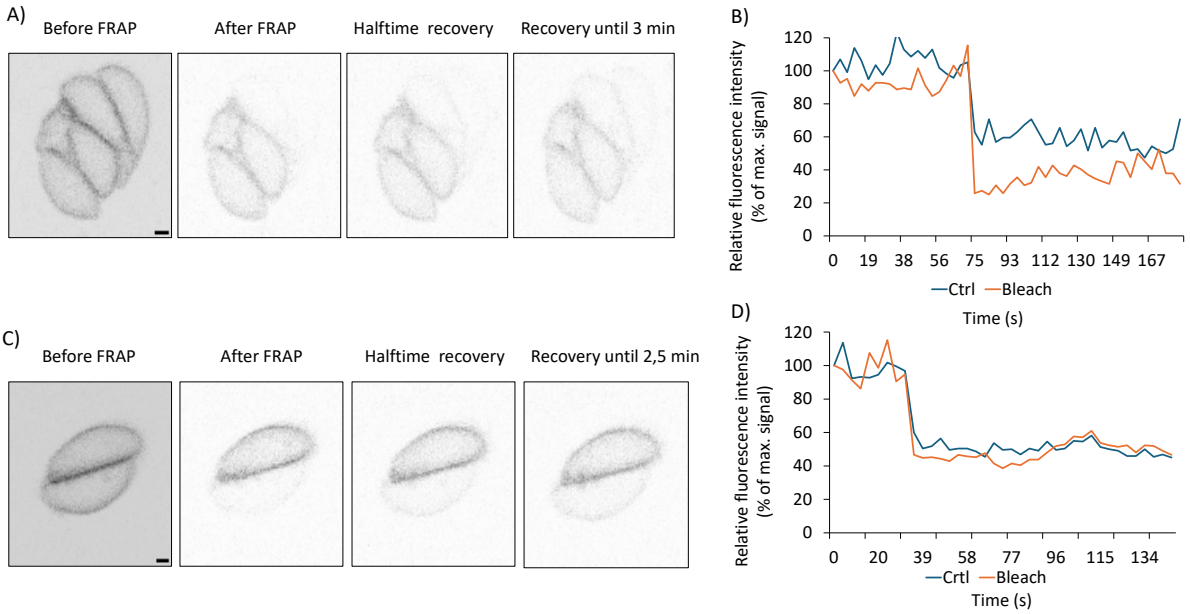

Figure 17 : ***Disorganised FRAP in 4-stage and 2-stage vacuoles. A)*** *FRAP of a 4-stage vacuole shows minimal recovery over three minutes.* ***B)*** *The control decreases to 60%, with recovery reaching 40% within three minutes.* ***C)*** *FRAP of a 2-stage vacuole shows slow recovery over 2.5 minutes.* ***D)*** *Pre-FRAP statistics show no significant recovery, and the unbleached parasites are similar effected by the FRAP as the bleached on. Showing an equalisation of membrane fluorescents over time. Scale bars: 1 µm and 2 µm.*

These findings underscore the dynamic yet regulated nature of plasma membrane flow in *Toxoplasma gondii* within organised vacuoles. While SAG1 can diffuse rapidly across individual parasite membranes, its movement between connected parasites is significantly slower, particularly as the structural complexity of the vacuole increases.

2.1.3 Analysis of Plasma Membrane Dynamics During Replication

Following the demonstration that SAG1 is a reliable membrane proxy and that parasites remain connected via the plasma membrane after replication, the next objective was to investigate how the plasma membrane changes during this process.

The HaloTag system enables precise tracking of SAG1 during replication by utilising dyes with distinct physical properties: membrane-non-permeable (MNP) and membrane-permeable (MP) dyes. These dyes are applied sequentially to distinguish between membrane-bound and internal SAG1 populations (Figure 18). The MNP dye cannot cross the plasma membrane and

therefore labels only the surface-exposed SAG1. In contrast, the MP dye can diffuse across the membrane, enabling visualisation of both surface and internal SAG1.

This ligand-binding system ensures that the first dye fully saturates the available tagged protein, so the second dye binds exclusively to newly synthesised, previously unlabelled SAG1 (233). This approach allows detailed analysis of plasma membrane inheritance and dynamics during replication.

Classification of SAG1-Halo Sub-Populations

To dissect the plasma membrane distribution, five distinct SAG1-Halo sub-populations were defined (Figure 18):

1. **PM-SAG1**: SAG1-Halo localised to the parasite surface, representing the plasma membrane exposed to the extracellular environment.
2. **Int-SAG1**: Internal SAG1 within vesicles, representing membrane not yet delivered to the PM.
3. **M-SAG1**: Maternal plasma membrane, including regions inherited from the mother cell prior to replication.
4. **n-SAG1**: Newly synthesised plasma membrane generated *de novo* during replication.
5. **Endo-SAG1**: Internalised (endocytosed) plasma membrane existing as vesicles within the parasite cytoplasm.

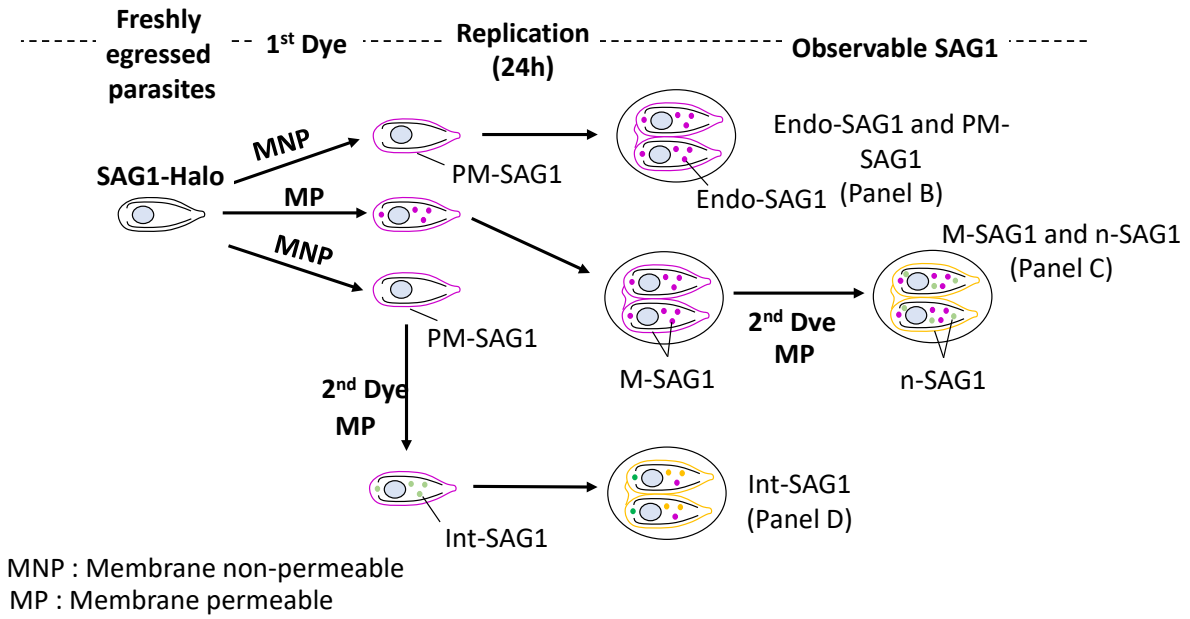

Figure 18: ***Staining strategy to investigate different SAG1 populations in extracellular and replicating parasites SAG1-Halo is labelled using three distinct strategies****:* ***MNP Labelling****: The membrane-non-permeable (MNP) dye labels the plasma membrane before replication. After replication, internalised SAG1 vesicles are highlighted as Endo-SAG1 (endocytosed SAG1).* ***MP labelling for M and n-SAG1****: The MP dye labels the plasma membrane and intracellular SAG1 from the M-SAG1. A second MP dye applied after replication labels the n-SAG1.* ***Sequential MNP and MP labelling****: The MNP dye initially labels the PM-SAG1. Following thorough washing, the second MP dye labels Int-SAG1. After replication, this strategy distinguishes between Endo-SAG1 and Int-SAG1.*

Labelling Strategies for Plasma Membrane Dynamics

1. PM-SAG1 and Endo-SAG1 (Membrane Inheritance and Endocytosis)

To study plasma membrane inheritance and endocytosis, parasites were labelled with an MNP dye for 1 hour, which exclusively marked the surface PM-SAG1. After washing and initiating replication, membrane distribution was monitored. Portions of the plasma membrane were observed to internalise into vesicles, classified as Endo-SAG1, representing endocytosed PM.

2. M-SAG1 and n-SAG1 (Maternal and Newly Synthesised Plasma Membrane)

To label newly synthesised SAG1, parasites were first incubated with an MP dye for 1 hour to label the M-SAG1. After replication, a second round of MP dye labelling was applied to mark n-SAG1. This approach enabled clear distinction between inherited maternal membrane and de novo synthesised plasma membrane during replication.

3. Int-SAG1 (Internal Plasma Membrane Reservoirs)

To identify internal plasma membrane reservoirs, a double-labelling strategy was used. The mother parasite's plasma membrane was initially labelled and saturated with an MNP dye for 1 hour, followed by three washes to remove excess dye. A second labelling step was then performed using the MP dye, which marked the internal SAG1 population, including endocytosed vesicles and other Int-SAG1.

2.1.3.1 Maternal PM SAG1 Inheritance by the Daughters

The fate of the maternal PM during replication was first investigated by quantifying the fluorescence intensity of PM-SAG1 at different replication stages.

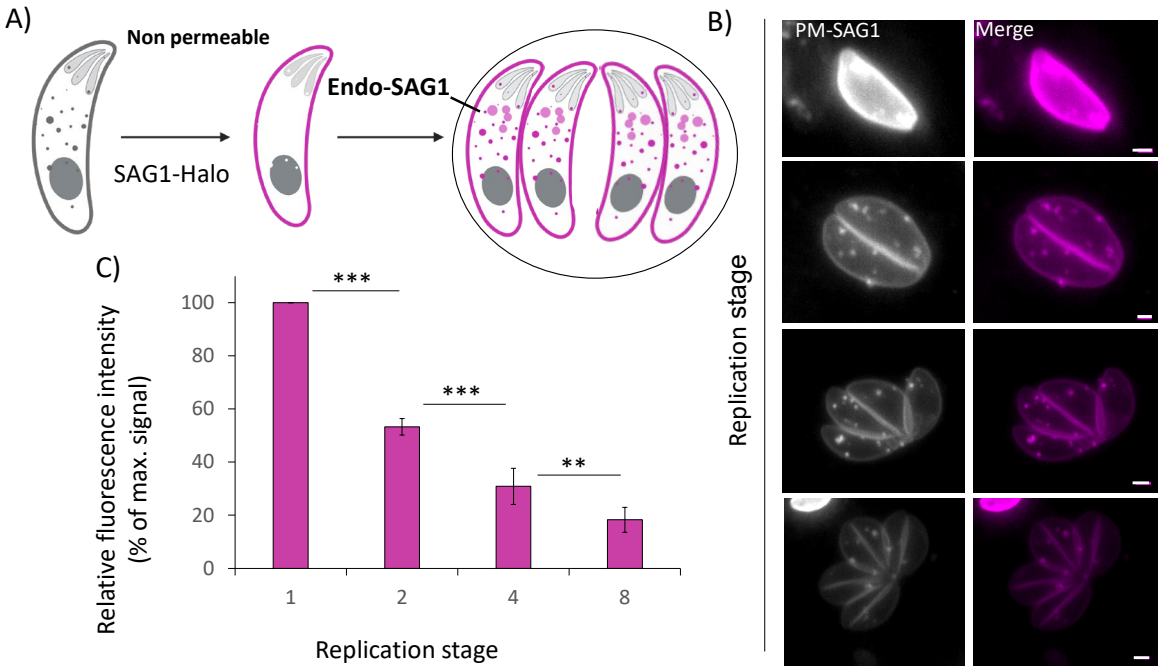

Figure 19: ***PM replication during parasite division. A)*** *Schematic representation of maternal (endo)-SAG1 during replication.* ***B)*** *Live-cell image showing the PM signal in replicating parasites labelled with the MNP dye, demonstrating a diminution of fluorescence during replication.* ***C)*** *Quantification of PM-SAG1 fluorescence intensity reveals a reduction to ~20% in eight-stage vacuoles. Created via BioRender Scale bar: 1 µm. ***p<0.001, **p<0.01.*

The relative fluorescence intensity of PM-SAG1 decreased progressively with each replication step (Figure 19B). In freshly invaded single-stage parasites, the fluorescence intensity was defined as 100%. This intensity dropped to approximately 50% in two-stage parasites, 25% in four-stage parasites, and 20% in eight-stage parasites (Figure 19C). Following a ~twofold

decrease with each round of daughter formation. These results suggest that daughter cells inherit the maternal PM in its entirety during each replication step.

2.1.3.2 De Novo SAG1 Complements PM Inheritance During Replication

In addition to PM inheritance, de novo of SAG1 will be integrated in the PM and is required to meet the increasing membrane demands during replication. To distinguish between maternal SAG1 (M-SAG1) and new SAG1 (n-SAG1), two sequential membranes permeable (MP) dye labelling steps were applied.

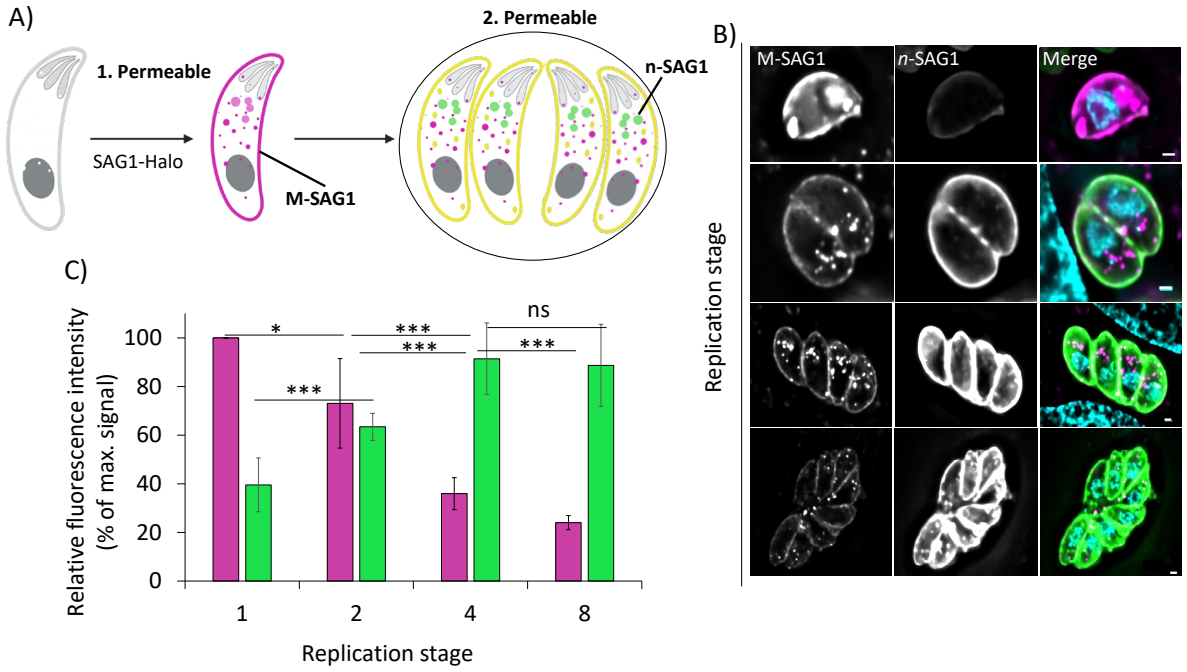

Figure 20: ***De novo SAG1 integration into the PM during replication****. **A)** Schematic representation of sequential MP labelling to differentiate M-SAG1 and n-SAG1. **B)** Live-cell images showing the M-SAG1 signal and n- SAG1. Revealing the reduced fluorescent signal in M-SAG1 while the fluorescents of n-SAG1 increases. **C)** Quantification of fluorescence intensity shows a slower decrease in M-SAG1 compared to PM-SAG1, while n-SAG1 signal increases and saturates at ~90% in four-stage vacuoles. Created with BioRender Scale bar: 1 µm. ***p<0.001, **p<0.01, *p<0.05, ns: non-significant.*

The fluorescence intensity of M-SAG1 followed a similar trend to PM-SAG1, decreasing from 100% in single-stage parasites to 70% in two-stage parasites, 40% in four-stage parasites, and 24% in eight-stage vacuoles (Figure 20C).

In contrast, n-SAG1 production began prior to replication. In single-stage parasites, n-SAG1 fluorescence intensity reached 40% and increased to 60% in two-stage parasites, eventually saturating at ~90% in four-stage vacuoles. Beyond this point, the signal remained stable,

reaching 91% in four-stage vacuoles and 88% in eight-stage vacuoles. These observations suggest that the plasma membrane of daughter cells is derived from the mother cell and formed de novo from internal SAG1 during replication.

2.1.3.3 Internal PM Reservoirs (Int-SAG1) Are Secreted During Replication

The M-SAG1 is composed of both PM-SAG1 and Int-SAG1. To investigate the role of Int-SAG1 during replication, the maternal plasma membrane and internal vesicles were labelled using a sequential MNP and MP dye strategy.

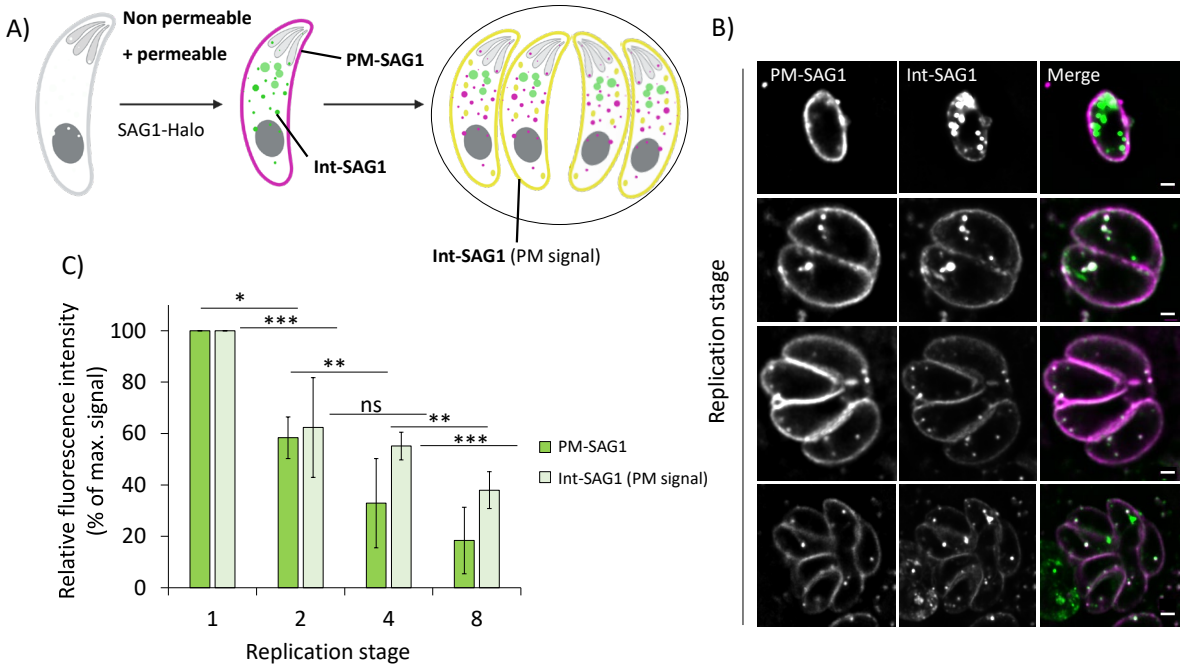

Figure 21: ***Internal PM reservoirs (Int-SAG1) during replication****. **A)** Schematic representation of internal SAG1 labelling. **B)** Live-cell images showing the reduction of PM-SAG1 and Int-SAG1 fluorescence during replication. **C)** Quantification of Int-SAG1 fluorescence shows a slower reduction compared to PM-SAG1, suggesting delivery to the plasma membrane. Created with BioRender. Scale bar: 1 µm. ***p<0.001, **p<0.01, *p<0.05.*

As previously observed, the surface PM-SAG1 intensity decreased with each replication step, confirming that the use of additional dyes did not interfere with the measurements (Figure 21B). Both Int-SAG1 and PM-SAG1 fluorescence intensities were reduced after each replication step. Int-SAG1 was detected both intracellularly and incorporated into the plasma membrane. A distinct difference in the inheritance patterns of PM-SAG1 and Int-SAG1 was also noted. Both Int-SAG1 and PM-SAG1 fluorescence decreased with each replication step. However, Int-SAG1 demonstrated a slower reduction. In two-stage vacuoles, ~60% of the Int-SAG1 fluorescence

signal was already detected at the plasma membrane. In four-stage vacuoles, the signal remained stable at ~55%, suggesting that internal SAG1 vesicles contribute to the plasma membrane SAG1 intensity even before replication begins. The progressive decline in fluorescence intensity of Int-SAG1 vesicles, from 100% in single-stage parasites to 58%, 32%, and finally 18% in eight-stage vacuoles, further supports the integration of internal membrane stocks to the plasma membrane.

These findings indicate that internal SAG1 reservoirs are delivered to the daughter cells and are subsequently integrated to the SAG1 stock at plasma membrane, contributing to its stability and slowing the decrease in fluorescence.

In summary, the fluidity and dynamics of the SAG1 were evaluated by FRAP experiments and confirmed that SAG1 is a good proxy for the analysis of membrane dynamics. In general the observed SAG1 fluidity at the membrane is consistent with measurements performed on other eukaryotic cells (233,240). In higher-stage vacuoles, SAG1 flow between parasites can vary, which could be due to the residual body acting as a bottleneck for diffusion of SAG1 proteins. Additionally, the complete inheritance of the old-SAG1 to daughter cells was visualised through the observed decrease in relative fluorescence signal with each doubling of parasites. Finally, the secretion and production of newly generated SAG1 were tracked, beginning in single-stage parasites and continuing throughout replication, until reaching a plateau of 90% relative fluorescence, satisfying the increased membrane requirements of the maturing daughter cells.

2.1.4 The Endo-Exocytosis Cycle and Secretion of Endocytosed Vesicles.

Following the demonstration that n-SAG1 and Int-SAG1 are secreted during replication, the next objective was to investigate whether an endo-exocytosis cycle exists in *Toxoplasma gondii* and whether endocytosed SAG1 (Endo-SAG1) is recycled and delivered back to the PM. Investigating the secretion of PM-SAG1 directly is challenging, as PM-SAG1 remains highly abundant at the plasma membrane, unlike Int-SAG1, which is predominantly vesicular following parasite invasion. Previous studies have shown that Int-SAG1 can be secreted and

deposited as trails behind extracellular parasites (210). To determine if secretion of endocytic material could also be detected in extracellular parasites, a trypsinisation assay was established to remove the PM-SAG1 signal selectively. Using this assay, parasites labelled with Endo-SAG1 vesicles were analysed for re-secretion (Figure 22).

Two parasite strains were used as controls:

1. **SAG1-Halo extracellular parasites**, freshly labelled with an MNP dye, served as a positive control for trypsin cleavage of extracellular PM-SAG1.
2. **IMC1-YFP-labelled parasites**, which express the inner membrane complex (IMC1) protein, served as a negative control. As IMC1 lies beneath the plasma membrane, it is expected to remain unaffected by trypsin treatment (241).
3. **Endo-SAG1,** labelled with MNP pre replication. Scratched and syringed before trypsinisation. Showed the presence of endocytosed vesicles after replication.

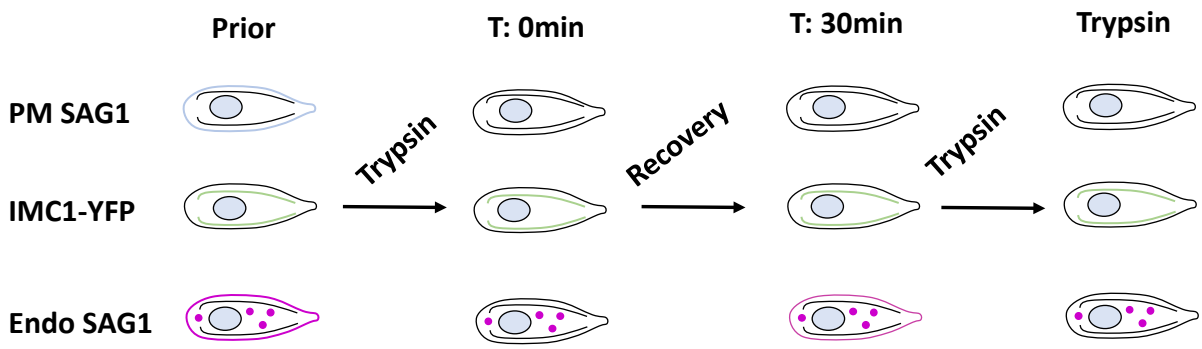

Figure 22: ***Schematic representation of the trypsinisation assay. A)*** *Schematic of trypsin treatment showing the labelling and measurement process before and after trypsinisation. Indicating the three different parasites used as well as the time course of the experiment. Pictures were taken prior trypsin and at 3 recovery timepoints until 30minuts when parasites were re-trypsinated.*

Trypsin treatment effectively cleaves extracellular plasma membrane proteins, including the external SAG1-HaloTag (241).

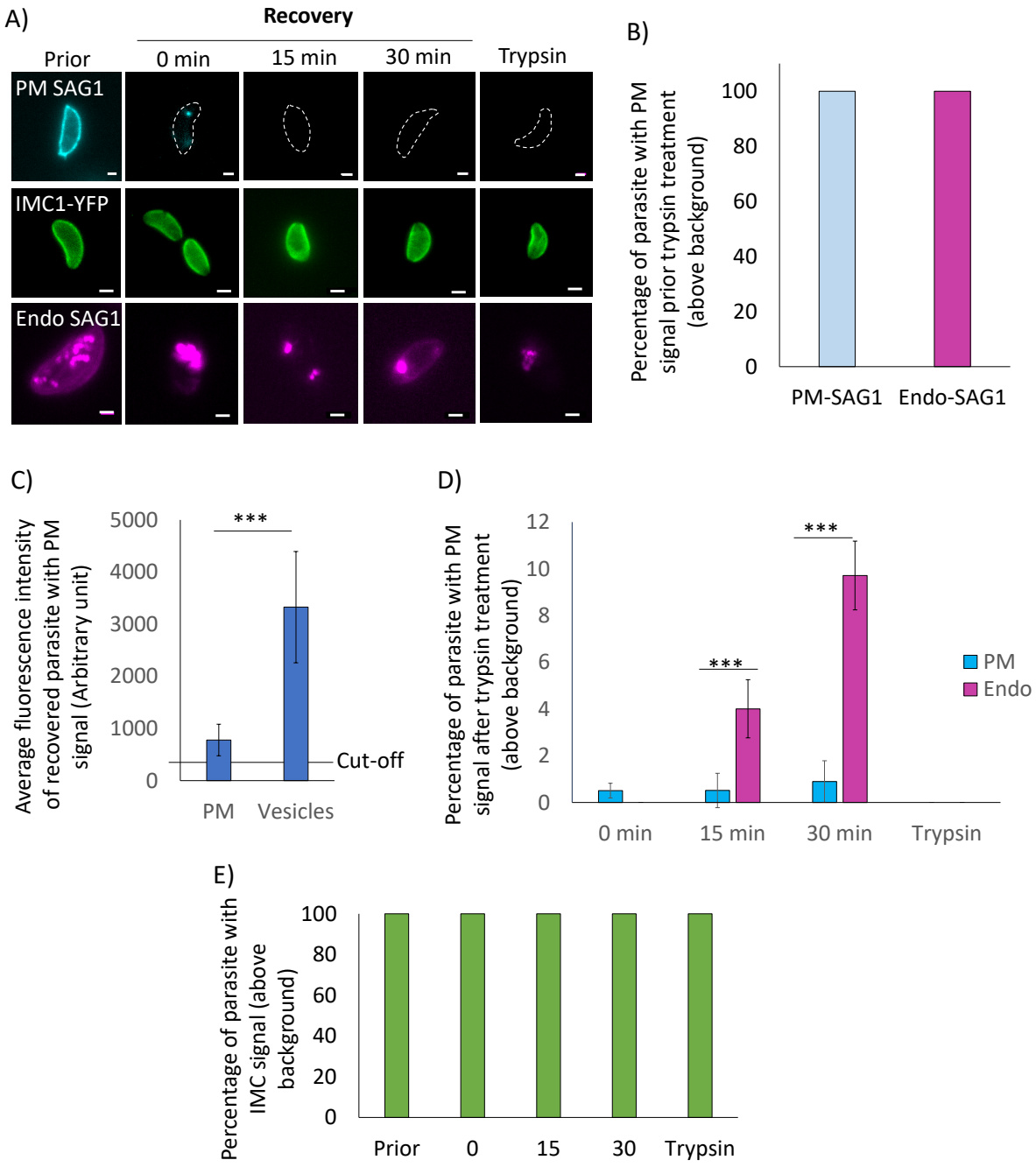

Figure 23: ***Trypsinisation assay A)*** *Schematic of trypsin treatment and recovery analysis.* ***B)*** *Percentage of parasites retaining PM signal before treatment. Showing no difference between Endo- and PM-SAG1 (100% on the surface of the parasites while internal SAG1 populations remain unaffected).* ***C)*** *Average fluorescence intensity of recovering parasites. Established for PM and Vesicles ~500 Arbitrary units* ***D)*** *Recovery of fluorescence in Endo-SAG1-labelled parasites, with no recovery in PM-SAG1-labelled parasites. Showing recover of 10% post trypsin PM intensity in End-Parasites* ***E)*** *IMC1-YFP control parasites showing no effect from trypsin treatment and remains at 100% of fluorescents intensity. Scale bar = 1 µm. ***p<0.001.*

Endocytosed vesicles, which are intracellular, remained unaffected by trypsin. Three differently labelled parasite groups were investigated using the trypsin assay (Figure 23). Fluorescence intensity measurements were recorded prior to treatment to establish baseline

values. Trypsin cleaved the extracellular SAG1-Halo tail, causing the fluorescence signal to vanish. As expected, IMC1-YFP-labelled parasites were unaffected by trypsin treatment and retained 100% of their fluorescence intensity (Figure 23E), since the IMC lies beneath the PM. PM SAG1 labelled parasites, showed no SAG1 signal following trypsinisation demonstrating the complete removal of surface-bound SAG1 (Figure 23D). To evaluate signal recovery, the average fluorescence intensity of the plasma membrane and vesicles was measured over a 30-minute recovery period. While PM-SAG1-labelled parasites showed no significant recovery during this time, Endo-SAG1-labelled parasites exhibited a 15% recovery of fluorescence intensity above the established threshold (Figure 23D). Re-trypsinisation after the recovery period resulted in the loss of the regained signal, confirming that the recovered fluorescence originated from the re-secretion of internalised SAG1-Halo vesicles to the plasma membrane.

Taken together these findings showed the re-recycling of endocytosed vesicle to the membrane in extracellular parasites. This provides further evidence for the presence of an endo-exocytotic cycle in *Toxoplasma gondii*, consistent with previous studies (210).

2.2 Trafficking of Plasma Membrane Vesicles

Investigation of membrane dynamics revealed a highly dynamic recycling and inheritance process during replication. This process enabled the visualisation of three distinct vesicle populations: PM/Endo-SAG1, Int-SAG1, and n-SAG1. Following the identification of these populations, the next step was to determine whether all three followed the same trafficking pathway within the parasite or utilised separate routes.

2.2.1 Intersection Between *de novo* and Recycling Pathways of SAG1

The trafficking routes and interconnection of the three distinct SAG1 populations were investigated, along with the role of the trans-Golgi network (TGN) and the plant-like vacuole compartment (PLVAC) in the endocytosis of SAG1 (242) were analysed next. Specifically, Int-SAG1 may represent a mixture of Endo-SAG1 and *n*-SAG1. It was hypothesised that if SAG1 recycling occurs, colocalisation would be observed between endocytosed SAG1 at the PM and Int-SAG1. In contrast, *n*-SAG1 would be expected to traffic independently.

To investigate whether endocytosed vesicles and newly generated vesicles share similar trafficking pathways, a triple-staining approach was developed. This method, based on sequential MNP and MP dye labelling, enabled the differentiation of:

- **Endocytosed PM-SAG1 vesicles** (labelled with MNP dye),
- **Old Int-SAG1 vesicles** (labelled with MP dye), and
- **Newly generated n-SAG1 vesicles** (labelled with MP dye).

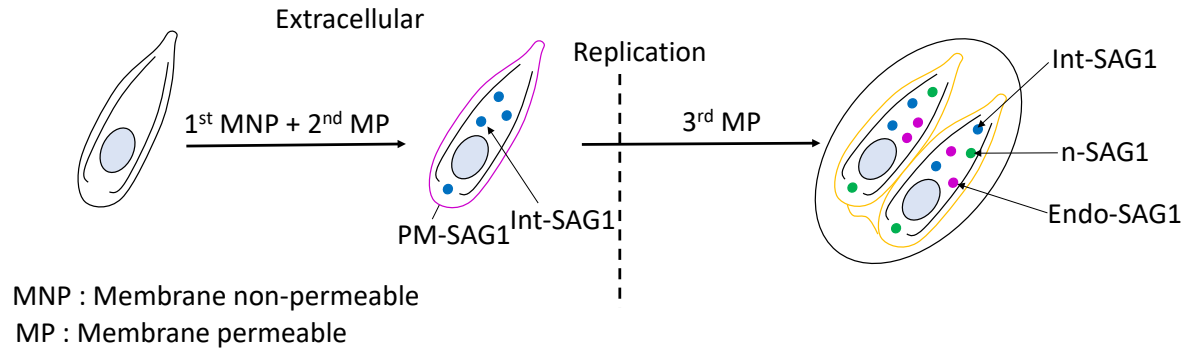

Figure 24: ***Schematic representation of the triple-labelling experiment*** *Step 1: The plasma membrane was labelled with MNP dye to identify endocytosed SAG1 (Endo-SAG1). Step2: Internalised Int-SAG1 vesicles were labelled with MP dye. Step3: Following replication, newly synthesised SAG1 (n-SAG1) was labelled with another MP dye.*

This triple-labelling strategy allowed the individual analysis of the three vesicle populations and their relationships.

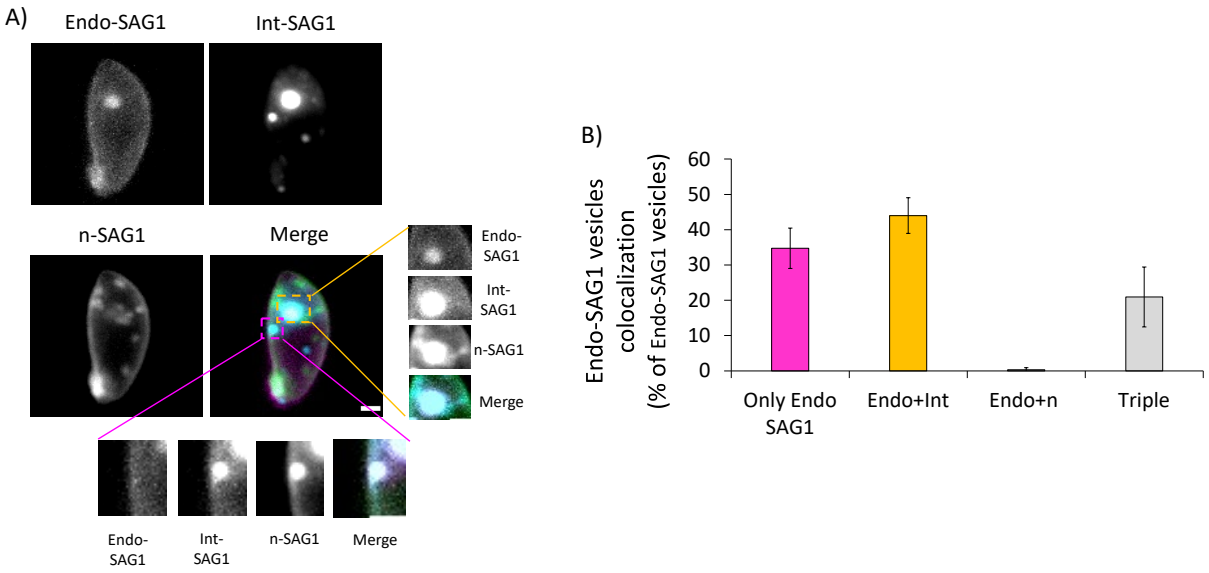

Figure 25: ***Triple-staining analysis of SAG1 populations****:* ***A)*** *Live-cell images showing individually labelled SAG1 populations: Endo-SAG1, Int-SAG1, n-SAG1, and their merged signals.* ***B)*** *Quantitative analysis of vesicle colocalisation. A total of 225 Endo-SAG1, 722 Int-SAG1 and 337 n-SAG1 were observed. Analysed were the different co-localisations of the Endo-SAG1 vesicles: single signal (Endo only), double signal (Endo-Int or Endo-n) and triple signal (Endo-Int-n), which amount to the totality of the Endo-SAG1 vesicles Triple staining revealed an overlap of ~15% for all three populations, with no significant colocalisation observed between Endo-SAG1 and n-SAG1 vesicles. Scale bar:1 µm.*

Quantitative analysis revealed the following levels of colocalization. The Endo-SAG1 and Int-SAG1 exhibited ~44% colocalisation, suggesting some overlap between endocytosed SAG1 and internal SAG1 reservoirs, whereas Endo-SAG1 and *n*-SAG1 did not display significant colocalization (Figure 25B), indicating that *de novo* synthesised SAG1 follows an independent trafficking route. Triple staining revealed ~20% overall colocalisation, suggesting that the three populations may intersect during trafficking to the plasma membrane. Alternatively, it is possible that a subset of *n*-SAG1 could be recycled and re-secreted.

The observed lack of significant overlap between Endo-SAG1 and *n*-SAG1 populations supports the hypothesis that endocytosed SAG1 and *de novo* synthesised SAG1 are at least initially trafficked independently and later merge to use the same pathway for delivery to the PM. In contrast, the partial overlap between Endo-SAG1 and Int-SAG1 suggests that these populations share a degree of connectivity, potentially reflecting a recycling mechanism.

The analysis of SAG1 trafficking pathways highlights the complexity of vesicle dynamics in *Toxoplasma gondii*. While Endo-SAG1 and Int-SAG1 partially colocalise at certain instances to be recycled back to the plasma membrane (PM), n-SAG1 appears to traffic independently, supporting the presence of distinct pathways for recycling and secretion. Endocytosed

material from the plasma membrane might be delivered to the trans-Golgi network, where interaction with n-SAG1 could occur. Here at the TGN, the different SAG1 populations could follow the same routes to the plasma membrane, as highlighted by the partial overlap observed in the triple labelling assay. To further analyse these hypotheses, colocalisation with marker proteins for the TGN and different known routes were examined in the following sections.

2.2.2 Investigation of SAG1 Vesicle Trafficking Pathway

To explore the trafficking routes of SAG1 vesicles and identify potential proteins or structures involved in SAG1 endocytosis, colocalisation assays were performed using selected marker proteins known for their roles in trafficking or association with proposed entry and exit points of endocytic pathways.

2.2.2.1 Marker Proteins

The marker proteins were chosen based on their known roles in vesicle trafficking, localisation, and involvement in endocytosis and exocytosis pathways. Rab5a and Rab5b are small GTPases involved in early endosomal vesicle trafficking in eukaryotic cells, and their homologues have been characterised in *Plasmodium* parasites. These proteins were chosen as potential candidates for vesicle trafficking in *Toxoplasma gondii* (68,203,243,244). Specifically, Rab5b, a cytosolic protein, has been shown in *P. falciparum* to regulate endocytosis and haemoglobin uptake at the cytostome, a structure specialised for nutrient uptake (68,203). The dense granule protein GRA2 was selected as a marker for the dense granules, unique secretory organelles found in apicomplexan parasites. Dense granule proteins are trafficked through the Golgi apparatus to the apical region of the parasite prior to secretion, where thy play a role in PV organisation and structure (53,245,246). TgTEP, a trans-Golgi network (TGN) protein, was used to highlight the Golgi trafficking pathway in *T. gondii* (247). ISAP1 and DrpC were chosen as markers associated with the micropore, a structure thought to mediate endocytosis in apicomplexan parasites. These proteins were considered as potential markers for endocytic entry points, given their localisation to the micropore in previous studies (62,248). Previous work by Koreny et al. demonstrated that

knockdown of K13 inhibited the endocytosis of SAG1, suggesting that the K13 micropore might facilitate PM internalisation. AAP3, a protein localised to the apical annuli, was selected as a marker for vesicle exit points. The apical annuli are recognised sites of exocytosis in *T. gondii*, known for mediating GRA protein export during host cell invasion and PV formation (53,56,249).

All marker proteins were YFP-tagged in a SAG1-Halo background, and integration was validated through fluorescence microscopy and integration PCR.

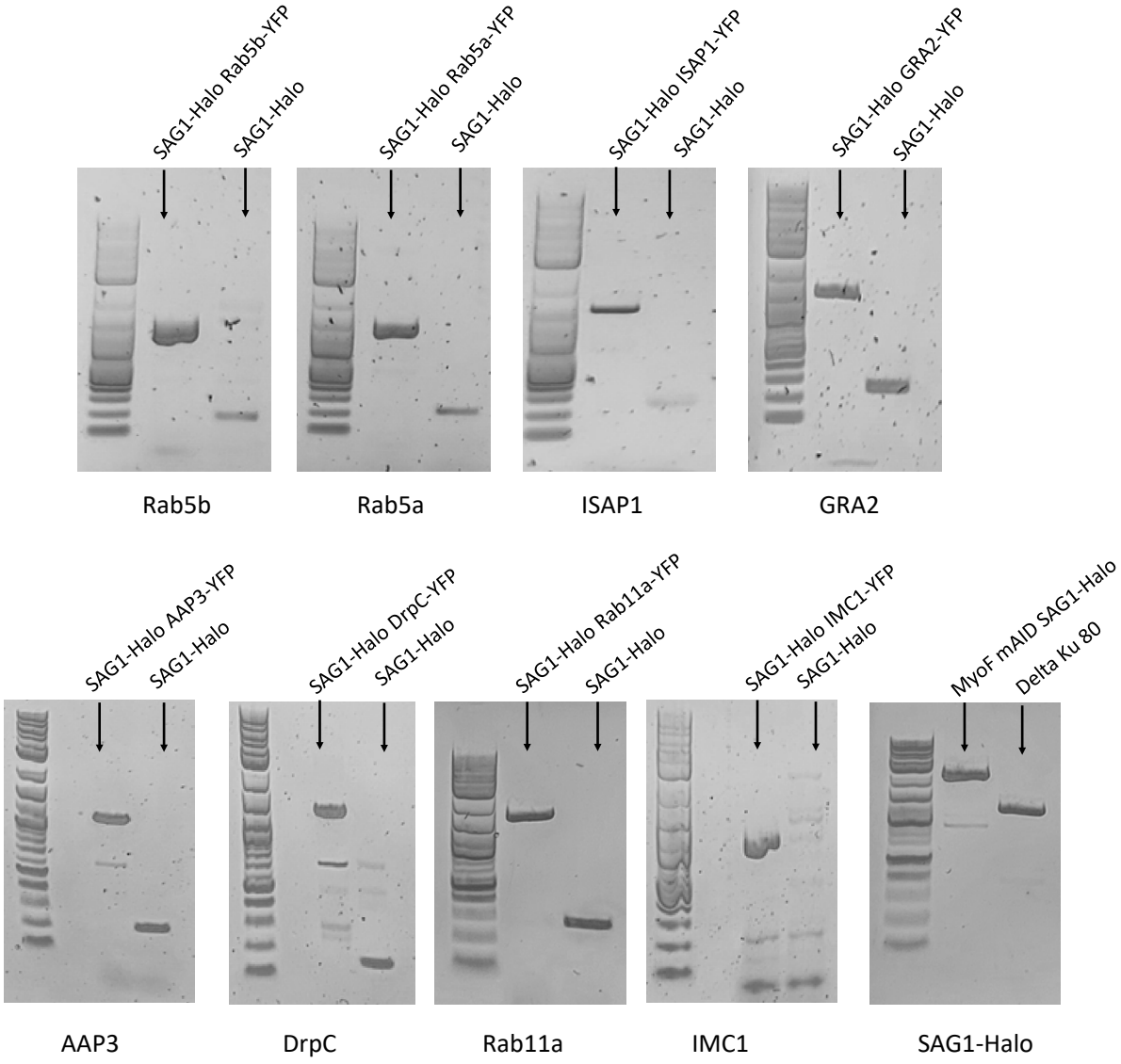

Figure 26: ***Genotyping of YFP-tagged parasites****. From left to right: Rab5b, Rab5a, ISAP1, GRA2, AAP3, DrpC, Rab11a, IMC1, and SAG1 Halo in the MyoF mAID strain. A significant YFP band of ~800 bp is observed. For SAG1 Halo primers were designed further apart, resulting in a YFP band of ~2 kb, and without YFP, a band of ~1 kb.*

2.2.3 Co-localisation with Marker Proteins and Pathways

For colocalisation assays, SAG1-Halo parasites were labelled with a membrane-non-permeable (MNP) dye and allowed to replicate for 24 hours.

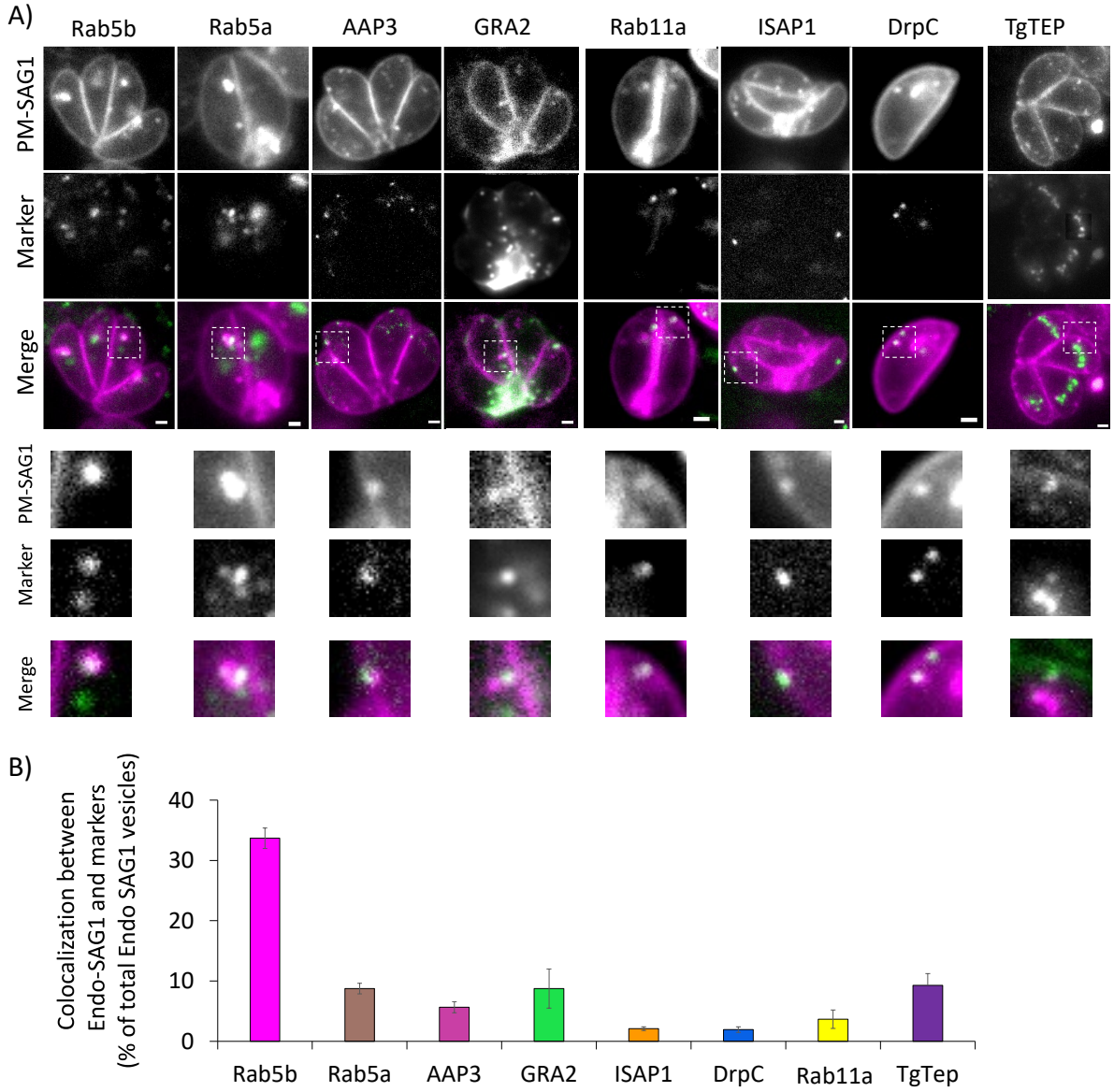

Figure 27: ***Colocalisation analysis of SAG1 vesicles with marker proteins A)*** *Live-cell images showing colocalisation of endocytosed PM-SAG1 (labelled with MNP) and YFP-tagged marker proteins. Zoomed in on colocalization of SAG1 Halo and the YFP marker signal.* ***B)*** *Quantitative analysis of colocalisation highlights the highest overlap between SAG1 vesicles and Rab5b and absence of colocalisation with other proteins. Scale bar: 1 µm.*

Colocalisation analysis with the selected markers revealed distinct levels of overlap with SAG1 vesicles (Figure 27A). ISAP1 and DrpC showed minimal colocalisation of ~2%, indicating limited interaction with SAG1 vesicles and suggesting that entry at the micropore is a fast and transient mechanism. AAP3 demonstrated ~5% colocalisation, suggesting a distinct trafficking of the SAG1 vesicles which is in agreement with the colocalisation found with the GRA2

vesicles here. GRA2 exhibited ~8% colocalisation, further pointing to a distinct trafficking of SAG1 independent of the dense granule secretion pathway. This suggests minimal overlap between SAG1 vesicle transport and the parasite's constitutive secretory system. TgTEP, the trans-Golgi marker showed ~9% colocalisation, indicating that the Golgi-ELC (early-late compartments) trafficking route does not significantly intersect with the SAG1 pathway. Rab5a and Rab11a: Both proteins showed minimal colocalisation (~8% for Rab5a and ~3% for Rab11a), indicating limited involvement in SAG1 vesicle trafficking. Rab5b exhibited the highest colocalisation (~33%) with SAG1 vesicles, suggesting a prominent role in SAG1 vesicle transport shown in Figure 27B.

Among the investigated candidates, Rab5b showed the highest degree of colocalisation with SAG1 vesicles, highlighting its potential role as a key trafficking factor for vesicle recycling in *Toxoplasma gondii*

2.3 Investigation Endocytosis: The Unique Role of Myosins

Following the investigation of SAG1 vesicle trafficking routes, it was necessary to identify motor proteins involved in the movement of endocytosed vesicles. Myosin F (MyoF) was chosen for analysis due to its conservation in apicomplexans (250) and its critical role in several trafficking pathways (245,251). A previously characterized MyoF-mAID strain, which allows knockdown of MyoF in an auxin-dependent manner, was endogenously tagged with SAG1-Halo and used in this study. To analyse endocytosis in the absence of MyoF, parasites were pre-treated with auxin to deplete MyoF. The induction time was selected based on Carmeille et al. (251). After labelling the parasites with MNP Alexa 488, the replication under auxin treatment was allowed to proceed 15 hours before analysis.

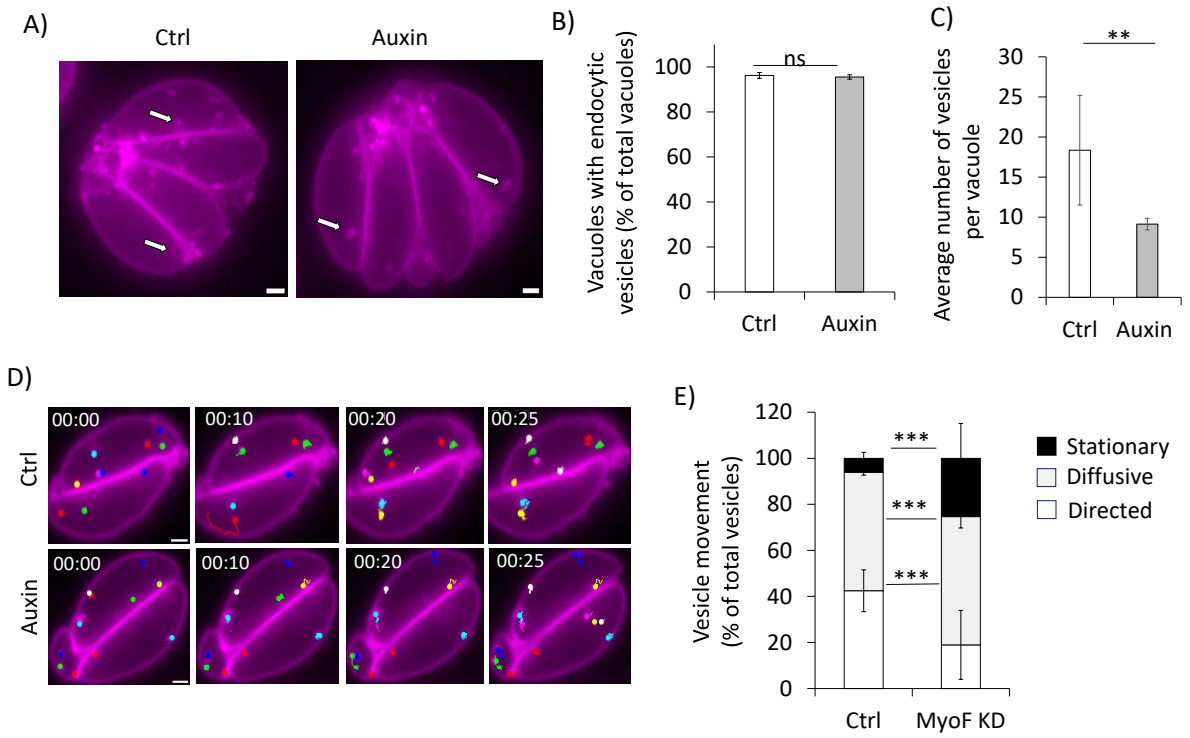

Figure 28: **Vesicle movement in the absence of MyoF A)** Live-cell images of 4-stage vacuoles (control and auxin-induced), showing a reduced vesicle count in the absence of MyoF .**B)** Statistical analysis showed the presence of endocytotic vesicles in all vacuoles analysed, both uninduced and induced. **C)** The average number of vesicles per vacuole indicates a reduction in endocytosed vesicles in the absence of MyoF. **D)** Vesicle tracking using ImageJ highlights increased stationary and twirling behaviour in auxin-induced parasites. A schematic illustrates vesicle movement within a 2-stage vacuole. **E)** Statistical analysis confirms an increase in stationary vesicles. *Scale bar: 1 µm. ***p < 0.001, **p < 0.01.*

A comparison between MyoF knockdown and uninduced parasites revealed no absence of endocytosed vesicles (Figure 28B). However, vesicles accumulated in the residual body, indicating that while endocytosis events still occurred, the vesicles were mis-trafficked. In control parasites, an average of ~18 vesicles per vacuole was observed, whereas in MyoF knockdown parasites, the number was reduced to ~10 vesicles per vacuole, suggesting a reduction in vesicle uptake in the absence of MyoF (Figure 28C).

To determine the role of MyoF in vesicle movement, MyoF knockdown (KD) parasites were compared to control parasites. In the absence of MyoF stationary vesicles increased from 6% in controls to 25% in induced parasites. Twirling behaviour was observed in ~55% of vesicles in induced parasites compared to ~51% in controls, showing a minor but measurable increase (Figure 28E). Free-moving vesicles decreased significantly from 47% in controls to 18% in induced parasites

These findings demonstrate the critical role of MyoF in endocytic vesicle movement, as its absence leads to vesicle mis-trafficking and reduced dynamics.

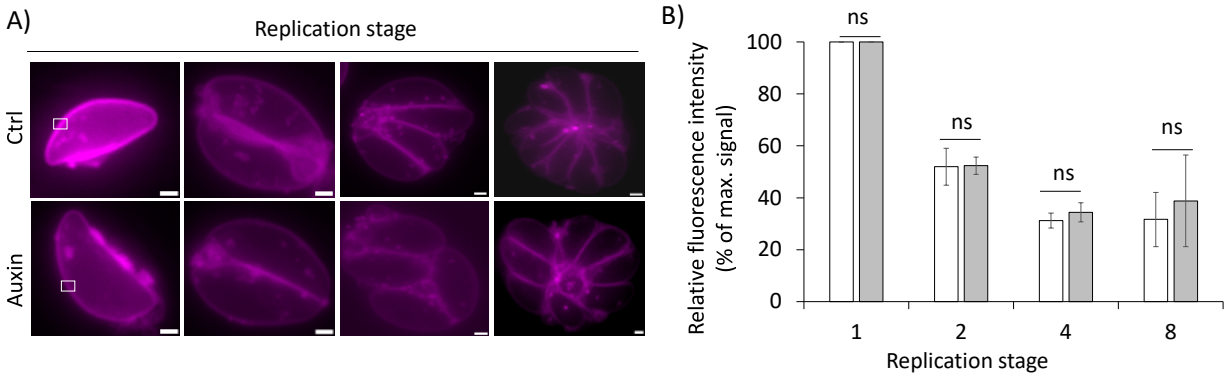

Figure 29: ***Membrane inheritance in the absence of MyoF****.* ***A)*** *Live-cell images showing membrane fluorescence (Alexa 488) across replication stages 1–8 for control and auxin-induced parasites. Note: Fewer vacuoles reached the 8-stage analysis due to slower or halted replication in MyoF knockdown parasites. Example of a ROI (region of interest) is indicated by the square in the single stage parasites. Measurements were always acquired on the membrane in all following replication steps with the same ROI* ***B)*** *Statistical analysis of fluorescence intensity during replication on the membrane reveals no significant difference between control and auxin-induced parasites. Scale bar :1 µm.*

Despite the observed defects in vesicle trafficking, MyoF depletion did not affect PM inheritance by daughter cells during replication (Figure 29A). The fluorescence signal in SAG1-Halo parasites followed the previously observed pattern of a two-fold reduction during each division step, in both control and auxin-induced parasites (Figure 29B). After confirming that MyoF impacts the movement of endocytosed vesicles but does not influence PM inheritance, a triple-labelling analysis was conducted to assess whether MyoF depletion alters the trafficking of distinct SAG1 sub-populations.

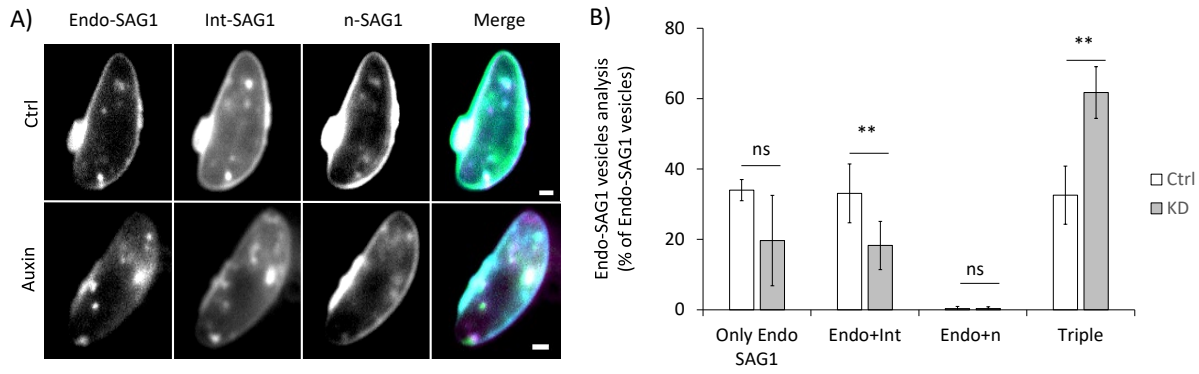

*Figure 30:**Triple labelling analysis of MyoF knockdown parasites A)** Live-cell images showing triple-labelling of Endo-SAG1, Int-SAG1, and n-SAG1 populations in control and auxin-induced parasites. **B)** Quantitative analysis reveals reduced colocalisation between Endo-SAG1 and Int-SAG1 vesicles in induced parasites, accompanied by increased triple colocalization. Scale bar: 1 µm. ***p<0.001, **p<0.01.*

The results showed a reduction in colocalisation between Endo-SAG1 and Int-SAG1 vesicles, decreasing from 40% in controls to 20% in MyoF knockdown parasites. Conversely, an increase in triple-labelled vesicles (Endo-SAG1, Int-SAG1, and n-SAG1) was observed, rising from ~40% in controls to ~60% in MyoF knockdown parasites (Figure 30). These findings suggest that MyoF depletion causes vesicle accumulation, resulting in increased overlap between n-SAG1, Endo-SAG1 and Int-SAG1.

Notably, the background strain (Tir1) used for the MyoF-mAID strain exhibited slower growth compared to the Δ80 DiCre SAG1-Halo strain. This reduced growth rate appeared to further influence vesicle movement and numbers, contributing to decreased vesicle dynamics and increased colocalisation due to slower vesicle trafficking.

The analysis of SAG1 vesicle trafficking demonstrated that MyoF plays a critical role in endocytosed vesicle movement. While endocytosis events still occurred, vesicles were mis-trafficked. MyoF depletion resulted in a significant reduction in free-moving vesicles and an increase in stationary vesicles. Interestingly, MyoF depletion did not impact plasma membrane inheritance during replication, as observed in both control and auxin-induced parasites. Triple-labelling analysis further revealed that MyoF knockdown alters the trafficking dynamics of SAG1 sub-populations, leading to increased colocalisation between newly synthesised and recycled vesicles.

These results highlight that the previously shown influence of MyoF on dense granule movement and microneme secretion, is now also demonstrated to play a key role vesicle trafficking of SAG1, establishing MyoF as a central motor protein for diverse trafficking events.

2.4 TgFLP2 and its Role in Vesicle Trafficking and Golgi Organisation

After investigating the molecular motors involved in endocytic vesicle trafficking, potential differences in membrane phospholipid composition were examined in collaboration with the Botté Laboratory. P4-ATPases are primarily responsible for mediating the translocation of phospholipids across membranes, a process essential for inducing membrane curvature and facilitating the trafficking of substances between organelles (252,253). In this study, the focus was placed on the P4-ATPase F2, the only essential P4-ATPase located at the Golgi apparatus (252). Its role in endocytosis and vesicle trafficking was specifically investigated to determine its involvement in these critical processes.

2.4.1 Impact of FLP2 on the trans-Golgi network (TGN)

As indicated above, FLP2 has previously been shown to localise to the Golgi apparatus in *Toxoplasma gondii* (109,254). In this study, a FLP2-mAID strain, generated in the Botté laboratory, was endogenously tagged with SortLR-Halo, a marker for the trans-Golgi network (TGN).

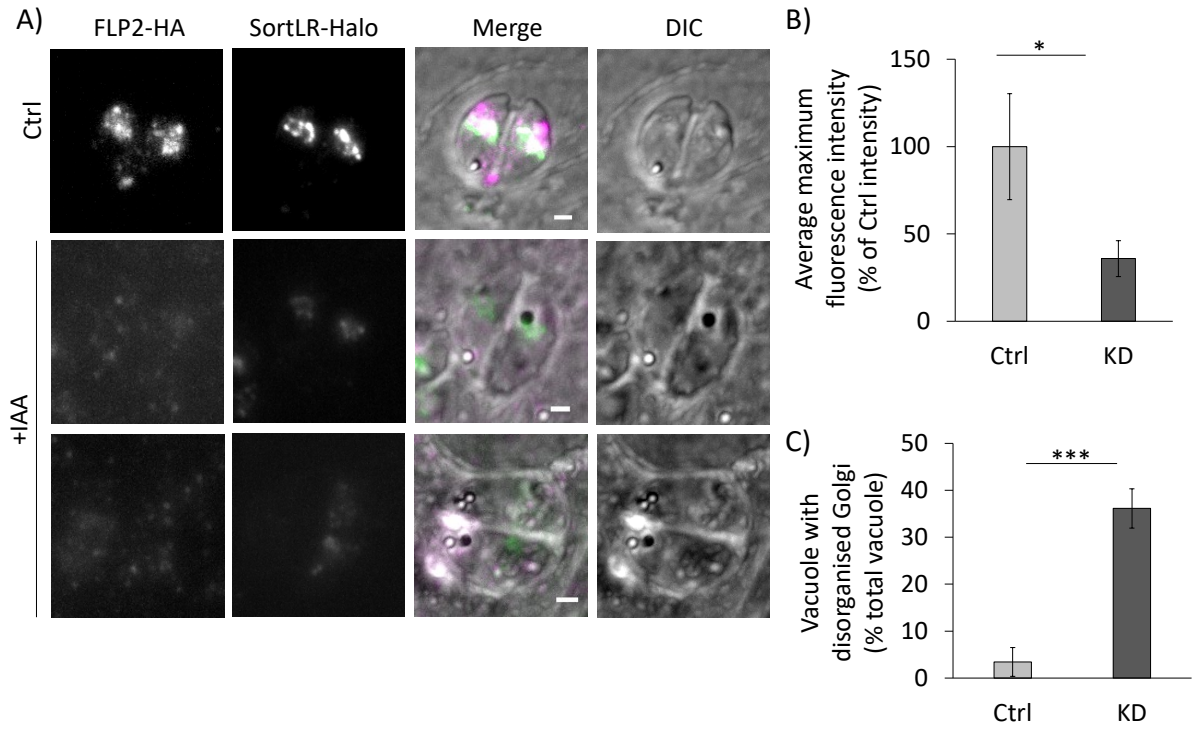

Figure 31: ***FLP2 localisation and Golgi organisation upon depletion A)*** *Colocalisation of FLP2-HA with SortLR-Halo in fixed images under induced (auxin-treated) and uninduced conditions.* ***B)*** *Fluorescence signal intensity of SortLR-Halo is significantly reduced in FLP2-depleted parasites.* ***C)*** *Golgi disorganisation is significantly increased in FLP2-depleted parasites compared to controls. Scale bar: 1 µm. ***p<0.001, *p<0.05.*

Colocalisation of FLP2-mAID with SortLR confirmed its localisation at the TGN. Depletion of FLP2 resulted in a significant reduction in SortLR fluorescence intensity, decreasing to 35% of the signal observed in uninduced parasites. Furthermore, FLP2 knockdown led to Golgi fragmentation, with disorganisation increasing to 36% in induced parasites compared to controls. These results demonstrate that FLP2 and therefore phospholipid composition is critical for maintaining Golgi organisation in *T. gondii*.

2.4.2 General Plasma Membrane Trafficking is Impacted by FLP2 Depletion.

After demonstrating the impact of FLP2 on the TGN, it was necessary to determine whether FLP2 also affects PM trafficking during parasite replication. To investigate this, SAG1-Halo was endogenously tagged in the FLP2-mAID strain, enabling the analysis of M-SAG1 and n-SAG1.

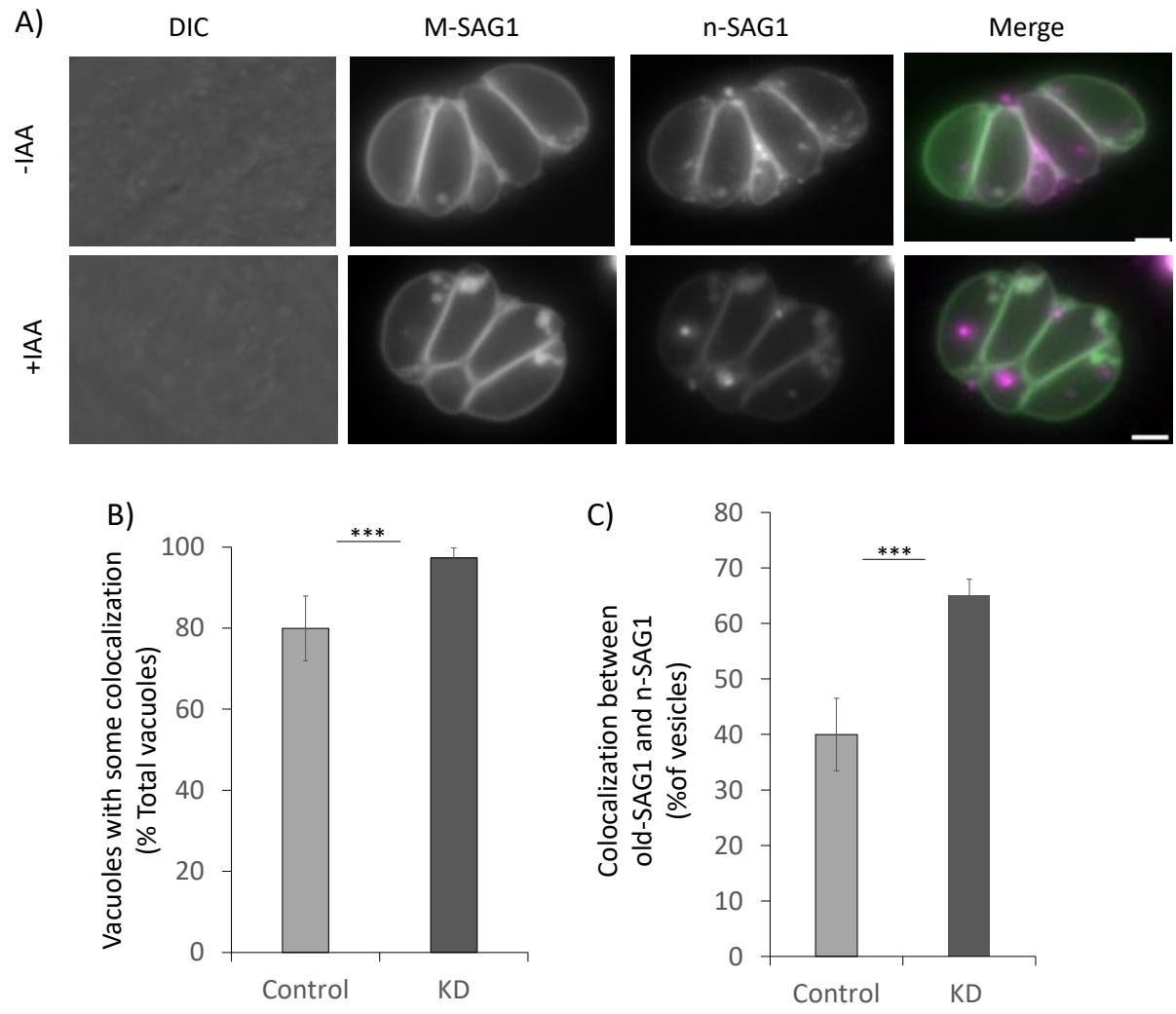

Figure 32: ***Impact of FLP2 depletion on M-SAG1 and n-SAG1 vesicles****. **A)** Representative images of M-SAG1 and n-SAG1 vesicles labelled with two MP dyes (Janelia 539 and 647) in control and FLP2 knockdown parasites.* ***B)*** *Statistical analysis shows increased colocalisation of SAG1 vesicles in FLP2 KD vacuoles (~95%) compared to controls (~80%).****C)*** *Increased colocalisation of M-SAG1 and n-SAG1 vesicles in FLP2-depleted parasites. Scale bar: 2 µm. ***p<0.001.*

As shown in Figure 32, depletion of FLP2 caused n-SAG1 and M-SAG1 vesicles to accumulate toward the parasite's tip, with a notable increase in vesicle size. Colocalisation of vesicles increased from 78% in controls to 95% in FLP2 knockdown vacuoles. At the individual vesicle level, colocalisation increased from ~40% in controls to ~70% in FLP2 KD parasites. These observations indicate that FLP2 depletion impairs the trafficking of both maternal and newly synthesised SAG1 vesicle populations. Observing the accumulation at the tip of the parasites raises the question of whether the arrested vesicles are near or even colocalise with the apical annuli. Unfortunately, this question remained unanswered by the conclusion of this thesis.

2.4.3 FLP2 and Its Importance for SAG1 Vesicle Formation

To further investigate the role of FLP2 in vesicle formation, FLP2-mAID-HA/SAG1-Halo parasites were analysed.

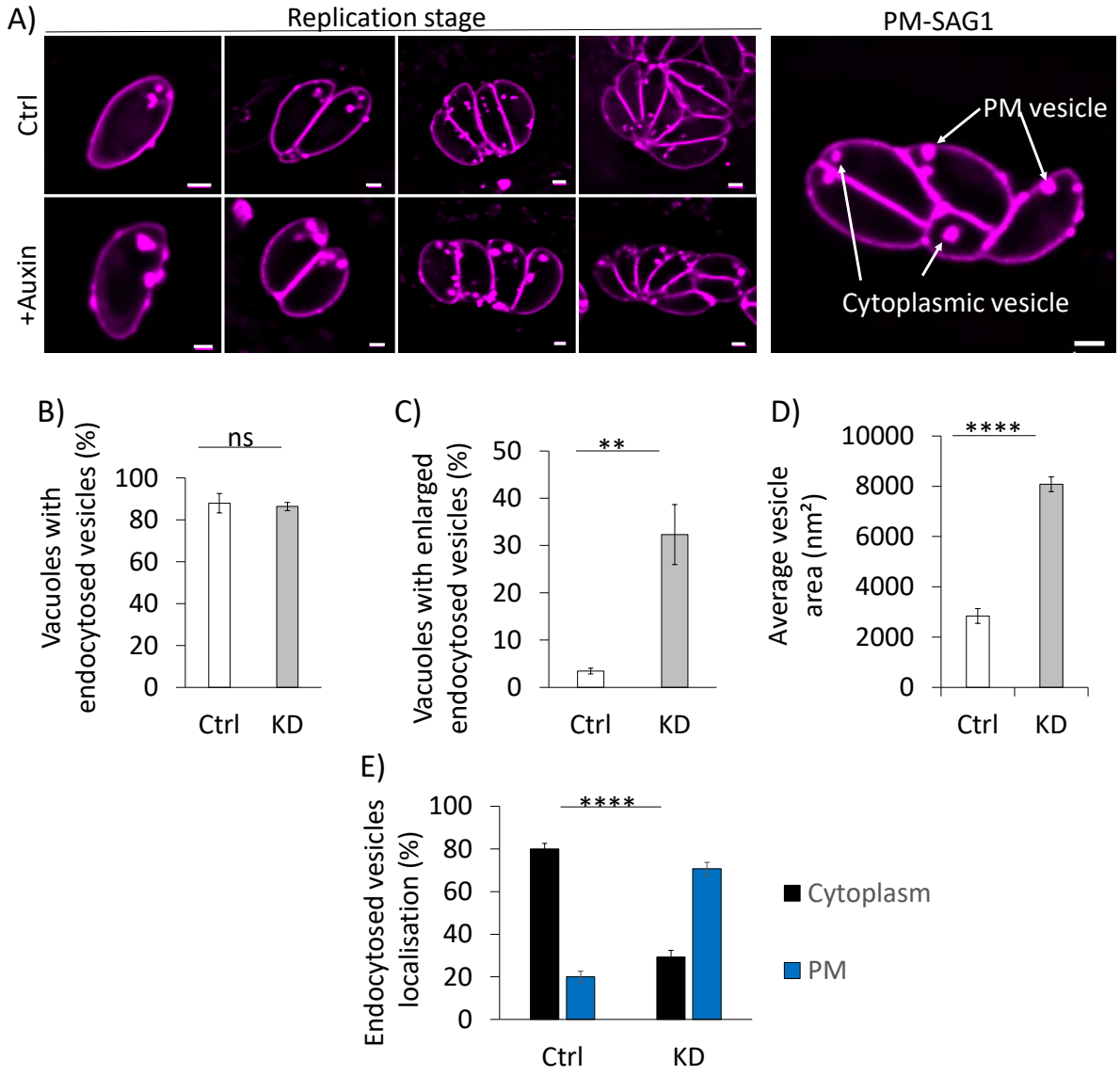

Figure 33: ***Effect of FLP2 depletion on SAG1 vesicle formation****.* ***A)*** *Live-cell images of SAG1-Halo in control and auxin-induced FLP2 knockdown parasites (15-hour induction).* ***B)*** *Quantification of vacuoles with endocytosed vesicles showed no significant difference.* ***C)*** *Statistical analysis reveals enlarged vesicle accumulation in FLP2 KD parasites (~8000 nm²) compared to controls (~3000 nm²).* ***D)*** *Vesicle localisation analysis shows increased accumulation at the plasma membrane in FLP2 KD parasites. Scale bar:1 µm. ****p<0.00001, **p<0.001.*

Depletion of FLP2 resulted in a significant increase in vesicle size and accumulation during replication. The proportion of enlarged vesicles increased from ~3% in controls to 32% in FLP2 KD parasites, with an average vesicle size increasing from 2500 nm² to 5240 nm². Depletion of FLP2 led to the enlargement and accumulation of endocytic vesicles during replication, as

previously observed for M-SAG1 and n-SAG1. The proportion of enlarged vesicles significantly increased from ~3% in uninduced parasites to 32% in FLP2 KD parasites (Figure 33D).

In addition, endocytic vesicles were observed to accumulate in proximity to the PM (Figure 33E). In control parasites, 80% of vesicles were localised to the cytoplasm, while 20% were associated with the plasma membrane. In contrast, FLP2 KD parasites exhibited an inverted pattern, with 30% of vesicles localised to the cytoplasm and 70% to the plasma membrane.

2.4.4 Endocytic Vesicles Are Not Stuck at the Micropore

To determine if endocytic vesicles were stuck at the micropore, the micropore markers ISAP1-YFP and DrpC-YFP were endogenously tagged into the FLP2-mAID/SAG1-Halo strain.

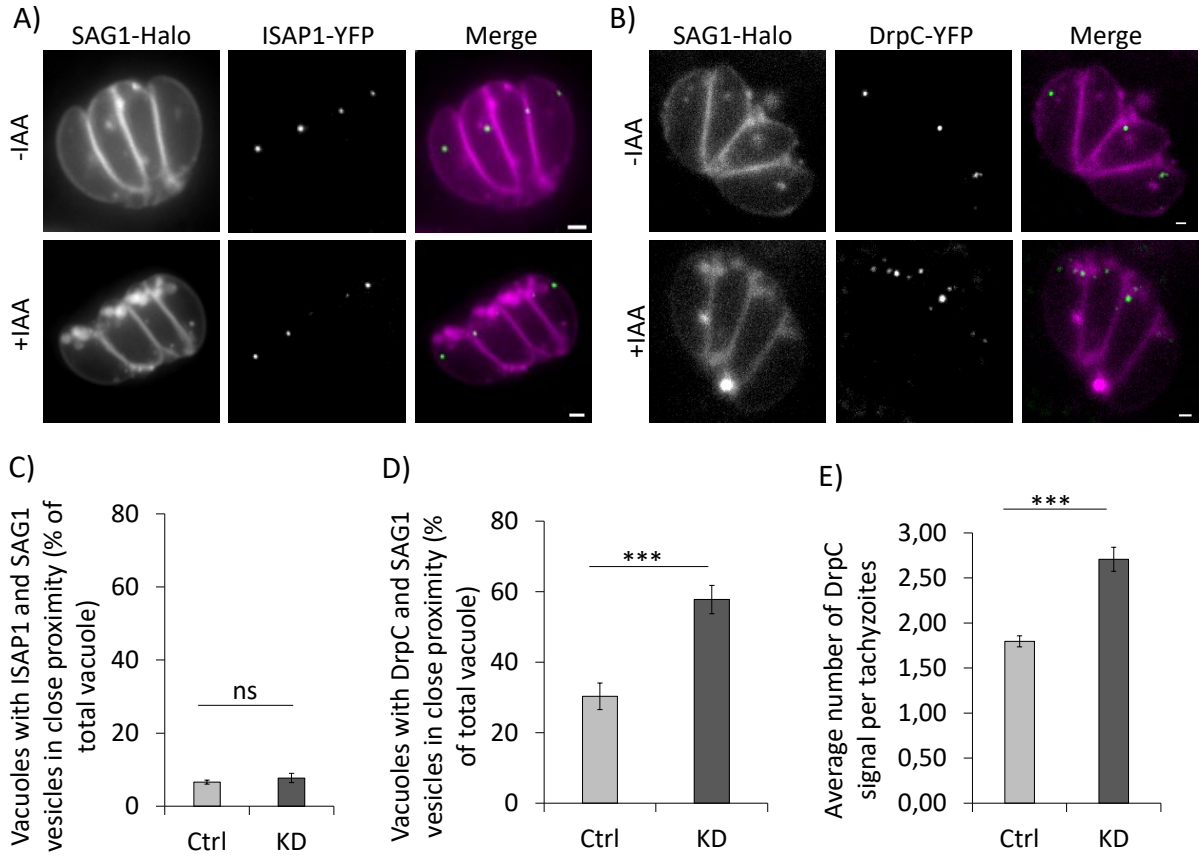

Figure 34: ***Investigation of micropore localisation of endocytic vesicles****. **A)** Representative live-cell images showing SAG1-Halo with ISAP1-YFP in control and FLP2-induced parasites. **B)** Live-cell images showing SAG1-Halo with DrpC-YFP in control and FLP2-induced parasites. **C)** Quantification reveals no significant colocalisation of ISAP1-YFP with SAG1 vesicles (~7% in both control and KD parasites). **D)** Statistical analysis shows increased proximity and interaction between DrpC-YFP and SAG1-Halo vesicles in FLP2 KD parasites. **E)** Elevated DrpC signal intensity observed in FLP2-depleted parasites. Scale bar: 1 µm. ***p<0.001.*

Despite the increased membrane localisation of endocytic vesicles, colocalisation with ISAP1 remained minimal, at approximately 7% in both control and FLP2 KD parasites (Figure 34C). This indicates that endocytic vesicles are not stalled at the micropore. Interestingly, a notable increase in colocalisation with DrpC was observed. In control parasites, 30% of vesicles colocalised with DrpC, whereas FLP2 KD parasites exhibited an increased colocalisation of 60% (Figure 34D). Additionally, the average number of DrpC signals per tachyzoite increased by 0.90 signals in KD parasites (Figure 34E), indicating elevated production of DrpC. This suggests an increased requirement for vesicle cleavage, possibly as the parasite attempts to process more rigid vesicles. DrpC, known for its role in vesicle cleavage in eukaryotic cells (64) may be recruited in greater numbers to compensate for changes in vesicle composition or rigidity caused by FLP2 knockdown.

These findings indicate that FLP2 is not essential for the formation of endocytic vesicles but is critical for their proper processing and trafficking. In the absence of FLP2, vesicles accumulate at the PM and exhibit increased size, highlighting defects in vesicle formation and processing. Furthermore, FLP2 KD parasites displayed vesicle accumulation near or at the membrane, rather than in the cytoplasm. This shift suggests that changes in lipid composition, resulting from FLP2 knockdown, affect vesicle trafficking and processing.

Finally, the aberrant translocation of phosphatidylserine (PS) caused by FLP2 depletion appears to disrupt Golgi organisation, which consequently impacts the entire endolysosomal compartment (ELC) system.

2.5 Discovery of the Plasma Membrane Reservoir (PMR)

The analysis of various replication assays revealed that single parasites formed an additional membranous structure on top of the PM. To determine whether this structure represents a biologically relevant feature, comparisons were made to a similar but more pronounced structure observed in the K13 KD phenotype, as described by Koreny et al (248). Yet, since this structure was also noticeable in control parasites, which typically replicate without abnormalities, it raises the question of whether this membrane structure represents a

purposeful generation of extra membrane required during replication or an artefact resulting from the SAG1-HaloTag.

In this thesis, these observed membrane structures will be referred to as "membrane reservoirs" or plasma membrane reservoirs (PMR).

2.5.1 Generation of the Membrane Reservoir for the Budding of Daughter Cells

To investigate the formation of this membranous structure, live-cell imaging of parasites expressing SAG1-Halo was performed during replication. The PMR was observed in 95% of parasites during replication, specifically during the transition from stage 1 to stage 2 (Figure 35A). The PMR appeared after parasite invasion and disappeared upon the completion of replication, suggesting a role as a membrane reservoir to facilitate parasite replication. To better understand the formation of these extra-membranous structures, detailed live-cell images of SAG1-Halo parasites during replication were analysed.

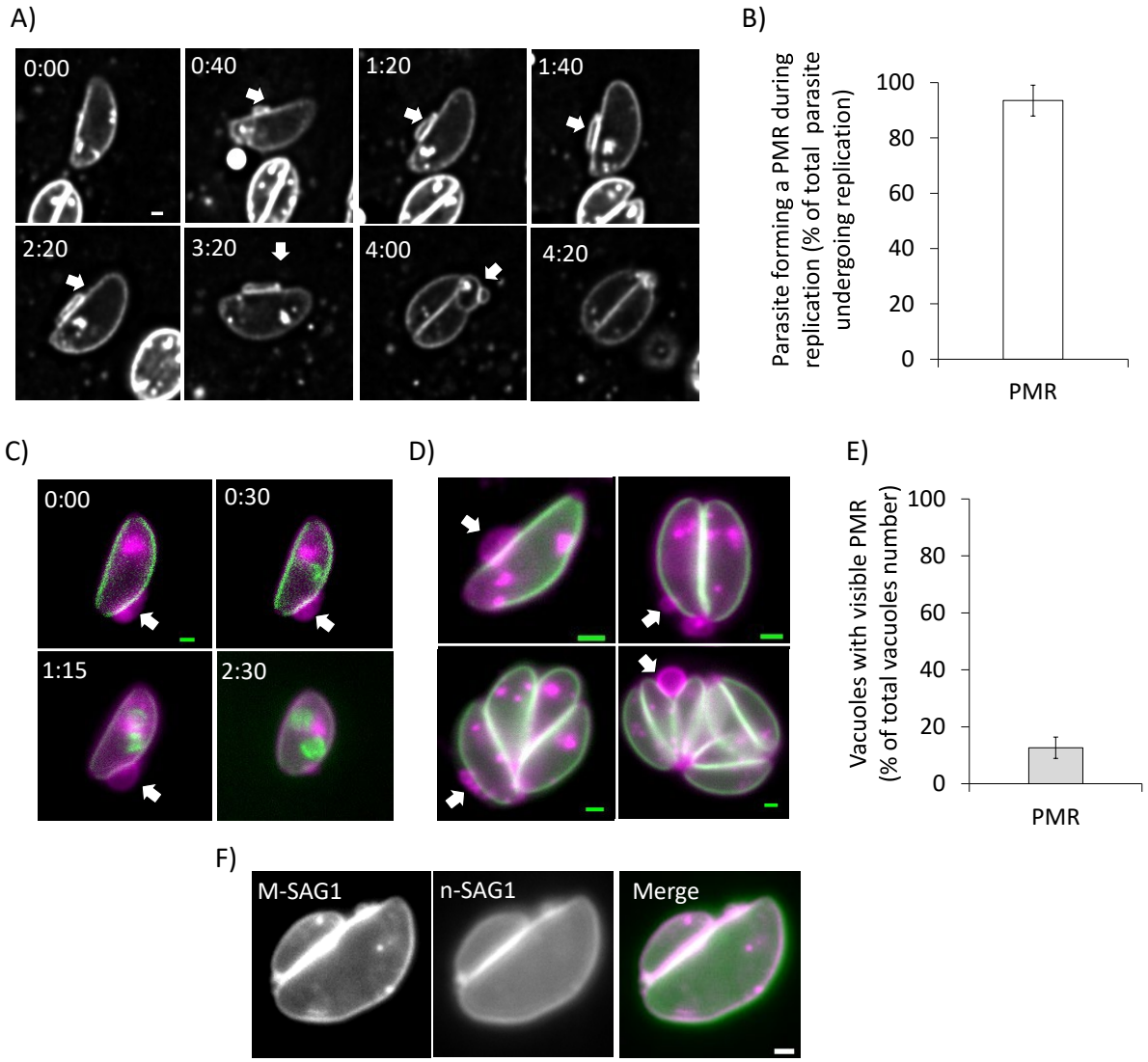

Figure 35: ***Membrane reservoir formation during parasite replication****. **A)** Live-cell video of parasites undergoing replication and forming membrane reservoirs. Time points range from 0–4 hours; at 0:40 min, the formation of the membrane reservoir can be observed until replication is complete. **B)** Statistical analysis of parasites during replication reveals that over 90% of parasites form a membrane reservoir (PMR). **C)** Time-lapse images of parasites expressing SAG1-Halo and IMC1-YFP show PMR generation, highlighting its distinction from daughter cell formation. **D)** Membrane reservoirs visualised at different replication stages (stages 1–8) in fixed parasites. **E)** ~13% of total vacuoles showed the PMR when unsynchronised. **F)** Double labelling of M-SAG1 and n-SAG1 populations at the PMR. The PMR is formed with both M-SAG1 and n- SAG1 populations, as shown through double membrane-permeable (MP) dye labelling. The first row shows SAG1-Halo-labelled PMRs. Scale bar: 1 µm.*

To highlight the appearance of the PMR, its formation was monitored relative to daughter cell IMC formation and in live cell videos (Figure 35). PMR formation was observed prior to the initiation of IMC development and therefore daughter cell formation (Figure 35), indicating that the reservoir forms during the early stages of replication in both live and fixed parasites (Figures 35C and D). Live-cell imaging established a time frame during which excess SAG1

accumulated on the membrane. The PMR became visible after parasite invasion and persisted during the internal formation of daughter cells (Figure 35A and Figure 37). Notably, as daughter cells began to bud, the mother parasite exhibited visible swelling, and the reservoir was subsequently reabsorbed into the plasma membrane. Figure 35E showed that in unsynchronised parasites, the PMR could be observed in approximately 12% of the vacuoles. To determine whether the PMR comprises M-SAG1, n-SAG1, or both populations, double labelling was performed (Figure 35F). The analysis revealed that the reservoir includes both M-SAG1 and n-SAG1 populations, supporting the hypothesis that the PMR functions as a storage system for plasma membrane components during parasite replication and facilitates the budding of daughter cells.

To confirm that the PMR is not an artefact caused by phototoxicity or the Halo dye in live-cell imaging, the IMC1-YFP tagged SAG1 Halo line was used (Figure 35) for fixed replication assays. Using this line, the presence of the PMR was validated in fixed and as shown before in live videos (Figure 35C-D). To further exclude the possibility that the PMR is a HaloTag artefact, experiments using transmission electron microscopy (TEM) and expansion microscopy (EX) were conducted. Both techniques confirmed the formation of the PMR in wild-type (WT) parasites.

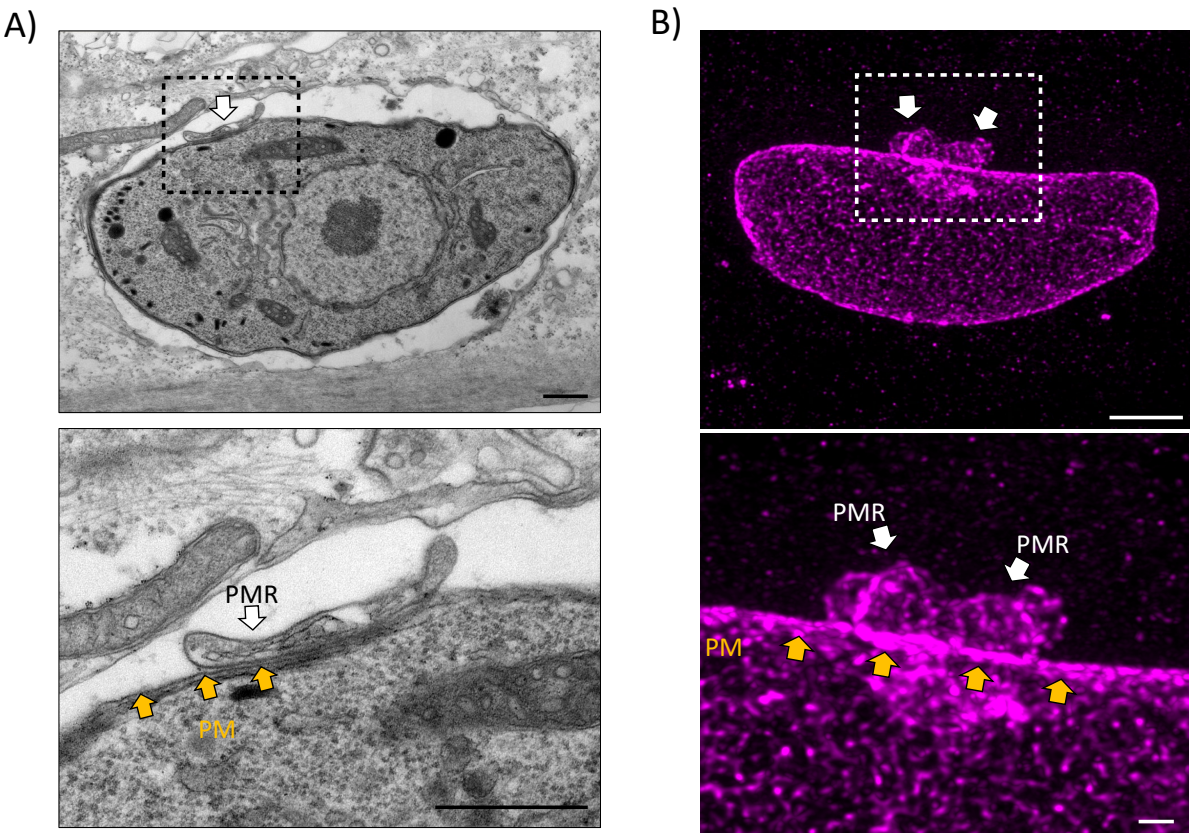

Figure 36: ***PMR validation using electron and expansion microscopy A)*** *TEM images of wild-type parasites showing the presence of the PMR.* ***B)*** *Expansion microscopy (EX) images, recorded in collaboration with the Soldati Lab, showing PMR formation in different parasites independent of the Halo tag. Scale bars: TEM: 5 µm; EX: 5 µm and 1 µm.*

The PMR was observed independently of the HaloTag and across multiple microscopic approaches. These findings demonstrate that the PMR is generated in every parasite and is unrelated to the presence of the HaloTag.

Live-cell videos show the formation of the PMR in invaded single parasites and its translocation along the parasite (Figure 37 0:00h-9:00h). During replication, the PMR moves along the parasite PM towards the residual body. After the establishment of daughter cells, the PMR is reabsorbed to facilitate daughter cell formation during the next round of replication (Figure 37 2:30-6:00h). Additionally, the PMR can form at any location on the parasite plasma membrane, including regions between replicating parasites (Figure 36 9:00h).

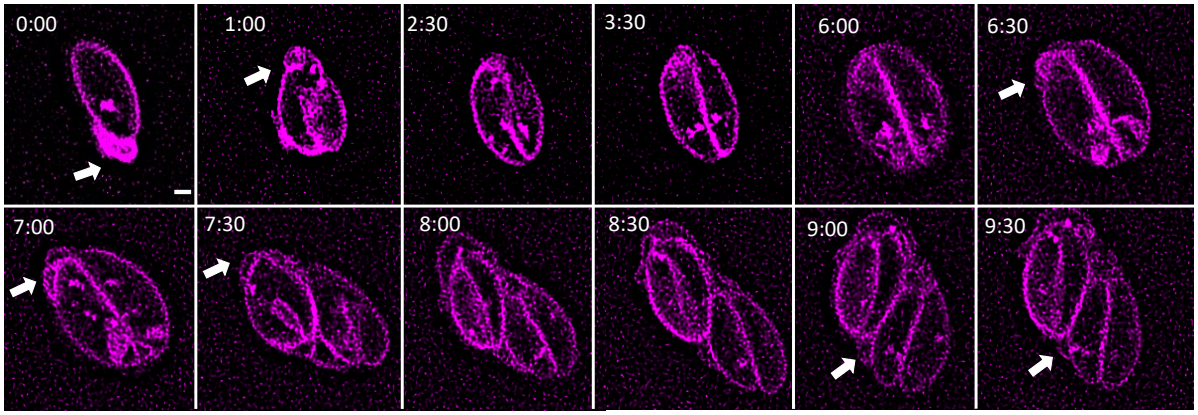

Figure 37: ***Dynamics of PMR generation during parasite replication****. Live-cell video showing the trafficking and dynamics of PMR formation around the parasite in hours Scale bar: 1 µm.*

Hypothetically, the PMR may play a dual role during parasite replication: 1) Facilitating daughter cell formation and budding and 2) Preventing membrane breakage during the swelling phase prior to the separation of daughter cells from the mother.

2.5.2 Micropores Control the Reabsorption of the Membrane Reservoirs.

Previous studies have suggested that the K13 micropore plays a role in membrane homeostasis (62,213). To investigate whether the micropore is related to the PMR, the colocalisation of K13 and the PMR was examined. Further the influence of MyoF was investigated regarding PMR formation.

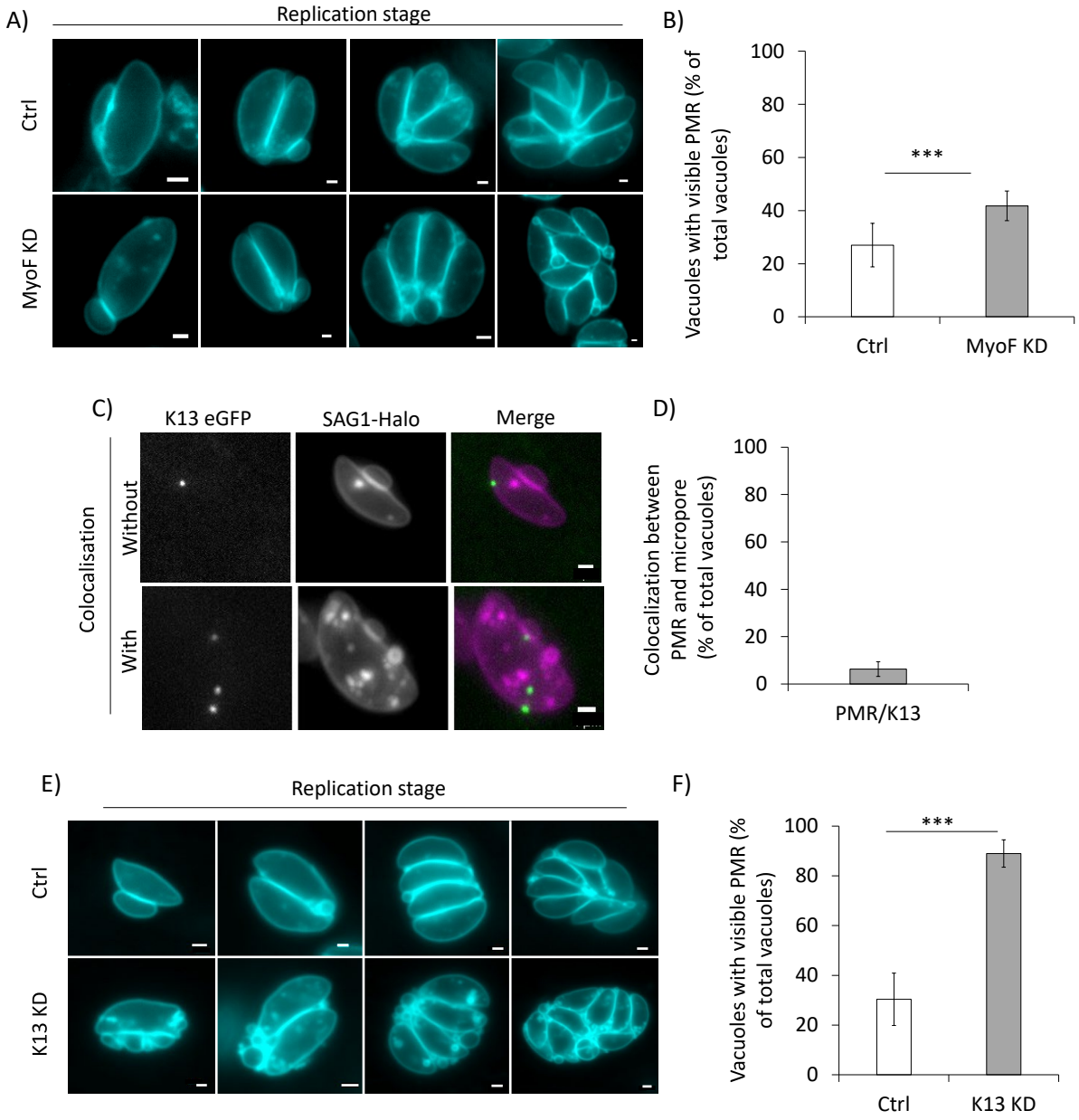

Figure 38: ***PMR formation in MyoF knockdown parasites. A)*** *SAG1-Halo-labelled control parasites and MyoF KD parasites showing an increase in visible PMR per vacuole in the absence of MyoF.* ***B)*** *Statistical analysis reveals a significant increase in PMR on the plasma membrane in MyoF KD parasites.* ***C)*** *PMR formation in K13 knockdown parasites. Live-cell images of K13-eGFP and SAG1-Halo-labelled parasites. The first row shows the appearance of an extra-membranous vesicle on the side opposite to K13-eGFP. The second row shows rare colocalisation between the PMR and K13.* ***D)*** *Statistical evaluation reveals that only 6% of K13 micropores colocalise with the SAG1-Halo PMR (n=100 micropores).* ***E)*** *Live-cell images of replicating parasites. The first row shows wild-type (WT) replication, while the second row shows replication in K13 KD parasites induced with anhydrotetracycline (ATc). An increase in PMR formation is visible around the parasite during stages 1–8.* ***F)*** *Statistical analysis reveals a significant increase in extra-membranous structures in K13 KD parasites compared to WT. Scale bar: 1 µm. ***p<0.001. Scale bar = 1 µm. ***p<0.0001.*

MyoF KD analysis of PMR formation revealed a significant increase in vacuoles with visible reservoir when MyoF was depleted, suggesting slowed or disrupted endocytosis in the

absence of MyoF. However, despite this disruption, the PMR was still formed and eventually reabsorbed, albeit with delays (Figure 38A-B). This disruption was less severe compared to K13 KD parasites.

Colocalisation assays confirmed that K13 and the PMR do not significantly colocalise (Figure 38C/D). The SAG1 reservoir can form at various locations on the parasite membrane. Due to the dynamic fluidity of the reservoir and its progressive growth during replication, a transient interaction between the micropore and PMR cannot be excluded. While the K13 micropore may act as a potential starting point for reservoir generation during daughter cell replication, the PMR appears to dynamically move along the parasite membrane as replication proceeds. This suggests the involvement of additional mechanisms in membrane uptake, with K13 potentially serving as a regulator of membrane homeostasis during reservoir formation.

To further explore this, K13 KD parasites were analysed to assess their impact on PMR formation. Results in K13 KD parasites showed a significantly increased presence of PMR on the membrane surface. PMR formation was enhanced in 90% of K13 KD parasites compared to 20% in control parasites. Additionally, the uptake of the PMR was severely restricted in the absence of K13. The loss of K13 disrupts the uptake process, resulting in excessive membrane accumulation on the parasite surface (Figure 38 E, F).

These findings suggest that the K13 micropore is not only involved in endocytosis but also plays a critical role in maintaining membrane homeostasis during PMR formation.

3. Discussion

3.1. SAG1 and the Fluidity of the Membrane

FLIP (Fluorescence Loss in Photobleaching) and FRAP (Fluorescence Recovery After Photobleaching) are valuable techniques for investigating the dynamics of fluorescently labelled proteins over time. In this thesis, the fluidity of the *Toxoplasma gondii* plasma membrane was assessed using the glycosylphosphatidylinositol (GPI)-anchored SAG1 protein as a proxy. This observation aligns with findings from eukaryotic membranes protein behaviour, particularly for GPI-anchored proteins (113,114,233,255). GPI-anchored proteins are known to exhibit lateral mobility typically 2–5 times faster than that of transmembrane proteins, approaching the diffusion coefficients of membrane lipids (256). Small, photobleached areas in single and double membranes recovered fluorescence within 20 seconds, indicating the lateral diffusion capability of GPI-anchored proteins (Figure 13-14A–C). However, when the bleached area was enlarged, fluorescence recovery in *T. gondii* was significantly prolonged, which deviates from typical FRAP patterns in most eukaryotic cells (114) (Figure 14D–F and Figure 16). Interestingly, similarly extended recovery times (up to three minutes) have been reported in *Plasmodium* FRAP experiments (257), suggesting that factors unique to apicomplexan parasites such as altered membrane/protein properties during replication(258) or the presence of inter-parasite connections in the parasitophorous vacuole (PV) like the basal body may influence membrane dynamics in the parasite.

Within the PV, parasites are interconnected via their basal body, which extend through the plasma membrane and interact with actin filaments (238), forming a syncytium. These connections facilitate the diffusion of cytoplasmic components, ensuring equitable distribution among daughter cells (212,259). Disruption of these interconnections can significantly alter membrane and protein flow between parasites. For instance, *act1* null mutants with a compromised actin network exhibit impaired cytoplasmic sharing and misaligned daughter cells due to cytoskeletal defects (46,51,223,260). Similarly, the absence of MyoJ or MyoI disrupts the residual body, thereby inhibiting the flow of cytoplasmic expressed GFP to daughter cells (261). However, the thin plasma membrane bridges

connecting parasites within the PV may create a diffusion bottleneck for membrane proteins, unlike the relatively unrestricted cytoplasmic diffusion observed for GFP (212).

FRAP experiments in 2-, 4-, and 8-stage vacuoles revealed slower recovery rates in replicating parasites (Figures 16–17), with further delays in vacuoles exhibiting disorganised or extended connections (Figure 17C–D). Parasites located farther from the basal pole or more distant daughter cells displayed longer recovery times, suggesting that elongation or disorganisation of basal body connections hinders membrane flow, potentially slowing or halting recovery altogether. Such limitations highlight challenges in using FRAP to measure membrane dynamics in replicating parasites.

Several factors may contribute to the observed slower recovery. In eukaryotic cells, FRAP is widely used to study membrane dynamics by bleaching a well-defined region of the membrane and monitoring the recovery of fluorescence. Recovery times can provide insights into the properties of target proteins within the membrane or the cell. Fast recovery typically indicates freely moving proteins, such as cytosolic proteins or lipids, whereas slow or no recovery suggests that the protein is either complex-bound, stationary, or slowly refilled (113,233).

Membrane fluidity is influenced by the lipid composition of the membrane, temperature, and protein density. Studies have shown that high protein density increases membrane tension, which can slow diffusion (93,262). GPI-anchored proteins, in particular, often reside in membrane microdomains such as lipid rafts (263,264) and diffuse from these domains across the membrane. The compartmentalised organisation of membranes, where proteins undergo hop diffusion, can reduce diffusion rates as molecules transition between dynamic compartments formed by the actin cytoskeleton and lipid rafts (265–268). In *T. gondii*, the residual body (Figure 14) may act similarly, localising proteins and consequently slowing their diffusion. During replication, additional factors such as increased secretion and production of SAG1 may lead to localised protein crowding, while heightened physiological tension at the basal body could compartmentalise GPI-anchored proteins between connected parasites and daughter cells. These factors, combined with high protein concentrations in confined regions, likely contribute to the reduced diffusion seen in replicating parasites compared to single parasites. As replication occurs within the PV, structural connections between daughter cells may weaken, leading to prolonged FRAP recovery (Figures 16–17).

Notably, in four-stage vacuoles, rapid fluorescence recovery was lacking when the typical rosette arrangement of daughter cells was either disordered or missing (Figures 17C). This observation supports the idea that basal body connections and the residual body play essential roles in facilitating efficient membrane diffusion. In other eukaryotic cells, GPI proteins can be secreted into the membrane in clusters before dispersing over time (269), suggesting a delay in protein dynamics after insertion into the membrane. A similar scenario may occur during replication in *T. gondii*, where SAG1 is secreted in clusters and temporarily remains immobile, further explaining the delayed recovery observed in replicating parasites.

To better understand the dynamics of membranes in parasites connected via the basal body, future research is needed to investigate PV organisation, protein distribution, and membrane concentration at the residual body. It is also important to examine how inter-parasite connections influence membrane protein dynamics, particularly under replication stress. Techniques such as multi-colour FRAP could differentiate between newly secreted and pre-existing SAG1 populations, providing insights into dynamic membrane behaviour. Advanced microscopy methods, including expansion microscopy to visualise basal body architecture, total internal reflection fluorescence (TIRF) microscopy, or super-resolution techniques such as PALM (Photoactivated Localisation Microscopy) and STORM (Stochastic Optical Reconstruction Microscopy), could offer higher spatial resolution. Single-particle tracking (SPT) may also provide quantitative data on the movement and residence times of individual fluorescent particles within defined regions (270).

Despite these complexities, the rapid recovery of SAG1-Halo in single parasites validates it as a reliable proxy for studying membrane dynamics. This conclusion is further supported by using SAG1-Halo labelling strategies to monitor membrane inheritance (Figure 19). These experiments demonstrated that PM-SAG1 is fully inherited by daughter parasites during replication and that newly synthesised SAG1 is generated to meet the increased demand for membrane components (Figure 20). Using this approach, it was also possible to show the contribution of Int-SAG1 to membrane inheritance via internal secretion (Figure 21). Collectively, these findings highlight the utility of SAG1-Halo as a tool for studying membrane fluidity, and the processes of membrane inheritance and secretion during replication in *T. gondii*.

3.2. The Endo-Exocytosis Flow in *T. gondii*

After analysing membrane flux in replicating parasites, the endo–exocytosis cycle was investigated through the newly established trypsinisation experiment. As expected, the recovered fluorescent signal displayed reduced intensity compared to the original vesicles, which can be explained by the fact that not all plasma membrane components are internalised into endocytic vesicles (Figure 23A). Only a small portion of the plasma membrane is incorporated into endocytic vesicles and subsequently re-secreted. Therefore, the proportion of re-secreted material is much smaller than the total plasma membrane surface area. Additionally, owing to lateral diffusion, secreted plasma membrane components are redistributed across the entire parasite surface, resulting in approximately a 10% increase after re-secretion in fluorescence relative to pre-trypsination labelled plasma membrane (Figure 23).

Earlier studies on cell membrane dynamics and SAG1 secretion relied on antibody assays that compared *T. gondii* at 4 °C and 37 °C (210), but these approaches were unable to capture detailed re-secretion kinetics in non-gliding parasites. Previous observations indicated that internally labelled SAG1 was present in trials of extracellular parasites (210), suggesting an extra-endocytic cycle for some internal SAG1 populations. However, the question remained whether endocytosed SAG1 vesicles could be returned to the plasma membrane. The dynamics of GPI-anchored proteins hinted at a clustered mechanism for their insertion into membrane microdomains (263,264), challenging the classical fluid mosaic and ‘fountain flow’ models. While the trypsinisation assay confirmed that SAG1 recycling can be visualised by measuring fluorescence recovery, this method could not delineate whether re-secreted SAG1 is delivered to specific membrane domains or determine the exact mechanism of vesicle fusion. It might involve either vesicle–vesicle fusion or a SNARE-mediated process. However, these dynamics lie beyond the resolution of the current used trypsinisation assay.

Demonstrating the full endo–exocytosis cycle might be more feasible in parasites actively gliding or replicating within host cells (Figure 19-21). During replication, nearly all membrane-bound SAG1 is redistributed to daughter cells, either via diffusion (as suggested by FRAP analyses) or more likely through the increased number of vesicles observed in replicating parasites. The fusion of endocytotic vesicle back to the membrane cannot be shown using the

trypsinisation assay alone. In single extracellular parasites under non-gliding conditions at 37 °C, the plasma membrane appears to reach a relatively homeostatic equilibrium with only minimal membrane re-secretion (~15%). By contrast, intracellular parasites display enhanced uptake and re-secretion of membrane components.

While the trypsinisation assay demonstrates that endo- and exocytosis occur in single-stage extracellular parasites, such that membrane-bound SAG1 can be stripped from the surface without causing immediate parasite death a more comprehensive characterisation of the endo–exocytosis cycle calls for further methodological integration. Combining trypsin assays with advanced fluorescence and microscopy techniques could help resolve both uptake and re-secretion events in greater detail.

Limitations of the Trypsinisation Technique and Alternative Approaches

Despite its utility, the trypsinisation method is not well suited for elucidating the precise secretion mechanisms of endocytosed vesicles. Therefore, adapting established assays from other eukaryotic systems could prove beneficial. For example, the confocal Fluorescence Recovery after Photoconversion (cFRAPc) technique is commonly used in eukaryotic cells to determine exocytosis levels (271,272). By fusing Dendra2 to the protein of interest, photoconversion can be performed in specific regions using a laser-scanning microscope (273). Under this method, Dendra2 is photoconverted within a chosen region (e.g. the membrane or vesicles), switching from green to red fluorescence. The non-photoconverted populations remain green, enabling distinct tracking of each population. Other potential photo-switchable dyes, such as mEos3.2, function similarly by switching from green to red upon exposure to 405 nm light (274).

A significant limitation of these photoconversion techniques is that they are less effective for proteins exhibiting rapid lateral diffusion, as the photoconverted signal would swiftly dissipate. Adapting these methods to *T. gondii* might thus require specialised photoconvertible dyes that switch only when vesicles are endocytosed, permitting targeted labelling within these compartments ideally switching through mechanical changes or pH changes. When these vesicles are subsequently re-secreted, they would display a distinct fluorescent signature, allowing them to be distinguished from the plasma membrane. One potential dye system involves rhodamine-based dyes, which can remain non-fluorescent until

activated at a specific wavelength, and may be used in combination with Halo dyes (275). Alternatively, a photoactivated GFP which requires activation at 495 nm (275,276), could be employed. Another promising approach is the Dronpa system, a photo-switchable protein that may also be exploited in this context (277).

In addition to photoconversion techniques, nanoplasmonic sensors may provide complementary tools for detecting vesicle secretion. These methods rely on plasmonic nanomaterials, which are highly sensitive to changes in the refractive index of their proximal environment. They can detect small biomolecular changes, such as binding events, and are already used for exosome detection when conjugated with antibodies (278).

Nonetheless, these techniques face challenges:

1. They require adaptation for live-cell imaging.
2. They work exclusively with antibody-conjugated molecules.

To integrate nanoplasmonic sensors into the SAG1-Halo assay, endocytosed vesicles being re-secreted would need to be tagged with specific antibodies and distinguished from the plasma membrane signal. Differentiating endocytosed vesicles from the plasma membrane remains challenging, especially if the vesicles are directly integrated into the membrane rather than released as exosomes (278), which does not appear to be the case here. A potential solution would involve tagging endocytosed vesicles with specific markers that alter their refractive index or fluorescence only upon secretion, enabling precise quantification of vesicle release (278,279). While nanoplasmonic sensors have been used for exosome detection, their application here would require a reliable means of discriminating re-secreted vesicles from the plasma membrane, which poses a technical challenge in *T. gondii*, especially if vesicles fuse directly with the membrane rather than bud off as exosomes (278,279).

Another promising avenue is Interference Reflection Microscopy (IRM), which detects membranes in close proximity to a coverslip by measuring interference patterns (280). Vesicle fusion or granule collapse appears as bright spots under IRM (280), reflecting changes in the local membrane area. However, applying IRM to live parasites requires immobilising them near the coverslip to maintain viability, and it remains uncertain whether SAG1 is an ideal

target for IRM detection. If vesicles fuse homotypically rather than collapsing into the membrane, IRM may not capture their fusion events.

Although these techniques are powerful, each poses limitations and would require substantial adaptation to *T. gondii*, particularly for extracellular parasites. Of the methods discussed, photoconversion-based approaches targeted to endocytosed vesicles offer the most promise for distinguishing re-secreted vesicles from the plasma membrane, enabling dynamic visualisation of the endo–exocytosis cycle. Moreover, investigating the cycle in gliding parasites, where the membrane must continually adapt, could yield additional insights into membrane turnover and recycling (255). Techniques such as TIRF or FRET microscopy might further elucidate how SAG1 is endocytosed and re-secreted at the plasma membrane.

During this thesis work, samples were submitted for correlative light and electron microscopy (CLEM), but no results have thus far been obtained. Further developments in imaging and labelling methods will help overcome the technical challenges posed by *T. gondii*, thereby advancing our understanding of the endo–exocytosis cycle for SAG1 and other essential membrane proteins.

3.3. Endocytosis Regulators and Vesicle Movement

Colocalisation analysis revealed that distinct SAG1 vesicle populations (M-SAG1, n-SAG1, and PM-SAG1) follow largely separate trafficking routes (Figure 25) and only colocalise to a small extent in single-stage parasites. Rab proteins, which function as molecular switches and coordinators of vesicle transport, were shown to interact specifically with endocytosed vesicles (128). Due to their central role in vesicle trafficking and their high degree of conservation across taxa, Rab proteins are well known for their roles in vesicle transport, acting as “barcodes” that mark vesicles for specific routes and target destinations (68,113,125,202,203). Consequently, identifying which Rab proteins participate in endocytosis is crucial for understanding the pathways of endocytic vesicles.

In *Toxoplasma gondii*, 15 genes encoding Rab proteins have been identified, a number that is comparable to other apicomplexan parasites (281). Some Rab proteins exhibit alternative

splicing, as in the case of Rab5, which has three isoforms like the mammalian Rab5, all sharing significant sequence similarity (282,283) or, as in the case of the three forms of Rab5 in *T.gondii* genes derived from the same ancestral gen called paralogue (284). Previous studies have implicated Rab5a and Rab5c involved in secretory organelle vesicle transport (284). In this study, colocalisation with Rab5b, Rab5a, and Rab11a was investigated (Figure 27B). Most colocalisation was observed between Rab5b and SAG1-Halo vesicles, supporting the hypothesis that Rab5b is involved in endocytosis and early endosome formation during membrane uptake. Aligning with its function of endocytosis in *Plasmodium* and the suggested role in early endosome formation followed membrane uptake (202,203).

In *Plasmodium falciparum*, PfRab5b interacts with PfRabsn5 and PfVPS45 to form a stable complex that regulates host cell cytosol uptake (HCCU) as well as the trafficking and digestion of haemoglobin within the food vacuole (203). Disrupting this complex severely impairs haemoglobin uptake, resulting in reduced haemoglobin accumulation (202,203). By contrast, in *T. gondii*, TgVPS45 appears to play a lesser role in trafficking host cell components to the vacuolar compartment (VAC) than it does in *Plasmodium* (285,286). Interestingly a distinction among Rab5 paralogues has been described in another parasites. In *Trypanosoma brucei* Rab5a-positive endosomes contain GPI-anchored transferrin receptors, whereas Rab5b-positive endosomes transport transmembrane proteins (287). This specificity in *T. brucei* is thought to reflect a mechanism whereby endocytosis depends on a protein's mode of membrane anchoring (287).

In mammalian cells, Rab5 plays a pivotal role in transitioning early endosomes to late endosomes. It is particularly important for the formation of early endosomes and vesicle budding, with overlapping functions among Rab5a, Rab5b, and Rab5c (288). Meanwhile, Rab7 and Rab9 act in the later stages of the endocytic pathway. Because Rab5 localises to the plasma membrane, it is a key target for GTPase activity in membrane uptake, especially in clathrin-coated vesicle formation (289). Rab5 also facilitates vesicle uptake and early endosome fusion in conjunction with early endosome antigen 1 (EEA1) (290). A Similar function could be shown in *Leishmania*, were Rab5b mediates the fusion of early endosomes, reinforcing the idea that Rab5b is a conserved and critical factor in vesicular transport (291). Highlighting the conserved function of Rab5 proteins throughout different eukaryotic systems.

Rab5a, the second isoform of the Rab5 family investigated in this thesis, was previously shown to be specifically involved in early endosome formation and the internalisation of host-derived material (201,284,292). In mammalian systems, Rab5a is particularly important for cargo sorting, clathrin-mediated endocytosis (CME), and signal regulation (292,293). However, in the present study, Rab5a demonstrated low colocalisation with endocytosed SAG1 vesicles in *T. gondii*. Given that clathrin-mediated endocytosis has not been observed in this parasite, and that Rab5a is involved in rhoptry and microneme secretion and trafficking in *T. gondii* (281), Rab5a may fulfil a different role in this organism than in other eukaryotic cells. This observation suggests that SAG1-containing vesicles might bypass conventional endosomal sorting pathways and instead undergo direct re-secretion. In contrast to the well-characterised Rab5a-dominated early endocytic trafficking in mammalian cells, the minimal colocalisation observed in *T. gondii* indicates that SAG1-containing vesicles likely rely on a specialised mechanism, thereby enabling rapid turnover and secretion.

The functional distinctions among Rab5 paralogues may also apply to SAG1 endocytosis in *T. gondii*. This notion is supported by the increased colocalisation of Rab5b with endocytosed SAG1 vesicles compared to Rab5a (Figure 27). Nevertheless, the role of the third isoform, Rab5c, which was not investigated in this thesis, cannot be excluded and may also contribute to SAG1 endocytosis. Further studies are required to determine whether Rab5c plays a complementary or distinct role in this process.

Beyond Rab5, the investigation of a third Rab protein, the Rab11a isoform, revealed low colocalisation with SAG1 vesicles (Figure 27). Rab11 is commonly associated with the exocytosis of recycled vesicles and trans-Golgi to plasma membrane transport. In *T. gondii*, Rab11 has an established role in dense granule transport and in the delivery of vesicles from the Golgi to the inner membrane complex (IMC), contributing to secretory organelle biogenesis (284). In this study, no significant colocalisation was observed between Rab11a and endocytosed SAG1 vesicles, suggesting that these vesicles do not rely on Golgi-mediated transport. However, colocalisation with newly synthesised SAG1 might still be informative in determining whether SAG1 is transported from the Golgi to the plasma membrane.

It is also worth noting that only one Rab11 isoform (Rab11a) was examined here. Hence, an isoform-specific transport mechanism for SAG1 cannot be excluded in *T. gondii*. Investigations

into the Rab11b paralogues may provide additional insights into the trafficking routes of endocytosed vesicles and further clarify whether different Rab11 paralogues have distinct roles in SAG1 transport.

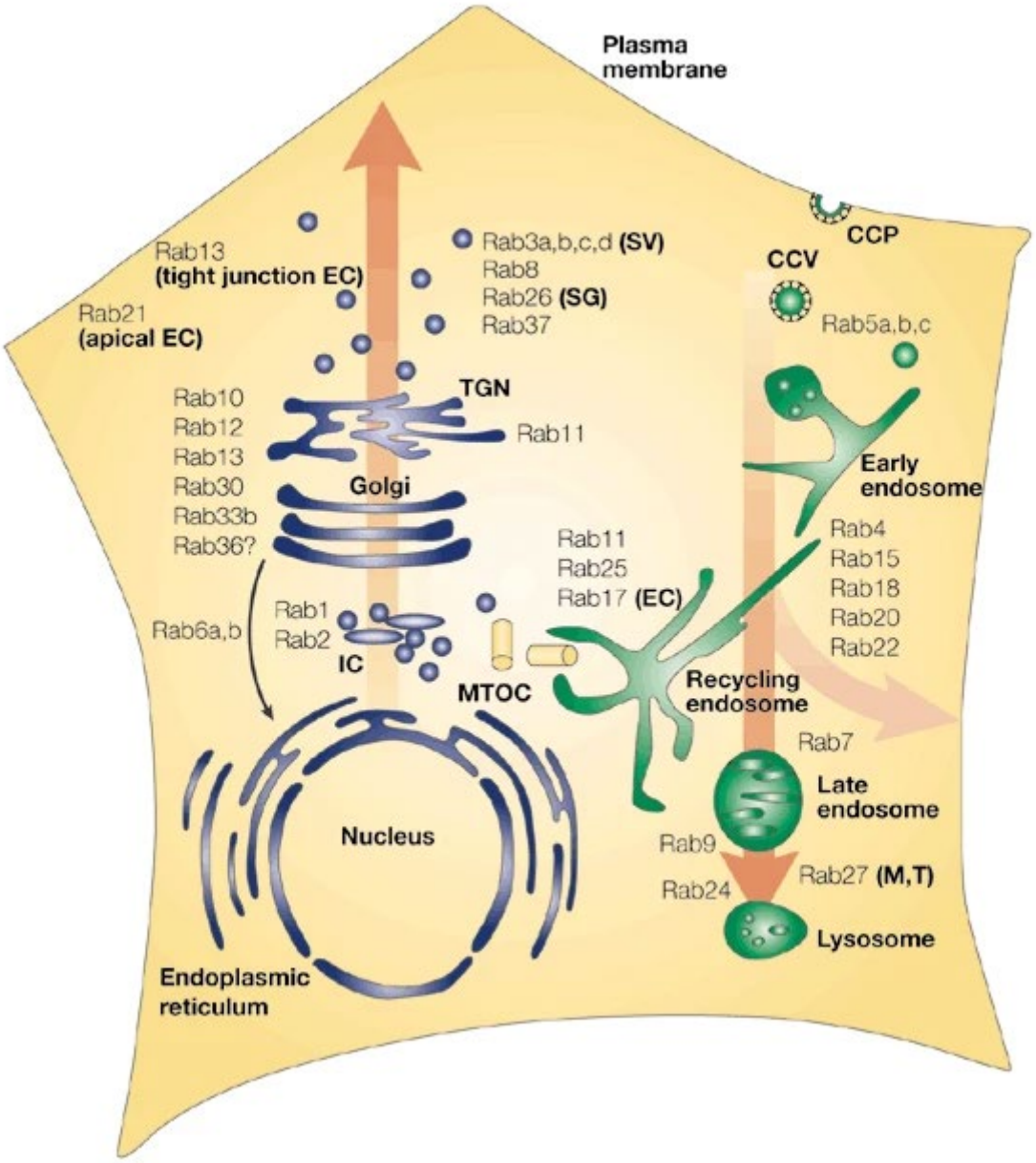

Figure 39: ***Overview of RAB proteins and their associated functions in exo- and endocytosis in eukaryotic cells****. The figure illustrates the diversity of Rab proteins, their individual roles in endocytic pathways, and their association with endosomes (290). Image adapted from Zerial and McBride 2001.*

The observed colocalisation with Rab5b (Figure 27) suggests similarities between *T. gondii* SAG1 endocytosis and vesicular trafficking in *Plasmodium* and *Trypanosoma*. Rab5 paralogues were shown to play distinct roles in vesicle uptake within early endosomes. In *Trypanosoma brucei*, Rab5b-positive endosomes contain GPI-anchored proteins, while Rab5a-positive

endosomes primarily contain transmembrane proteins. This differentiation based on anchoring mechanisms might be reason for the enhanced colocalisation with Rab5b compared to Rab5a in the colocalisation assays and might support the hypothesis that GTPase isoform specificity determines protein uptake pathways. Which further seems to be consistent with the established ability of endocytosed GPI-anchored proteins to follow different endocytic routes depending on their role in cell physiology (294). Further investigation in SAG1 specific transport is needed to get a deeper inside into Rab protein trafficking.

Previous studies showed Rab11a colocalisation with dense granule proteins and their secretion at the apical end of *T. gondii* (246). The low Rab11a colocalisation shown in this thesis could have two explanations: (1) SAG1 bypasses recycled endosomes altogether, or (2) Rab11 function is paralogue specific. *T. gondii* encodes two Rab11 paralogues Rab11a and Rab11b resembling the functional specialisation observed among Rab5 paralogues. Future colocalisation experiments with Rab11b might clarify whether this paralogue plays a distinct role in SAG1 trafficking. In other organisms, tissue-specific Rab11 paralogues have been associated with unique uptake mechanisms (295). Additionally, in *Trypanosoma*, Rab11 is implicated in compartment definition and recycling, notably in directing variant surface glycoproteins (VSGs) to the plasma membrane (296,297).

In addition to the Rab proteins used for colocalisation in this study, *T. gondii* encodes at least 15 Rab proteins and 12 are expressed by the tachyzoite (284). Further colocalisation experiments with Rab4 (284), Rab7 (243,284), or Rab1b (298,299), among others, may offer deeper insights into the parasite's endocytic trafficking pathways.

Vesicle sorting at the Golgi

The endomembrane system regulates both secretory and endocytic pathways, encompassing the endoplasmic reticulum (ER), Golgi apparatus, lysosomes, endosomes, and the plasma membrane (101,125). To explore a possible Golgi-mediated role in SAG1 endocytosis, colocalisation experiments were conducted with TgTEP (Toxoplasma Tepsin), a trans-Golgi-associated protein (247). Minimal overlap between TgTEP and SAG1-Halo vesicles was observed, indicating that SAG1 endocytosed vesicles are likely not sorted or modified at the Golgi. Consistent with this, endocytosis assays in TgTEP knockout (KO) parasites revealed no significant effect on SAG1 endocytosis (300). Given that these analyses focus exclusively on

endocytosed vesicles, which are presumed to originate at the cell membrane (Figure 27), the Golgi apparently does not have a central role in trafficking endocytosed SAG1. This highlights the need to investigate alternate routes and regulatory mechanisms.

Micropore and Alternate Mechanisms

The micropore has been implicated as the entry point for endocytosed material in *T. gondii* (61,62). Although direct evidence for SAG1-Halo vesicle entry via the micropore remains elusive, previous studies have shown that the micropore contains a K13 ring embedded in the IMC and adaptor proteins (AP-1, AP-2α, and AP-2μ), while Dynamin (DrpC) at the base of the tunnel facilitates vesicle cleavage (61,63,64). In this study, a high colocalisation of ISAP1 and DrpC with SAG1-Halo vesicles was not observed. However, endocytosis at the micropore may occur too rapidly to be effectively visualised using the microscopy techniques employed in this thesis. It remains uncertain whether all endocytosis pathways in *T. gondii* rely on the micropore and dynamins, which are key players in clathrin-mediated endocytosis in eukaryotes, but whose roles in this parasite have not yet been demonstrated (301).

In other protozoan models, the start of endocytosis employs diverse mechanisms. *Trypanosoma* forms clathrin-coated pits at the flagellar pocket, recruiting adaptor proteins such as TbEpsinR and TbCALM, but not AP-2 (197,198). By contrast, *Plasmodium* employs endocytosis for haemoglobin uptake at the cytostome, involving AP-2 adaptors and Kelch13 (199–203). It is therefore plausible that *T. gondii* adopts a hybrid endocytic system, integrating both clathrin-dependent and clathrin-independent processes, depending on the specific cargo and physiological context. Recent studies in *P. Falciparum* found clathrin to be involved with AP1 and the haemoglobin uptake shedding new insides on endocytosis in apicomplexan parasites (302).

Interestingly, as SAG1 vesicles accumulate at the plasma membrane, as observed in FLP2 knockdown experiments, a higher colocalisation with DrpC becomes evident (Figure 34 and FLP2 Discussion). This observation suggests that FLP2 depletion may enhance DrpC recruitment to vesicles at the plasma membrane, potentially implicating DrpC in the vesicle accumulation phenotype. Alternatively, the immobility of the SAG1 vesicles may facilitate the visualisation of their interaction with DrpC.

Apical Annuli and Alternative Secretory Pathways

In *T. gondii*, five apical annuli proteins have been identified (56). Chelaghma et al. reported that the annuli participate in dense granule exocytosis (53). This study explored the potential involvement of apical annuli 3 (AAP3) as a site for SAG1 exocytosis. However, only low levels of colocalisation were observed between SAG1 vesicles and AAP3. Furthermore, GRA2, a protein associated with modifying the PV, similarly exhibited minimal overlap with SAG1 vesicles. These findings suggest that, in contrast to GRA proteins, which are secreted specifically at the apical annuli (53,55–57), SAG1 endocytosed vesicles may not be secreted via this pathway.

This aligns with the limited interaction between Rab11A, known for its role in transporting GRA proteins from the trans-Golgi network (TGN) to the apical end (246) with SAG1 vesicles. The minimal colocalisation of GRA2 with SAG1 vesicles and its known association with PV and intravacuolar network (IVN) (303) further suggest that GRA2 may not be an appropriate marker for studying SAG1 trafficking. Nevertheless, the large family of GRA proteins in *T. gondii* (304) cannot be entirely excluded as potential contributors to SAG1 vesicle trafficking.

These observations indicate that SAG1 exocytosis diverges from the classical route used by dense granule proteins and may require a different apical annuli component, an alternative SNARE protein, or an entirely separate exocytic pathway. It would therefore be of interest to examine whether SAG1 vesicles colocalise with microneme proteins, which are secreted via the conoid, (54) or whether they resemble rhoptry discharge by forming a rhoptry secretory apparatus (RSA) that docks to an apical vesicle (AV) (55,305).

Further to colocalisation studies with microneme and rhoptry proteins, other GRA proteins and Rab proteins like Rab6 (known to be involved in F-actin transport), (251) could provide additional insights into the regulatory factors and pathways governing SAG1 trafficking. Such studies would clarify whether SAG1 vesicles follow a unique exocytic pathway or share mechanisms with other secretory proteins in *T. gondii*.

In eukaryotes, exocytosis is often seen to be SNARE-dependent vesicle fusion or full-collapse fusion, requiring a large pore that has not yet been documented in *T. gondii* (306). The ‘kiss-and-run’ mechanism, characterised by a transient small pore, is also possible but has been

mainly studied in specialised neuronal cells (307). Whether comparable exocytic processes occur in *T. gondii* demands further investigation. It is also conceivable that homotypic fusion, the fusion of two similar membranes without requiring specific exit proteins such as SNAREs or Rabs, plays a role (121), although this was beyond the scope of the present thesis.

Overall, understanding the trafficking pathways, entry sites, and release mechanisms of SAG1 vesicles requires more extensive investigation. One potential approach involves tagging Rab5b with biotin to identify interaction partners, thereby shedding light on Rab5b's function in endocytic trafficking (40). The proximity-labelling nature of such techniques may capture a broad spectrum of proteins that are encountered during vesicle trafficking. Nonetheless, proximity labelling remains a valuable strategy for mapping the vesicle's pathway through the parasite. Another promising avenue is BioID or TurboID tagging of Rab5b (40), which could similarly reveal critical interaction networks. Likewise, "Localisation of Organelle Proteins by Isotope Tagging" (LOPIT) (308) offers a powerful method for mapping vesicle trafficking routes. When combined with selective trypsinisation of the membrane, it may be feasible to extrude intracellular or endocytosed vesicles and analyse them via mass spectrometry. Given Rab5b's central role in endocytic events, it is a prime candidate for such characterisation studies in *T. gondii*.

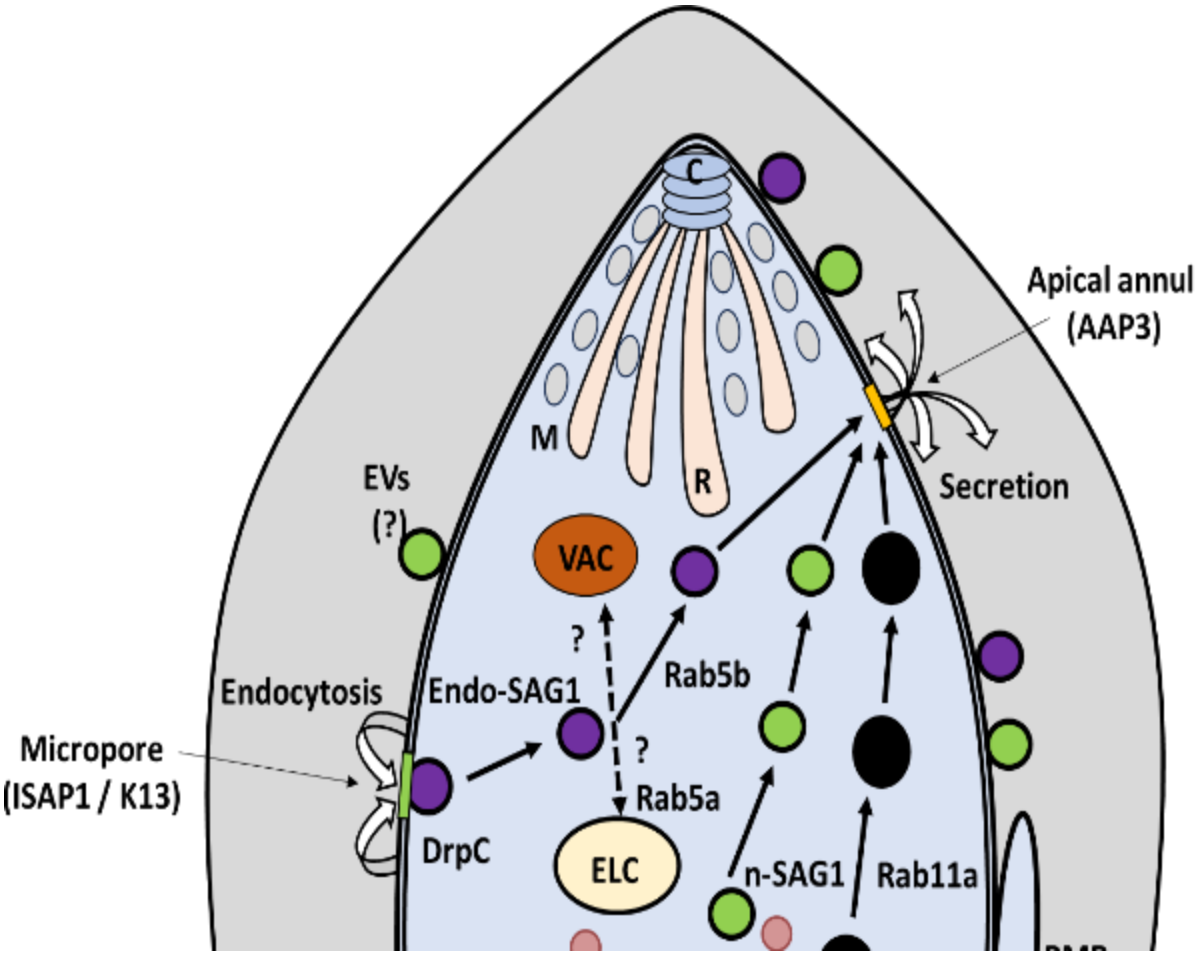

Figure 40: ***Schematics of SAG1 potential vesicle trafficking through the parasite****. These schematics illustrate that the trafficking of different SAG1 populations operates independently. Furthermore, they demonstrate the interaction of endocytosed SAG1 with Rab5b, but not with Rab5a or Rab11a.The diagrams should highlight the distinct vesicle populations, tracing the journey of endo-SAG1 from the micropore to the annuli, and n-SAG1 from the Golgi to secretion.*

The colocalisation assays conducted in this study focused exclusively on endocytosed vesicles, leaving open the possibility that the trafficking routes for newly synthesised SAG1 vesicles may differ. Newly synthesised proteins, including SAG1, must pass through the ER and Golgi for post-translational modifications and packaging into COPI or COPII vesicles (90,102). Sorting for GPI-anchored proteins at the Golgi can vary by cell type, leading to diverse trafficking routes to the plasma membrane (256,309). While it is plausible that recycled and newly synthesised SAG1 vesicles intersect at the TGN, triple-labelling experiments performed in this thesis (Figure 26) showed only partial overlap between the three SAG1 populations. This partial overlap suggests transient or specialised interactions during their respective trafficking pathways within the parasite. However, further investigation is necessary to determine the precise nature of these interactions and identify the mediator proteins involved.

Clarifying whether these vesicles carry nutrients, receptors, or plasma membrane components is crucial for understanding their role in parasite biology. At present, the specific cargo of these vesicles remains unknown, demanding deeper exploration of their functions. Collectively, these data underscore the complexity and dynamism of SAG1 trafficking pathways, suggesting that *T. gondii* uses diverse and possibly unique mechanisms to regulate endocytosis and exocytosis.

3.4. MyoF: The Motor Protein for Vesicle Movement

Myosins are motor proteins that move along actin filaments using their myosin head domain, their tails often bind to cargo such as endocytosed vesicles (123). In *Toxoplasma gondii*, myosins are best known for their role in the actin-myosin motors contributing in gliding motility and host-cell invasion, where they are crucial for the parasite's glidosome (79). Recently, the Heaslip lab identified MyoF as a key player in rhoptry and dense granule trafficking, as well as a factor influencing Golgi development and apicoplast inheritance (251). In non-apicomplexan parasites such as *Trypanosoma cruzi*, MyoF is also expressed in the endocytic pathway (310), suggesting that MyoF may have a broader role in vesicle transport.

In this study, MyoF was investigated to assess its role in endocytosis and the trafficking of various SAG1 vesicle populations. Significant differences were observed in vesicle movement depending on the presence or absence of MyoF. When MyoF was absent, vesicle motion progressively slowed and ultimately ceased, leading to vesicle accumulation in the residual body, showing the impaired trafficking of SAG1 (Figure 28D–E). Despite this disruption, membrane inheritance by daughter cells during replication remained unaffected (Figure 29). This suggests that while MyoF is not explicitly required for the initial endocytic uptake of vesicles, it likely contributes to their subsequent intracellular movement within the parasite's cytoplasm.

Triple-labelling experiments revealed a slight increase in the accumulation of all labelled vesicles, coupled with a decrease in 'endo-int' vesicles. These findings indicate a general disruption of the vesicle trafficking system, with n-SAG1, M-SAG1, and PM-SAG1 vesicles all accumulating within the parasite (Figure 30). Although MyoF appears to play a crucial role in

vesicle transport, the motor protein(s) directly responsible for endocytic uptake in *T. gondii* remain unidentified.

In other eukaryotic cells, myosins mediate both long- and short-distance cargo transport by attaching vesicles to actin filaments for movement towards lysosomes, the Golgi, or other destinations (123,148). In *T. gondii*, MyoF is one of 11 myosins known in the parasite and, together with MyoA, is conserved within the apicomplexan phylum (245,251,304,311,312). It has also been implicated in apicoplast inheritance, working in conjunction with actin and Formin-2 to ensure correct organelle division (245,251,311). However, while MyoF's involvement in the movement of SAG1 vesicles was demonstrated in this study, it was not shown to affect SAG1 endocytosis per se. The precise mechanism by which MyoF might influence SAG1 vesicle trafficking remains unclear.

In eukaryotic cells, myosin isoforms perform diverse roles. For example, Myosin IE is associated with vesicle assembly during clathrin-mediated endocytosis (148), while Myosin VI isoforms regulate endocytosis and vesicle sorting in specific tissues (123). Generally, myosin mediate organelle motility, including mitochondrial positioning and ER dynamics (123,312,313). In general Myosin I supports short-range membrane transport and endocytosis, whereas Myosin V mediates Golgi-to-plasma membrane transport (123,148). TgMyoF exhibits remarkable structural similarity to Myosin Va in eukaryotes (251), which has multiple roles depending on isoform and cell type. Among the three Myosin Va isoforms in humans, the most abundant is highly enriched in the brain, where it participates in exocytosis alongside t-SNARE proteins (314,315). In dendritic cells, Myosin Va mediates mRNA transport (316), while Myosin Vb facilitates endosome recycling (317). This structural conservation suggests functional parallels but also highlights the potential for isoform-specific roles. In protozoa like *Entamoeba histolytica*, Myosin IB interacts with EhFP10 to facilitate phagocytosis and pinocytosis via actin cytoskeleton regulation (318).

In eukaryotic cells, vesicle movement relies on the cytoskeletal network, which provides tracks (actin filaments and microtubules) and mechanical force (motor proteins). In *T. gondii*, MyoF and actin cooperate in dense granule trafficking and organelle segregation, such as in the apicoplast (245,251). However, a similar interaction specifically involving SAG1-Halo vesicles was not observed in this study. Myosin types mediate distinct cargo trafficking activities along

actin filaments: For example Myosin I anchors actin to the plasma membrane, facilitating membrane bending and supporting endocytosis (319), while Myosin II drives clathrin-independent endocytosis (320). Myosin Vb is particularly associated with Rab11-positive recycling endosomes this association with Rab11 could not be found for SAG1 Halo vesicle, and Myosin VI isoforms are specialised for apical vesicle transport in polarised cells (321,322). These might underscore the type- and paralogue-specific roles of myosins, raising the possibility that other myosins in *T. gondii* may contribute to SAG1 vesicle trafficking.

The halted vesicle movement observed in this study indicates a role for MyoF in vesicle transport. However, its role in exocytosis and endocytosis remains inconclusive. This is evidenced by the unaffected membrane distribution to daughter cells (Figure 29) and the continued presence of endocytosed SAG1-Halo vesicles inside the parasite, irrespective of MyoF knockdown. Collectively, these results highlight MyoF's contribution to intracellular trafficking while suggesting the involvement of additional or alternative motor proteins in SAG1 endocytosis.

As part of this network, actin is known to fulfil diverse functions in eukaryotic cells, including supporting short-range vesicle transport near the plasma membrane and facilitating endo- and exocytosis (142). It also supplies the mechanical force for membrane budding and vesicle scission (145,146). Given its well-established roles in vesicle generation and intracellular sorting, actin might serve as a critical component of endocytosis in *T. gondii* (146,162,323). However, experimental challenges prevented studying actin directly in this thesis. The treatment with actin-depolymerising drugs such as Cytochalasin D (CytoD) (324), generated autofluorescence and the CytoD resistant cells showed excessive cell overgrowth, complicating microscopic analyses. Advanced imaging tools and single-particle vesicle tracking could potentially overcome these technical obstacles, yielding more definitive insights into actin's role in endocytosis.

Considering that actin and myosin are highly conserved throughout the Apicomplexa and play analogous roles in diverse eukaryotes, they remain likely candidates for powering endocytosis. Indeed, in mammalian cells, actin polymerisation near the plasma membrane drives both clathrin-mediated and clathrin-independent endocytosis (162,186), while myosin motors facilitate vesicle movement along these actin tracks (325).

In this study, MyoF was confirmed to have a role in SAG1 vesicle transport, a specific function in SAG1 endocytosis remains unproven. Future research should investigate other myosin isoforms in *T. gondii*, given the diversity of myosin functions in cell biology. For example, Myosin A supports gliding motility and mitochondrial inheritance, whereas Myosins B and C remain poorly characterised. MyoJ and MyoI are critical for residual body integrity and mediate the flow of GPI-anchored proteins to daughter cells (261), making them intriguing targets for endocytic pathway exploration, along with MyoH, which operates within the conoid (326). Ultimately, dissecting the interplay of these motor proteins with actin will illuminate the molecular mechanics of SAG1 endocytosis.

Potential Roles of Other Motor Proteins

Because MyoF the class XIV myosins, which are unique to apicomplexans, may not participate in endocytic trafficking, it is plausible that alternative motors are directly responsible. Kinesins and dyneins, well characterised for anterograde and retrograde microtubule-based transport, respectively, are also prime candidates (149,327). These proteins move cargo directionally along microtubules and could thus participate in vesicle transport within the parasite.

Microtubules form another polarised component of the cytoskeletal network and are anchored at the MTOC (69,149). While actin generally supports short-range transport, microtubules mediate longer-range movements, for instance between the ER and Golgi (69). Notably, actin and microtubule networks function cooperatively to promote efficient vesicle transport (144), enabling vesicles to switch smoothly between these filament systems. Although dense granule transport in *T. gondii* does not appear to rely on microtubules, (47,245) SAG1 vesicles may use different pathways. In many eukaryotes, kinesin (types 1, 2, and 3) and dynein (328) can shuttle vesicles from and to the plasma membrane and back in a bidirectional manner, often handing them off to myosin motors for actin-based transport (325,329). Such a mechanism, if present in *T. gondii*, would align with the observed termination of SAG1 vesicle movement in the absence of MyoF, while endocytic uptake itself remains unaffected (Figure 28-29). The initial transport phase could be microtubule-mediated, with vesicles later transferred to MyoF to actin pathways, thus explaining the partial but not absolute block in SAG1 trafficking when MyoF is disrupted.

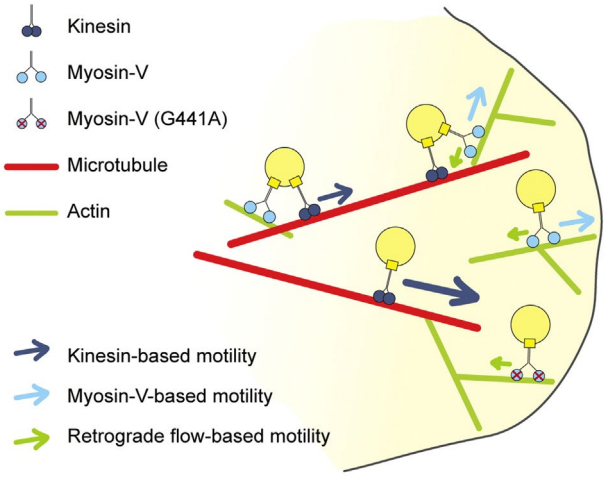

Figure 41: ***Interaction between actin****, Myosin and microtubules to ensure transport from and to the membrane. Picture from current biology (150). Image from Kapitein et al. 2013.*

Finally, it cannot be excluded that some SAG1 vesicles are transported through passive diffusion within the parasite cytoplasm, particularly near the plasma membrane, where molecular crowding might facilitate random collisions akin to smaller molecules (330). Alternatively, vesicle movement might occur passively via cytoplasmic streaming, a phenomenon observed in eukaryotes (331,332). Notably, the potential interaction of MyoF with kinesin could provide deeper insights into SAG1 endocytosis. This hypothesis is supported by studies in other eukaryotes, where Myosin V interacts with kinesins in dendritic cells and plays a role in endosomal recycling in HeLa cells (150,333,334). The interplay of multiple routes, microtubule, actin, and diffusion based, could ensure robust vesicle traffic under varying conditions.

3.5. FLP2: what Role Plays the Membrane Composition in Endocytosis

In this thesis TgFLP2 mAID parasites were investigated for the role of FLP2 in endocytosis trafficking and trans-Golgi vesicular trafficking. Trans-Golgi trafficking is important for both endocytic and exocytic events in eukaryotic cells, and in *Toxoplasma gondii*, it is especially crucial for the transport of secretory proteins such as dense granules, rhoptries, and micronemes. Secretion depends on the secretory pathway, in which proteins are trafficked

from the endoplasmic reticulum (ER) to the Golgi and then translocated to the endosome-like compartments (ELCs) via TgSORTL. This pathway is essential for the maturation of these proteins and their subsequent secretion (335).

Here, it was demonstrated that FLP2 is not directly involved in endocytosis. But absence of FLP2 resulted in parasites with disorganised Golgi and lower levels of SortLR (Figure 31) and accumulation of aberrant big vesicles inside the parasite (Figure 33-34). FLP2 appeared to be crucial for efficient trafficking and correct Golgi morphology but was not found to inhibit SAG1 endocytosis. Flippases are enzymes that translocate membrane lipids and proteins from one leaflet of a bilayer to the other, thereby maintaining lipid asymmetry (214). This asymmetry is essential for processes for instance signal transduction and membrane bending, and its inhibition can severely impair or even block endocytosis in eukaryotic cells. P4-ATPases promote lipid asymmetry, particularly at the TGN, and their disruption can lead to widespread defects in vesicular trafficking (106). While some P4-ATPases localise to various secretory pathway membranes (336), P5 ATPases, predominantly reside in the ER (337). Across eukaryotes, three clades of P4-ATPases (P4A, P4B, and P4C) have been identified (337) with members playing diverse roles in vesicle formation and trafficking (107–109). To function correctly, they require CDC50 as a β-subunit to form heteromeric complexes (338). A similar role is indicated for FLP2 as it is also localised in the Golgi.

In Humans P-type ATPases form a large transport family that includes H^+ ATPases and SERCA ATPases and comprise 14 P4-ATPases that function as phospholipid Flippases (339). In humans the ATPases are divided into five classes, many of which are central to endo- and exocytic mechanisms (340). For example, ATP11C acts as an ‘eat-me’ signal (341), while ATP8A1 is critical for membrane trafficking within recycling endosomes (342). The closely related *Caenorhabditis elegans* TAT-1 is implicated in maintaining endo-lysosomal compartments and sorting endocytic cargo (343), highlighting the conserved roles of P4-ATPases in vesicular trafficking and Golgi dynamics across species (342).

Making FLP2 an interesting target for investigation endocytosis and vesicle trafficking in *T. gondii*. While in *Toxoplasma gondii*, flippases appear to play key roles in secretion of the secretory organelles, and organelle membrane maintenance. Recent studies identified a heterocomplex of CDC50.4 and ATP2B/ATP2A that functions as PS flippases at the plasma

membrane and influences microneme exocytosis (109,215). This complex, which is highly conserved across the Apicomplexa phylum, has been implicated in flipping phosphatidylethanolamine (PE) and PS in *Plasmodium chabaudi*, as well as internalising NBD-labelled PS in *P. falciparum* (344) .Genome analyses show that *P. falciparum* encodes three P4-ATPases, two are essential in blood-stage parasites (345) whereas *T. gondii* expresses five ATPases (346).

The absence of FLP2 resulted in parasites with disorganised Golgi and lower levels of SortLR (Figure 31). The loss of SortLR may disrupt the TGN, which is responsible for vesicle sorting (107,108), ultimately leading to the collapse of the Golgi. Showing that FLP2 appeared to be crucial for correct Golgi morphology but was not specifically related to endocytosis aligning with the function and localisation in other investigated eukaryotic cells. While one of the four CDC50 proteins in *Toxoplasma gondii* localises to the Golgi, (346) interactions between FLP2 and CDC50 have not yet been demonstrated.

Similar disruptions in vesicular trafficking have been observed in *Saccharomyces cerevisiae*. The absence of P4-ATPases in yeast leads to misdistribution of aminophospholipids, delayed endocytosis, and vesicle-budding defects at the cell membrane, stemming from Golgi-derived secretory vesicles. The Drs2p ATPase exhibits phenotypic similarities to TgFLP2 mutants, including TGN protein mislocalisation, Golgi swelling, reduced clathrin levels, and defects in vesicle budding (347). Similar effects have been observed in the depletion of other P4-ATPases, such as the endosome-associated Neo1p, which caused defects in receptor-mediated endocytosis (348), and MGATP2 in rice plants, where its absence reduced the secretion of extracellular enzymes (349) as well as in *Arabidopsis thaliana*, ALA3 (a Golgi-localised P4-ATPase) is vital for secretory vesicle formation (350). These findings collectively suggest that P4-ATPases are essential for vesicle formation across species in different stages of intracellular trafficking (351) as seen in FLP2 KD parasites. These parallels highlight the role of P4-ATPases in maintaining membrane asymmetry and indicate that FLP2 deficiency in *T. gondii* likely alters membrane biophysical properties, contributing to SAG1 vesicle accumulation and Golgi fragmentation.

The colocalisation of M-SAG1 and n-SAG1 was slightly altered in the absence of FLP2, with increased colocalisation between the two populations (Figure 32). This finding highlights an

effect on the trafficking of both old and newly synthesised SAG1 populations. Interestingly, the absence of FLP2 led to the aberrant formation of giant SAG1 vesicles on the parasite membrane. Additionally, the loss of FLP2 resulted in increased vesicle fusion inside the parasite, involving both de novo and endocytic SAG1 pathways, although these pathways themselves appeared unaffected by the absence of FLP2 (Figure 33). These vesicle accumulations were found to be associated with DrpC but not the ISAP1 (Figure 34). In the FLP2 mutant, DrpC was heavily recruited to the aberrant vesicle formations, suggesting a supporting role in vesicle cleavage and its specific recruitment to endocytosed vesicles. The observed increase in DrpC fluorescence may indicate, that the parasite is experiencing issues with membrane cleavage or curvature.

The accumulation of enlarged endocytosed vesicles at the plasma membrane was striking, indicating alteration of the vesicle transport resulting from the absence of FLP2. Vesicle formation has been shown to be influenced by plasma membrane composition, ion concentrations, and clathrin (352,353). Clathrin, which is typically associated with the Golgi, may play a role here. The absence or dysfunction of the Golgi could be related to the increased fusion of SAG1 vesicles. This dysfunction appears to be recognised by the parasite, leading to an overproduction of DrpC.

It can be speculated, that these effects result from a potential shift in membrane tension: vesicles with an altered lipid composition may become more rigid. Consequently, increased recruitment of cleaving proteins, such as DrpC, would be required to overcome this rigidity. Overproduction or heightened recruitment of DrpC may represent a compensatory mechanism to counteract vesicle rigidity or alleviate membrane tension caused by lipid imbalances. Alternatively, the prolonged cutting time required for scission of these rigid vesicles might make the scission process more readily observable in *T. gondii*. The apical accumulation of vesicles were not micropore related but if these vesicles accumulate at the apical annuli could not be investigated during this thesis it might be interesting to include this colocalisation in further study.

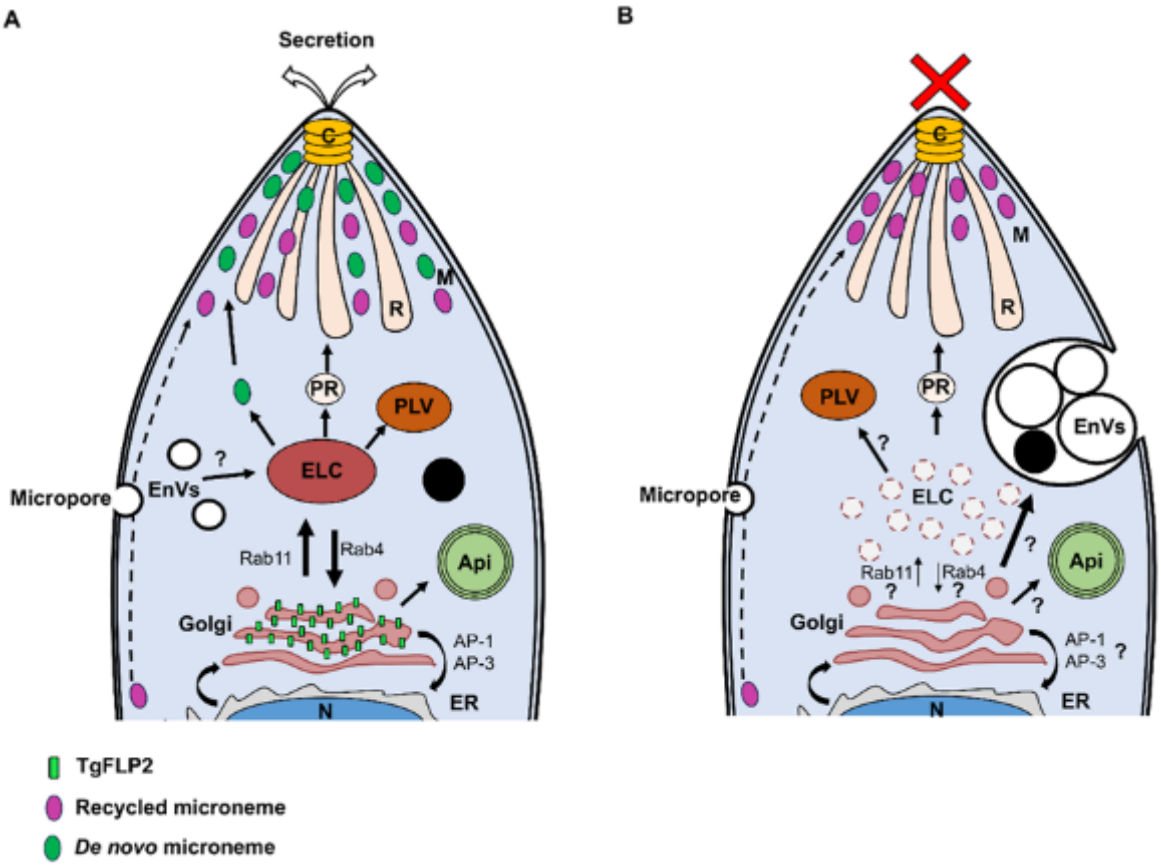

Figure 42: ***Overview highlighting vesicle transport with and without FLP2. A)*** *Overview of endocytosed vesicle movement to the ELC.* ***B)*** *disruption and fragmentation of the ELC in the absence of FLP2, leading to increased endocytosis vesicle fuse and accumulation on the membrane.*

Two models have been proposed to explain how P4-ATPases facilitate vesicle scission. The first model suggests that P4-ATPases catalyse inward-directed phospholipid translocation across the lipid bilayer, creating an imbalance in phospholipids that drives inward membrane bending and budding (354,355). The second model posits that ATP-driven lipid translocation generates a membrane environment conducive to vesicle budding by increasing the concentration of aminophospholipids (356,357). Both mechanisms highlight the critical role of P4-ATPases in endocytotic and exocytotic processes, as evidenced by their ability to induce endocytotic-like vesicles and accelerate endocytosis (358,359).

Which one of the two models is accurate in *T. gondii* needs to be investigated. But the principles seem to apply to *T. gondii*, where FLP2 deficiency disrupts normal SAG1 vesicle trafficking. P4-ATPases have been shown to play crucial roles in endocytosis and vesicle trafficking across various eukaryotic model organisms, depending on their localisation (340). It can be speculated that FLP2 performs a similar function, as its depletion resulted in vesicle

accumulation and Golgi fragmentation, suggesting that these functions are broadly conserved across species. However, further investigation is needed to determine the extent to which P4-ATPases in *T. gondii* mirror their counterparts in other eukaryotes. Nevertheless, the functional similarity between P4-ATPases in *T. gondii* and those in other systems remains to be fully elucidated. These findings suggest that the roles of P4-ATPases in *T. gondii* are likely diverse, with additional flippases potentially contributing to endocytosis and vesicle trafficking.

Further investigation of other flippases in *T. gondii* may provide insights into membrane homeostasis and endocytosis. For example, ATP2B/ATP2A, previously identified as PS flippases at the plasma membrane (109,215) could be a promising starting point for future studies. Moreover, TgP4-ATPases have been localised to various cellular compartments, with TgP4-ATPase1 and TgP4-ATPase2 salvaging host-derived lipids, TgP4-ATPase3 playing a role in the lytic cycle, and TgP4-ATPase2/5 present in the plasmalemma and cytomembranes (346).

Future studies comparing *T. gondii* ATPases with those in yeast and other eukaryotes could provide valuable insights into FLP2's specific functions. Additionally, floppases and scramblases, which transport lipids in the opposite direction or in both directions, may influence membrane composition and vesicle fission. A deeper understanding of P4-ATPase roles in *T. gondii* membranes and organelles is essential for explaining how lipid composition impacts inter-organelle vesicular trafficking and endocytosis.

3.6. PMR: the Membrane Reservoir affected by K13 and MyoF

During live-cell investigations, it was shown that the PMR forms on the cell membrane. This structure is transient, with neither its position nor size fixed. Strikingly, these PMRs always formed during replication and disappeared as soon as the daughter cells completed their maturation (Figure 35). These PMRs resembled the aberrant structures observed in the K13 KD. Previous studies may have misinterpreted PMRs as artefacts resulting from cell fixation and permeabilization techniques. However, using the SAG1-Halo technique, which enables live-cell imaging, it was demonstrated that reservoir formation is not an artefact of labelling techniques, but a natural biological phenomenon. PMRs were found in all replicating

parasites, confirming they are not a product of dying parasites (Figure 38). Another reason PMRs could be missed is their fusion with the residual body during replication, which makes it difficult to distinguish the two structures (259,360).

Still questions remain about the function of the PMR as a reservoir and the mechanisms underlying its generation and absorption. In *Plasmodium* parasites, a similar formation of additional membrane during development and division has been observed (257). In contrast, membrane reservoirs identified in *Drosophila* cells during cellularisation exhibit a fold-like structure, which unfolds as the cell grows (361), rather than the accumulation seen in *Toxoplasma*. However, in dividing eukaryotic cells, membrane accumulation similar to the PMR can also be observed, driven by both endocytosis and exocytosis (362,363). Furthermore, caveolae are considered membrane reservoirs in eukaryotic cells which was not shown for apicomplexan parasites like *T. gondii*. These specialised, tight membrane structures can flatten and disassemble under mechanical stress, increasing the cell surface area and preventing membrane tearing (364). The overall function of these membrane reservoirs is to act as pool for rapid integration in the PM, when needed. This can be for membrane homeostasis and repair of trauma induced damage of the PM (365,366). The PMR in *T. gondii* differs significantly from other known membrane reservoirs but exhibits similarities to membrane blebs, which are transient, balloon-like structures on the plasma membrane of cancer cells. These blebs are particularly important in amoeboid migration and cell survival under stress conditions (367). Cancer cells proliferate at a rapid rate and migrate through various tissue structures, experiencing significant plasma membrane tension stress, which shows parallels to the behaviour observed in *T. gondii*. It remains debatable whether the increased PMR formation in *T. gondii* arises from a greater demand for membrane material during replication or if it represents a distinct mechanism unrelated to the responses to mechanical stress seen in other systems.

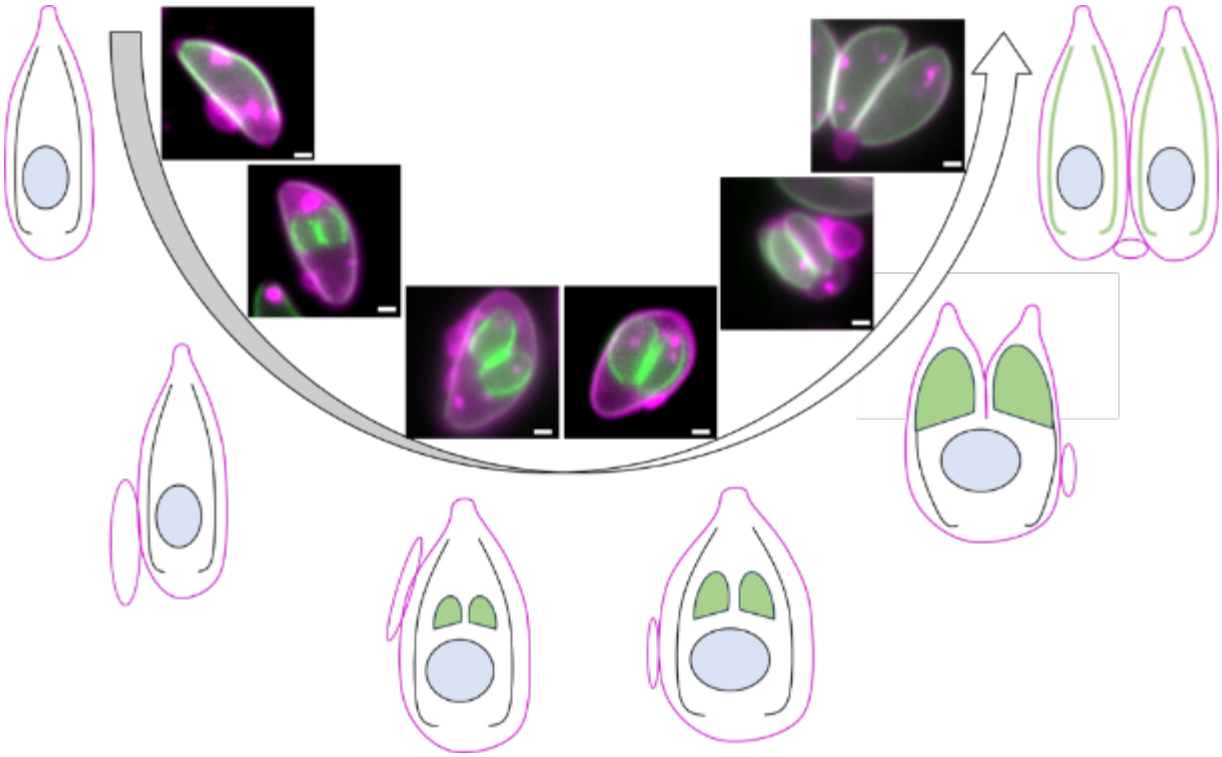

Figure 43: ***Example schematics of the formation of the PMR in time with the formation of the daughters****. Here, SAG1 Halo is magenta, and IMC1 YFP is green. It shows the formation of the PMR before daughter cell formation starts and its translocation to the basal area of the parasites at the end of daughter formation.*

An in-depth analysis of the K13 knockdown revealed a significant accumulation of the PMR on the cell surface of dividing parasites, exceeding what was observed in the absence of MyoF (Figure 38). This finding underscores the role of K13 in maintaining membrane homeostasis and functioning as a gatekeeper for membrane reservoir uptake. Colocalisation studies between K13-eGFP and the PMR yielded no significant results. Given that the PMR is secreted from the plasma membrane and translocated across the entire parasite, a stable localisation with K13 was not anticipated.

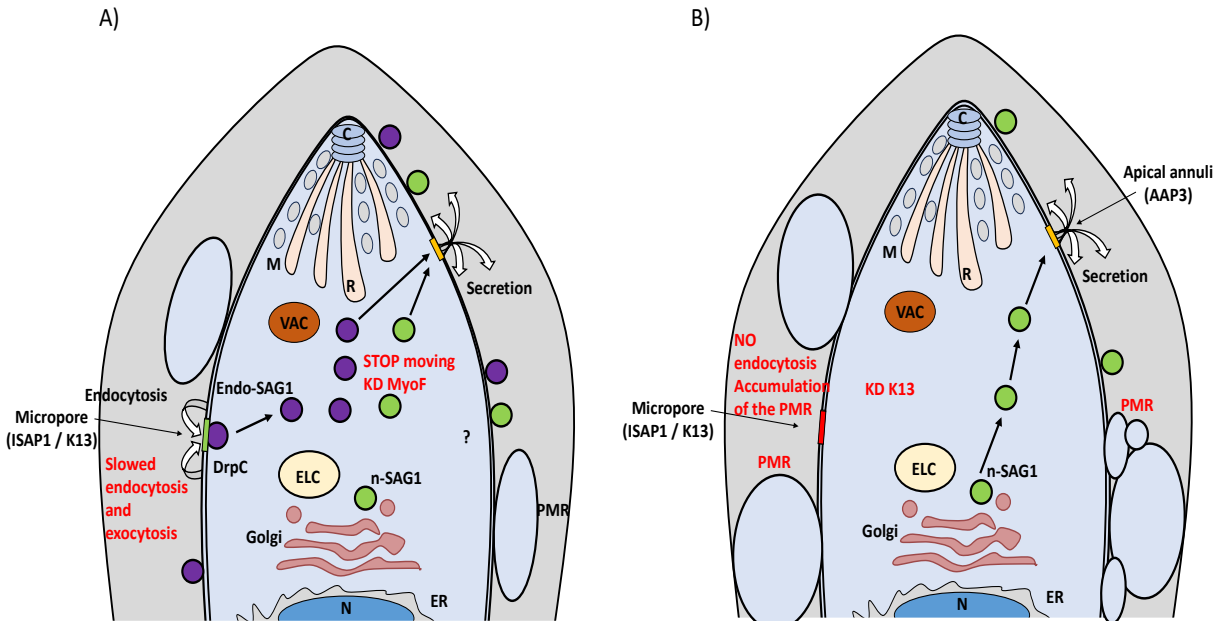

Figure 44: ***Comparison schematics of MyoF KD and K13 KD. A)*** *Showing the slowed endocytosis in the MyoF knockdown to* ***B)*** *The complete abolished endocytosis without K13 and increased accumulation of the PMR.*

In *Plasmodium falciparum*, the K13 protein has been associated with artemisinin (ART) resistance by altering the uptake of haemoglobin at the cytostome (200,202–205). This highlights the role of K13 in endocytosis in *Plasmodium*, particularly in the uptake of host cell material. Initially, the micropore in *Toxoplasma gondii* was also thought to play a role in nutrient uptake. More recently, it was discovered that the K13 pore has a direct connection to the parasite plasma membrane and is heavily involved in endocytic events (61,62). Its absence led to an increase in aberrant membrane structures on the parasite membrane and ultimately resulted in parasite death. In contrast, Wan et al. demonstrated that nutrient uptake from the host cell relies on endocytic events occurring at the micropore, suggesting that parasites starve and die in the absence of the K13 pore (62).

The question remains whether the micropore has an additional role in nutrient uptake. Its precise function in endocytosis or general membrane uptake is still under investigation, approached through a SILAC experiment. SILAC (Stable Isotope Labelling by Amino Acids in Cell Culture) is based on the incorporation of heavily labelled amino acids. The idea is, that parasites in heavily labelled host cells would scavenge host nutrients, and take up the heavy amino acids (368). A comparison between control and K13 KD parasites should clarify whether the micropore is involved in nutrient uptake. If the micropore plays a role, KD parasites should show no trace of heavy-labelled amino acids from the host cells. Through the amount of SILAC

integration in the host cell a direct quantification of the uptake amino acids in the parasite can be shown, and this over the whole proteome and where the amino acids are processed. This provides a more detailed analysis than what is achievable with GFP. Other host cell uptake assays, which rely on fluorescently labelled host cells, have shown limited success (369). All these approaches have weaknesses and limitations in elucidating the overall function of the micropore in nutrient uptake and endocytosis. Further investigations into the micropore should focus on host cell protein and nutrient uptake, to improve our understanding of these unique cell structures and their roles in endocytosis.

3.7. Conclusion and Remarks

Using Halo technology and relying on dyes with distinct physicochemical properties, it was possible to visualise PM dynamics in replicating parasites, trace membrane inheritance to daughter cells, and investigate the different SAG1 sub-populations. This study highlights the complexity of endocytosis in *Toxoplasma gondii*. In *Plasmodium*, endocytosis is tightly regulated to facilitate haemoglobin uptake from the host cell, involving an endocytic complex consisting of PfRabsn5, PfRab5, and PfVPS45. In contrast, endocytosis in *Toxoplasma gondii* appears to be regulated differently.

This study successfully identified Rab5b as the most prominent candidate for vesicle trafficking. This finding shows clear alignment with Rab5b's established role in haemoglobin endocytosis in *Plasmodium falciparum* (201,203) as well as its involvement in endocytosis at the flagellar pocket in *Trypanosoma* (197) and its relationship with early endosomes in *Leishmania* parasites (370).

Myosin F (MyoF) was shown to be essential for general vesicle transport, including the trafficking of SAG1 vesicles, GRA proteins, and micronemes, validating its previously suggested role in vesicular trafficking. However, MyoF's direct involvement in membrane endocytosis could not be confirmed and may depend on other motor proteins, requiring further investigation. Furthermore, this thesis highlighted the importance of phospholipid composition in the trans-Golgi network (TGN) and vesicle trafficking.

By employing various microscopy techniques, this work validated the plasma membrane reservoir (PMR) as a genuine biological structure, rather than an artefact. It demonstrated a novel mechanism of PMR formation in *T. gondii*, which is comparable to membrane reservoir formation observed in eukaryotic cells. Additionally, the study confirmed the involvement of K13 in PMR uptake and membrane homeostasis.

Through these findings, this thesis sheds light on endocytosis in *Toxoplasma gondii*, a process that has previously been difficult to study. However, the precise trafficking mechanisms and protein interactions remain unclear, necessitating further research to fully understand endocytosis in *Toxoplasma*.

Supplemented Information will be provided on an CD Room at the end of this thesis. Containing Videos of vesicle moving in MyoF KD.

4 Material and Methods

4.1.1 Equipment

Table 1: Equipment used in this study

Machine	Manufacturer
Ad-Nucleofector ™	Lonza
Centrifuge %810R & 5910 R & 524 R	Eppendorf
Centrifuge MIKRO 200R	Hettich
ThermoMixer ®C & ThermoMixer® Comfort	Eppendorf
Microwave Inverter	HARP
-86°C ULT freezer	Hair Biomedical
HWAEUS PICO 21 Centrifuge	Bio-Rad $ Peqlab
Vortex Genie 2 ™	Bender &Hobein Ag Zurich, Switzerland
Agarose gel electrophoresis	Eppendorf
Refrigerated incubator Shaker Innova 4230	New Brunswick scientific
Analytic balance	Satorius, KERN
Dynamag™ -2 magnet	Thermo Fischer Scientific
FACSAria™ III	BD Biosciences
FastGene blue/green LED transilluminator	Nippon Genetics
Fridge	Siemens & Bosh
Genius dry bath incubator	Major Science
UM300 incubator	Memmert
Hercell ™240i incubator	Thermo Fischer Scientific
Innova™ 4200 incubator	New Brunswick Scientific
HERAsafe HS15 laminar flow hood	Thermo Heraeus
ENVAIReco® Comfort Plus laminar flow hood	ENVAIReco
3D STED microscopy	Abberior Instruments
Inverted Leica SP8X WLL confocal	Leica
Primovert microscope	Zeiss

Axiovert A1 microscope	Zeiss
DMi8 microscope	Leica
NanoDrop® ND- 100	Thermo Fischer Scientific
Neubauer haemocytometer	Carl Roth
Odyssey CLx	Li-Cor Bioscience
pH meter	Mettler Toledo
Accujet ® pro pipette	BrandTech
ErgoOne pipettes	StarLab
P93D printer	Mitsubishi
RICOH IM C5510A printer	RICOH
SB2 rotator	Stuart
MiniProtean SDS-Page & blotting	BioRad
Titertek shaker	Flow Laboratory
Mastercycler Pro thermal cycler	Eppendorf
Vacuum pump	A.Hartenstein
Vortex	Scientific Industries, Bender & Hobein GmbH
WB-12 water bath	Phoenix Industries

4.1.2 Computer Software

Table 2 Computer Software and online resources

Software	**Source**
Adobe Acrobat Reader	ADOBE System Inc
ApE Plasmid Editor v3.1.2.	Davis and Jorgensen 2022
Basic Local Alignment search tool (BLAST)	National institute for Biotechnology Information
Clustal Omega & MUSCLE	EMBL-EBI Medeira et al.
Eukaryotic Pathogen sgRNA Design Tool (EuPAGDT)	Peng and Tarleton, 2015
Gimp v2.10.34	GIMP's Team

FIGI Image V1.54f	Schindelin et al. 2012
Inkscape v1.3	GIMP
LasX v3.4.183668	Leica Microsystems
VEuPathDB & ToxoDB	Amos et al., 2022 Kissinger et al., 2003
Office 365 APPs for Enterprise v2308	Microsoft
BioRender	BioRender 2024

4.1.3 Consumables and reagents

4.1.3.1 Consumables

Table 3: Consumables used during this study

Product	**Source**
Eppendorf Tubes 1,5 / 2mL	Eppendorf
Cryovials, Falcon tubes (15mL /50mL), TPP cell culture vessels	Faust
Microscopy coverslips	A.Hartenstein
Microscopy slides, Parafilm	ROTH
Serological pipettes, aspirating pipettes	Starsted
Needles, gloves, syringes	SMS Medipool
Micropipette tips	StraLab
PCR tubes, Petri dishes, reagent reservoir	Avantor
Ethanol >99,5% PH.Eur.,reinst	ROTH
DNA LoBind Tube 1,5mL	Eppendorf
PCR Consumables/PCR-Product	Sapphire
Nitril NextGen Small	Meditrade
Biozym LE GeneticPure Agarose	Biozym
ROTIPHORESE r %0x TAE Puffer	ROTH

Glass bottom 96 well plates; uSlide 8 well Glass Bottom.	ibidi
Glass bottom dish 20mm micro-well # 1.5 cover glass	IBL
Bacteria cell spreaders, Sterile Filter Nylon 0,2um;	Roth

4.1.3.2 Kits

Table 4: Commercial kits

Kit	Manufacturer
ExtractMe Genomic DNA kit, ExtractMe Plasmid Mini kit, ExtractMe DNA clean-up & Gel-out kit	Blirt
P3 primary cell XL nucleofection kit	Lonza

4.1.3.3 Buffer & Solutions

Table 5: Buffer, solutions, and media prepared or modified in the house

Solutions	Components
LB medium	10 g/L tryptone, 5 g/L yeast extract, 10 g/L NaCl
LB media + Ampicillin	10 g/L tryptone, 5 g/L yeast extract, 10 g/L NaCl, Ampicillin 1ml/L
50% glycerol	50% glycerol (v/v) in ultrapure water
Supplemented DMEM	500mL DMEM 10% FCS (v/v) 4mM L-glutamine, 20ug/mL gentamicin
2x Freezing medium	50% FCS (v/v) , 20% DMSO (v/v), 30% supplemented DMEM (v/v)

1X TAE	1:50 50x TAE in water
Agarose	0,8-2% (w/v) agarose 1x TAE
4% PFA	1:5 20% PFA in PBS
Blocking Buffer	3% BSA (w/v) in PBS
Permeabilising buffer	0.2% (v/v) triton TX-100 on blocking buffer
Annealing buffer	10mM Tris-bases pH 7,5-8 50mM NaCl, 1mM EDTA

4.1.4 Reagents

Table 6: Commercial chemical and biological reagents

Product	**Source**
Trypsin EDTA	Biochrom L2143
4-20% Mini-PROTEAN TGX gels	BioRad 4561093
GelRed	VW 41003
Agarose	Hartenstein CA47
DMEM high glucose	Merck D6546
DMSO	Carl ROTH 4720.4
Ethanol	Carl ROTH T171.4
FBS	Merck F2442
Mounting Prolong gold	Thermo Fischer
Immersion oil Leica	Thorlabs MOIl-10LF
Isopropanol	Carl ROTH 9866.1
L-glutamine	Merck G7513
Lens Tissue	Thorlabs MC-50E
Methanol	Carl Roth 0082.2
Dulbecco's PBS	Merck D8537
20% paraformaldehyde	Electron Microscopy science 15713
Sodium acetate	Merck S2889
TAE	Carl Roth CL86.2

IAA	Merck 45533
rCutSmart	NEB B6004
BsaI HFv2	NEB r3733
1 kb + DNA ladder	NEB N0550
dNTPs	NEB N0447
Q5 HF DNA polymerase	NEB E0555
Quick load purple	NEB B7025
T4 DNA ligase	NEB M0202
T4 Buffer	NEB B0202S

4.1.4.1 Antibodies

Table 7: Primary antibodies

Antibody	**Dilution**	**Source**
HA rabbit	1:1000	Cell Signal tech 3724

Table 8: Secondary antibodies used for Halo and Immunofluorescence assays

Antibodies	**Concentration**	**Source &Cat. No**
Halo Tag Alexa Fluo 488	0,2uM	Promega
Halo Tag Alexa Fluo 660	0,2uM	Promega
Halo Tag oregon green	0.2uM	Promega
Janelia Fluor HaloTag ligand 549	200nM	Promega
Janelia Fluor HaloTag ligand 647	20nM	Promega

4.1.4.2 Drugs

Table 9: Drugs

Drug	**Stock concentration**
Ampicillin (100x)	100mg/mL H2O
Rapamycin (1000x)	50uM in DMSO
Auxin	500mM
Anhydrotetracycline (ATc)	1mg/ml in Ethanol used 1/1000 Clontech Labs

4.1.4.3 Oligos

Table 10: Oligos generated for this study

Oligos	Number in Lab	Gene	Sequence
gRNA fw	5028	SAG1	**AAGTT**GTGGAGTTTGCCGGGGCTGCA**G**
gRNA rev	5029	SAG1	**AAAAC**TGCAGCCCCGGCAAACTCCAC**A**
homology primer fw	5025	SAG1	GGGGATCGCCTGAGAAGCATCACTGTACCGTGAAACTGG AGTTTGCCGGGGCTAAAATTGGAAGTGGAGGA
homology primer rev	5026	SAG1	ATGGAAACGTGACTGGCTGTTCCCGCAGCCGATTTTGCTG ACCCTGCAGCCTTGTCGTCATCGTCTTTG
genotyping primer fw	5082	SAG1	ATCAAGAAGGAAGCATTTCCAG
genotyping primer rev	5083	SAG1	CCTTTGTCGATTTGAGAAGTGAG
gRNA fw	6594	SortLR	AAGTTGCTCCTACAGAGCTGCAAGAG
gRNA rev	6595	SortLR	AAAACTCTTGCAGCTCTGTAGGAGCA

homology primer fw	6596	SortLR	TTCCGCGTCTGGCGCCGCCGCGATTCGACGAGGATAACGT CGAACTTCTTGCTAAAATTGGAAGTGGAGG
homology primer rev	6597	SortLR	AAAGACATGCGAGACACGAAAGAGAGCCGTCTTCGGCGG AAGCTCCTACAATAACTTCGTATAATGTATGCTATACG
genotyping primer fw	6598	SortLR	CTGAGCAGGAGACGTCTCT
genotyping primer rev	6599	SortLR	AGATTTCCTTTGCAGGCACA
gRNA fw	7820	GRA2	AAGTTACTACGACGAAAGTGATGCGCG
gRNA rev	7821	GRA2	AAAACGCGCATCACTTTCGTCGTAGTA
homology primer fw	7822	GRA2	TGGAGCCCCAACAGCGGGCCGCACACGTGCCCGTCCCAG ACTTTTCGCAGGCTAAAATTGGAAGTGGAGG
homology primer rev	7823	GRA2	TTTTCACTGATCGGCTTTGTAGACTTCTCCCTTCAGCGGCTT TCCAGCCTATAACTTCGTATAATGTATGCTATACG
genotyping primer fw	7824	GRA2	GAAACTCGCGAATGTGGAGA
genotyping primer rev	7825	GRA2	ACAAGACCACCTCCCCA
gRNA fw	8093	DrpC	AAGTT ATGAAACTGTGTGGCTTGTGC G
gRNA rev	8094	DrpC	AAAAC GCACAAGCCACACAGTTTCAT A
homology primer fw	8095	DrPc	GTCAACCTGCAGGAAGTTCCGGTCGGCTTCCGTCACCGTT GAATGGGGCTGCTAAAATTGGAAGTGGAGG
homology primer rev	8096	DrpC	CAAATGTTTCTTCGCTGTTCTTCCCAGTGCTCTGGCGAAGT GGGCCAGCAATAACTTCGTATAATGTATGCTATACG
genotyping primer fw	8097	DrpC	CAGGGAAGGAACGGGAAG
genotyping primer rev	8098	DrpC	GAAGGCTTCAGTATGGAGGG
gRNA fw	8099	AAP3	AAGTTAGTTGATTTGTCGTAAAAAAG
gRNA rev	8100	AAP3	AAAACTTTTTTACGACAAATCAACTA
Homology fw	8101	AAP3	AGGCAGGCGATACAGAAGAAATCGCAGCTCTTGTTGAAG TTGATTTGTCGGCTAAAATTGGAAGTGGAGG

Homology rev	8102	AAP3	GAGGGTATTTTCTGGACTACGTGCTGACGCGCTGTCTCTG CAGACCGTTTATAACTTCGTATAATGTATGCTATACG
Genotyping fw	8103	AAP3	GAGGCGAGGCCCC
Genotyping rev	8104	AAP3	GCAGGCGTCGCCAAC
gRNA fw	8147	ISAP1	AAGTTGTTACCGAAGCAACGCGGTAGG
gRNA rev	8148	ISAP1	AAAACCTACCGCGTTGCTTCGGTAACA
Homology fw	8149	ISAP1	TGCCCCCTTATGCATGGGGAGTGCCTCGTGTGGTTACCGA AGCAACGCGGGCTAAAATTGGAAGTGGAGG
Homology rev	8150	ISAP1	CTTCTATCTTATGGAGAGGTGTGGTGCGGCAGAATTCACA TCACCCTCTAATAACTTCGTATAATGTATGCTATACG
Genotyping fw	8151	ISAP1	CACGTCGCATCTGACCTAC
Genotyping rev	8512	ISAP1	GTAGGTCAGATGCGACGTG
gRNA fw	8602	Rab5b	AAGTTGCAGCTGAAGCAGAGCATGA G
gRNA rev	8603	Rab5b	AAAACTCATGCTCTGCTTCAGCTGC A
Homology fw	8604	Rab5b	gtacagCCAAGGAAGTTTTTGAaCAaCTcAAaCAaAGtATGAT GGAaTTaGCTAAAATTGGAAGTGGAGG
Homology rev	8605	Rab5b	gaagtcaaggaactccatgcagaagaaaagtaaaaaagaactggaggagt ATAACTTCGTATAATGTATGCTATACG
Genotyping fw	8606	Rab5b	ctttcgacgttttcgtgtc
Genotyping rev	8607	Rab5b	ctctcaggctgggctccgt
gRNA fw	8608	Rab5a	AAGTTATTTCTGTAAGAACTGTTTCTG
gRNA rev	8609	Rab5a	AAAACAGAAACAGTTCTTACAGAAATA
Homology fw	8610	Ran5a	AAGAACAGAAGTCTTCTTCGAGCTCGTGGTGTGCATGTGG AGGCAAAAGTGCTAAAATTGGAAGTGGAGG
Homology rev	8611	Rab5a	ctttaaaatcgaaaacaaagagtcgaaggcctcagtcctcaaagccgagaA TAACTTCGTATAATGTATGCTATACG

Genotyping fw	8612	Rab5a	GCTTTCAACTGAACAAGACG
Genotyping rev	8613	Rab5a	cagcctgagacaccggag

4.1.4.4 Plasmids

Table 11: Plasmids

Name	Information	Source
Cas9_YFP	pTUB1-Cas9-HA-NLS-eYFP-NLS/ pU6-ccdb-tracrRNA	Curt-Varesano et al., 2016
Halo plasmid	pUC19_LIC_Halo-LoxP	Meissner LAB
YFP plasmid	Puc19_LIC_Halo_LoxP	Meissner Lab

4.1.5 Cell line and parasite strains

Table 12: Bacteria

Strain	Competence	Source
DH5a	Chemically competent	NEB

Table 13: Mammalian cell lines

Line	Source	Origin
Human Foreskin Fibroblasts (HFFs)	ATCC SCRC-1041 ™	Homo Sapiens

Table 14 Toxoplasma gondii strains

Number	Strain	Resistance	Strain origin and parental strain
1	RH ΔKu 80 DiCre	Cat/ delta hxgpt	Hunt et al. 2019
2	RH ΔKu80 DiCre SAG1 Halo	Cat/ delta hxgpt	Dr. Simon Gras
3	RH ΔKu80 DiCre SAG1 Halo Rab5a YFP		2
4	RH ΔKu80 DiCre SAG1 Halo Rab5b YFP		2
5	RH ΔKu80 DiCre SAG1 Halo DrpC YFP		2
6	RH ΔKu80 DiCre SAG1 Halo ISAP1 YFP		2
7	RH ΔKu80 DiCre SAG1 Halo AAP3 YFP		2
8	RG ΔKu80 DiCre SAG1 Halo floxed301410 mCherry		Dr. Jenessa Grech
9	RH ΔKu80 DiCre SAG1 Halo GRA2 YFP		2
10	RH Tir1 ty MyoF HA mAID	Cat/ Δhxgpt Δuprt t	Dr. Oefa Heaslip (251)
11	RH Tir1 MyoF HA mAID SAG1 Halo		9
12	FLP2 mAID HA		Botte laboratory
13	FLP2 mAID HA SAG1 Halo		11

14	Tet K13 HA		Waller laboratory
15	Tet K13 HA SAG1 Halo		13
16	eGFP K13 SAG1 Halo		Waller laboratory

4.2 Methods

4.2.1 Bacterial methods

Transformation of bacterial plasmid ligated into pGM 747: 25-50ul DH5a chemical competent bacteria were thawed on ice and incubated with 5-10 ul plasmid for 30 min-1h on ice. This was followed by a 30s heat shock at 42°C. The bacteria were recovered for 2 min on ice, plated onto LB agar plate + ampicillin, and incubator for 14-18 hours, then single bacterial colonies were picked and incubated in LB media + ampicillin at 37°C for another 14-18h.

4.2.2 Molecular Biology technics

4.2.2.1 Polymerase chain reaction (PCR)

Polymerase chain reaction is a method used to amplify DNA fragments. PCR was performed using Q5 DNA polymerase or Taq DNA polymerase with the corresponding buffer (Q5 Reaction Buffer or ThermoPol buffer), according to the manufacturer's protocol. The annealing temperatures were determined using primers and calculated using the NEB Tm calculator. In total, 35 cycles were performed.

4.2.2.2 Agarose gel electrophoresis

DNA electrophoresis was performed to separate and analyse the amplified DNA fragments. TAE agarose gels containing 0.8-2% w/v) agarose were stained with GleRed and run at 90V for 30-120 minutes. Visualization on a UV transilluminator

4.2.2.3 DNA restriction

Depending on the amount of DNA being digested and the concentration of enzymes, the amount of restriction enzymes (used according to the manufacturer's instructions) varies, as well as the incubation times. In the analytical digest, the amount of DNA used was less then 1ug, resulting in a reaction volume of less than 10ul.

4.2.2.4 DNA purification

DNA was purified using the ExtractMe DNA Clean up Kit according to manufacturer's instructions

4.2.2.5 sgRNA preparation and ligation

Ordered oligos were resuspended according to the manufacturer's instructions (Thermo Fisher Scientific). 2ul of a 1:10 dilution (10uM) was hybridised in 20 µl DNA oligo annealing buffer using a thermocycler at 95°C for 5 min with a ramp to 26°C(RT). 5 µl of hybridised oligos were ligated into 50ng of the Cas9-eYFP plasmid using T4 DNA ligases. Ligation was incubated overnight at room temperature for transformation into bacteria.

4.2.2.6 Plasmid DNA isolation from bacteria

Plasmid isolation was performed using 2 +2 mL (4mL total) bacteria culture using ExtracMe plasmid mini kit (Blirt)

4.2.2.7 gDNA isolation from *T. gondii*

gDNA was extracted from 1mL freshly lysed *T. gondii* tachyzoites using ExtractMe genomic DNA kit

4.3 Cell culture

4.3.1 Growth and generation of transgenic T.gondii

T. gondii tachyzoites were maintained at 37°C with 5% CO2 growing in human foreskin fibroblasts (HFFs; ATCC, SCRC 1041) cultured in Dulbecco's Modified Eagle Medium (DMEM Sigma) supplemented with 10% fetal bovine serum (FBS BioSell), 4mM L-Glutamate (Sigma), and 20ug/ mL gentamycin(Sigma) as previously described

4.3.2 Cryopreservation

Intracellular *T. gondii* tachyzoites were dissociated using a cell scraper, diluted 1:1 in 2x freezing medium, transferred into cryovials, stored in the freezer at -80°C for short term storage and transferred into a nitrogen tank for long term storage. They can be thawed again at RT and parasites can be transferred onto a new culture dish with an HFF monolayer. The DMEM was changed either 5h later or the next day.

4.3.3 Generation of transgenic parasites

Tachyzoite gene modification using transient Cas9 transfection. The strain was generated as described for Cas9 tagging (371). Guide RNAs targeting the regions of interest were designed using EuPaGDT (372). Briefly, gRNA oligos were annealed, ligated into the Cas9 vector, and verified by sequencing (Eurofins Genomics). The template DNA was generated by PCR amplification using Q5 High-Fidelity DNA Polymerase (New England BioLabs). The repair template was purified using a PCR Purification Kit (Blirt). Ethanol precipitation was performed using 100 µL of PCR mix +10-15ng purified Cas9 guide + 0.1x 3M NaAc pH5.2 and 3x 100% EtOH. Samples were stored overnight at -20°C or for 1h at-80°C then pelleted at 20,000 × g for 30 min-1h in a cold centrifuge. DNA pellets were washed twice with 70% EtOH before air dried

Parasite transfection: Tachyzoites were transfected with up to 20 µg of the repair template. transfected cells were transfected with the Amaxa 4D-Nucleofector system (Lonza AAF-1003X).

~1x10^6 parasites were centrifuged and resuspended in 50µl of P3 buffer, and the transfection mix (100ul) was transferred into a cuvette (P3 Primary cells 4d-Nucleofactor X kit L, Lonza). Electrophoresis was performed using program F1-158. After transfection, the parasites were resuspended in 1mL of fresh DMEM and transferred onto a fresh HFF dish.

4.3.4 Strain isolation using Fluorescents sorting (FACS)

The parasites were mechanically egressed 24 to 48 h after transfection, passed through a 3 µm filter and the parasites which transiently expressed Cas9-YFP were enriched via FACS 23 (FACSARIA III, BD Biosciences) and sorted into 96-well plates (a minimum of 5 events per well). The resultant clonal lines were screened by IFA for SAG1 labelling, and integration was confirmed by PCR and sequencing (Eurofins Genomics).

4.4 Halo assays

Labelling of the PM-SAG1 and visualisation of the endocytosis / Endo-SAG1

Fresh tachyzoites expressing SAG1-Halo were mechanically egress, filter (3µm) and were resuspended in cold DMEM media containing Halo membrane non-permeable dye Alexa 660 or 488 dye (Halo-Alexa Fluor®-488/660 1:1000 Promega) for 1 h. Parasites were spined at 2500 Revolutions Per Minute (RPM) for 5 min and media was exchanged, this was repeated three times, to remove any unbound ligand. Parasites were then transferred to Ibidi live cell dishes covered with HFF for overnight replication before imaging.

Labelling of the maternal M-SAG1 and visualisation of the n-SAG1.

Fresh tachyzoites expressing SAG1-Halo were mechanically egress, filter (3µm) and were resuspended in cold DMEM media containing Halo membrane permeable dye, Janilla 646 (Janeli Fluor®-646, 1:1000, Promega) for 1 h. Parasites were spined at 2500rpm for 5 min and media exchanged, three times, to remove any unbound ligand. Parasites were then transferred to Ibidi live cell dishes covered with HFF for overnight replication. After replication, a new labelling with media containing Halo membrane permeable dye, Jan 549, (Janelia Fluor®-549,

1:1000, Promega) was performed for 1h at 37°C. After 3 washes to remove any unbound dye left, parasites were imaged.

Labelling of the Int-SAG1 and tracking of the distribution to the daughter cells

Fresh tachyzoites expressing SAG1-Halo were mechanically egress, filter (3µm) and were resuspended in cold DMEM media containing Halo membrane non-permeable dye Alexa 660 or 488 dye (Halo-Alexa Fluor®-488/660 1:1000 Promega) for 1 h. Parasites were spined at 2500 RPM for 5 min and media exchanged, three times, to remove any unbound ligand. Parasites were then resuspended in cold DMEM media containing Halo membrane permeable dye Janila 549 or 646 (Janila Fluor®-549,646 1:1000, Promega ®) for 1 h. Parasites were spined at 2500 RPM for 5 min and media exchanged, three times, to remove any unbound ligand. Parasites were then transferred to Ibidi live cell dishes covered with HFF for overnight replication before imaging.

Endo-SAG1, Int-SAG1 and n-SAG1 colocalization.

For the analysis of the Endo-SAG1 vs n-SAG1 vesicle colocalization, triple labelling was performed as described above. Parasites were transferred on Ibidi live cell dishes covered with HFF for overnight replication. Parasites were then Fixed with 4% paraformaldehyde and imaged with Z-stack. The analysis focused on stage one parasites to avoid the obtention of too much de novo material in the recycling steps. Per replicate, at least 25 parasites were analysed for a total of about 100 Endo-SAG1. The different colocalization possibilities were counted and expressed as a percentage of the vesicles analysed. The experiment was performed with three independent biological triplicates. The values are then expressed as the mean values of the three independent experiments ± SD. Videos were analysed via Fiji.

Evaluation of the re-secretion of PM-SAG1 endocytosed vesicles

Parasites were labelled as described above with Alexa 660/488 (non-permeable Halo-Alexa Fluor®-488/660, 1:1000; Promega). The cells were transferred to HFF for overnight replication, followed by scratching, syringing, and trypsinisation. The second group was labelled as described above. All parasites were washed with DMEM without FCS and trypsinised by incubation with 30 mg/ml trypsin in DMEM without FCS at 37°C for 30 min. Parts of the parasites were imaged on live cell dishes coated with poly-L-lysine for 20 min (dishes were

washed with sterile H20 prior to use). The remaining parasites were washed with DMEM containing 10% FCS to stop trypsinisation. The cells were incubated in 10% trypsinization for 1h to see recovery and then transferred to live cell dishes. Additionally, the parasites were trypsinised to investigate the origin of the recovered signal. For analysis, control parasites were labelled (prior to trypsin), trypsin (time 0), 10 min recovery, 30 min recovery, 60 min recovery, and after re-trypsinisation.

After trypsinisation parasites were analysed for recovery signal above the background cut off in ImageJ and percentage of recovery above background was measured for trypsinization parasites (replicated and non-replicated) recovery was measured over 60 min in 3 independent experiments with at least 100 parasites

4.5 Phenotypic assays

Induction of KD:

MyoF: As previously described for MyoF mAID parasites, MyoF-mAID SAG1-Halo parasites were induced +/- auxin for 4h prior to labelling and experiments.

K13: As previously described, T4-S1 K13 SAG1-Halo parasites were induced 24h +/- anhydrotetracycline (ATC) prior labelling and experiments

Live replication assay

SAG1-Halo and SAG1-Halo IMC1-YFP parasites were labelled with the Halo membrane permeable dye Janila 646 (Janila Fluor®-646 1:1000, Promega ®) for 1 h. After 3 washes to remove any excess of dye, the parasites were transferred to Ibidi live cell dishes covered with HFF. Parasites were allowed to invade for 1h-2h to obtain enough invasion events to reach an average of 10 parasites per FOV. After the invasion, the excess of parasites was removed by 3 washes. Live cell dishes were then transferred to the Leica-DMI8, heated at 37°C under a chamber containing 5% CO2. Laser power and exposure were adjusted to the lowest values allowing reliable imaging. Imaged were taken every 20-30 minutes to follow the plasma membrane behaviour during replication for 12h. The experiment was performed with three independent biological triplicates. The values are then expressed as the mean values of the

three independent experiments ± SD. Videos were analysed via Fiji. Additionally, *iΔHATgK13-SAG1-Halo* parasites were induced with ATc (0.5 ug/ml) for 48h and labelled with Janelia 647 (permeable Halo-Janelia Fluor®-647 1:1000 Promega) and left to replicated overnight and analysis for changes in reservoir formation.

Fixed replication assay

For fixed replication, parasites were labelled in the same way as in the live replication assay, but before imaging, parasites were fixed with 4% paraformaldehyde (PFA Roche (10% dilution) for 10 min and analysed directly.

Immunofluorescence labelling

As described above, the samples were fixed in 4% PFA for 20 min. Blocked in PBS + 0,2% triton + 3% BSA for 30 minutes before 1h of first antibody labelling in the blocking solution. Samples were washed 3x times before secondary Ab labelling for 45 min in blocking buffer (AB+ blocking) washed and 1x time washed with Hoechst in PBS (1:50000) and mounted with ProLong™ Gold (with or without DAPI) sealed with nail polish.

Colocalization assay with YFP markers

For all colocalization assays, all parasite lines were labelled with the Halo membrane non-permeable dye Alexa 660 (Halo-Alexa Fluor®660 Promega concentration 1:1000) for 1 h. Parasites were spined at 2500rpm for 5 min and media exchanged, three times, to remove any unbound ligand. Parasites were then transferred to Ibidi live cell dishes covered with HFF for overnight replication. Parasites were then fixed with 4% paraformaldehyde and imaged. For the percentage of vacuole colocalization, 10 fields of view were imaged with stacked pictures along the Z-axis (Z-stack) for a total of at least 100 vacuoles. For the percentage of vesicle colocalization, about 25 vacuoles where colocalization was observed were analysed for a total of at least 100 endocytic vesicles per replicate. Colocalization with the YFP markers was calculated. The experiment was performed with three independent biological triplicates. The values are then expressed as the mean values of the three independent experiments ± SD. Videos were analysed via ImageJ

Vesicles tracking

For tacking the Endo-SAG1 vesicles, parasites were labelled as described above with the Halo membrane non-permeable dye Alexa 488 (non-permeable Halo-Alexa Fluor®-488 1:1000 Promega). Parasites were transferred to Ibidi live cell dishes covered with HFF for overnight replication. The induction of the MyoF-KD was performed as described above and maintained during replication. Live cell imaging was then performed for 30 seconds taking 1 frame per second with the Leica DMI8 100x. At least 100 vesicles were analysed per replicate. Vesicles were manually analysed for movement with ImageJ, and divided into three categories: directed movement, diffusive movement or stationery as previously described (34).Co-Localisation between old and new in FLP2 parasites

FLP2 parasites were induced with auxin for 4h before labelling. The control parasites were unidentified. Parasites were first labelled with Janelia 549 for 1h then washed three time with 10mL of DMEM and transferred to live cell dishes (70-100µL) for overnight replication. Before Imaging, parasites were labelled with Janelia 647 for 1h and three times before imaging with Leica DMi8. The induced parasites were kept under auxin conditions for the entire experiment. Colocalisation was analysed using ImageJ for double signal overlapping in the parasites.

Fluorescence recovery after photobleaching and FRAP

For analysis of the membrane dynamics, Sag1 Halo parasites were inoculated on Ibidi live cell dishes covered with HFF and labelled with Oregon green for 1h and washed prior to imaging. (Halo-Oregon green 1:1000 Promega). Photobleaching on the Leica-DMI8, with a FRAP unit, was recorded at objective 100x on single parasites for a complete period of 50 seconds. (10s before bleach, 1s 100% laser power (bleaching event), 39 seconds recovery). The imaging area was selected to allow the presence of at least another invaded tachyzoite to allow to determine the photobleaching induced by the recording. A total of 25 parasites per replicate were recorded. The experiment was performed in triplicates. Analysis was performed via ImageJ, values were normalised using the control parasites and then converted to percentage using 10s recorded before the bleaching as control of pre bleached (100%).

Confocal FRAP / FLIP approach

For the FRAP of stages 4 to 8, Leica SP8 with an FRAP module at the BMC was used. Parasites were recorded for 20sec pre bleach. Bleach was performed with a FLIP over 10sec until the fluorescent signal of the bleached area is gone. Recovery was recorded every 5 s for 7–10 min. Fluorescents were measured on bleached parasites and compared with non-bleached parasites of the same PV. The number of parasites analysed was not statistically significant.

Quantification of the PMR formation:

For experiments of quantification of the PMR, the different SAG1 Halo parasite lines were labelled with the Halo membrane non-permeable dye Alexa 488/660 (Halo-Alexa Fluor®488/660 1:1000 Promega) or the Halo membrane permeable dye Janila 594/646 (Janila Fluor®-549/646 1:1000, Promega ®) or a combination of both (see labelling strategies) for 1 h as described above. Parasites were transferred to Ibidi live cell dishes covered with HFF for overnight replication. About 10 fields of view were imaged with Z-stack for a total of at least 100 vacuoles. For quantification of the PMR, we counted the number of parasites showing membrane loops or accumulation above the plasma membrane. The results are expressed as a percentage of the total parasite population imaged. The experiment was performed with three independent biological triplicates. The values are then expressed as the mean values of the three independent experiments ± SD. Images were analysed via Fiji.

SAG1-endocytosis assays in FLP2 parasites

For extracellular tachyzoites, the SAG1-Halo strain was labelled with the non-permeable Alexa 660 dye (1/1000) in cold media for 1 h. Parasites were washed 3× to remove excess ligand. Parasites were incubated at 4 °C or 37 °C on the FBS coated live-cell dishes (Ibidi live-cell dishes, 29 mm) for 1 h prior to live imaging, as described below, for evaluation of internalization of the SAG1 signal. For SAG1 recycling assays of intracellular tachyzoites, parasites were labelled with Alexa 660 as above and then inoculated onto HFF monolayers in Ibidi dishes. Parasites were allowed to replicate for 24 h prior to imaging. For endocytosis assays with K13-depletion, iΔHA-TgK13-SAG1-Halo parasites were first induced for 48 h with or without ATC, before mechanical egress, filtering and labelling. Parasites were then allowed to reinfect new HFFs cells, grow for 24 h under the same ATc treatment and were then imaged live, as described below, for evaluation of internalization of the SAG1 signal. Endocytic activity

was assessed by the presence of the PM-SAG1 vesicles (non-permeable halo-Alexa Fluor®-660) and the percentage of parasites showing the presence of vesicles was determined. Mean values of three independent experiments ± SD were determined. The mean number of PM-SAG1 vesicles/parasite was determined from the total number of vesicles inside vacuoles divided by the number of parasites in the vacuole. For membrane accumulation, we scored aggregation of PM-SAG1 as signal in the residual body or outside the typical parasite plasma membrane. For these analyses at least 25 vacuoles per replicates were used and mean values of three independent experiments ± SD were determined. All SAG1-Halo images were acquired on a Leica-DMI8, objective 100x with the LasX software (v3.7.4). Imaged were deconvolved using Huygens essential software (v18.04) and batch express processing. Fiji (v1.53c) was used to analyse the picture and all count were made manually.

4.6 Microscopy and Image analysis

Widefield microscopy

Unless stated otherwise, all images were acquired on a Leica-DMI8, objective 100x with the LasX software (v3.7.4) (41). Fiji (v1.53c) was used to analyse the picture and all counts were made manually. LasX software (v3.7.4 and v.5.3.0) from Leica was used to obtain parasite imaging data

Visualization of PMR by Ultrastructure Expansion Microscopy (U-ExM)

Freshly egressed RH tachyzoites were allowed to infect HFFs in DMEM, supplemented with 5% FBS. After 1 hour of infection cells were washed to remove the extracellular tachyzoites and preserve only the intracellular parasites and allowed to replicate for 3h.

U-ExM was performed via published protocols for T. gondii. In brief, coverslips coated with the HFF cells infected with the parasites were typically not fixed before immersion in a 0.7% formaldehyde/1% acrylamide (FA/AA) solution for 5 hours at 37 °C. The coverslips were then overlaid with a monomer mixture (19% sodium acrylate/10% acrylamide/0.1% bis-acrylamide) supplemented with 0.5% ammonium persulfate (APS) and 0.5% tetramethylethylenediamine (TEMED) to initiate gel polymerization. After a 30-minute incubation at 37 °C, the fully

polymerized gels were detached and subjected to a 30-minute incubation at 95 °C in denaturation buffer (200 mM SDS, 200 mM NaCl, 50 mM Tris, pH 9). The gels were expanded overnight in successive water baths. The following day, the gels were shrunk in PBS, sectioned, and agitated for 3 hours at 37°C in a solution of appropriate primary antibodies diluted in freshly prepared 2% PBS-BSA. After three 10-minute washes in 0.1% PBS-Tween, the gels were incubated for 3 hours at 37°C (agitated and in the dark) with the appropriate secondary antibodies. After three additional 10-minute washes in 0.1% PBS-Tween, the gels were expanded overnight in water. Imaging was performed using a Leica TCS SP8 inverted microscope equipped with an HC PL Apo 100×/1.40 Oil CS2 objective and HyD detectors. Z-stack images were acquired via Leica LAS X software and deconvolved with the built-in "Lightning" mode or manually using Huygens deconvolution software. Image processing was conducted via ImageJ software, and maximum projections were generated for publication.

Ultrastructure TEM

For looking at the plasma membrane connection of parasites from the same vacuoles, and PMR, RH parasites were transferred to Ibidi µ-dishes previously seeded with HFF cells. After 24 h of replication, the parasites were fixed with 2.5% glutaraldehyde in 0.1 M phosphate buffer pH 7.4. The parasites were washed three times at room temperature with PBS (137 mM NaCl2, 2.7 mM KCl, 10 mM Na2HPO4, 1.8 mM KH2PO4, pH 7.4) and post-fixed with 1% (w/v) osmium tetroxide for 1 h. Subsequent to washing with PBS and water, the samples were stained en bloc with 1% (w/v) uranyl acetate in 20% (v/v) acetone for 30 min. Samples were dehydrated in a series of graded acetone and embedded in Epon 812 resin. Ultrathin sections (thickness, 60 nm) were cut using a diamond knife on a Reichert Ultracut-E ultramicrotome. Sections were mounted on collodium-coated copper grids, post-stained with lead citrate (80 mM, pH 13) and examined with an EM 912 transmission electron microscope (Zeiss, Oberkochen, Germany) equipped with an integrated OMEGA energy filter operated in the zero-loss mode at 80 kV. Images were acquired using a 2k × 2k slow-scan CCD camera (Tröndle Restlichtverstärkersysteme, Moorenweis, Germany).

For Statistic testing One-tail ANOVA was performed as required.

Confocal

A Leica DMi8 microscope equipped with SP8 imaging and an FRAP module was used. LasX software was used for the acquisition. Analysation was performed with ImageJ

FLIP/FRAP

Imaging was performed using a Leica TCS SP8 inverted microscope equipped with an HC PL Apo 100×/1.40 Oil CS2 objective and HyD detectors. Z-stack images were acquired via Leica LAS X software and deconvolved with the built-in "Lightning" mode or manually using Huygens deconvolution software

Image analysis

The Leica LasX software was used for Image analysis. All Images were processed and analysed with Fiji (ImageJ) software

5 References

1. Kwong WK, Irwin NAT, Mathur V, Na I, Okamoto N, Vermeij MJA, et al. Taxonomy of the Apicomplexan Symbionts of Coral, including Corallicolida ord. nov., Reassignment of the Genus Gemmocystis, and Description of New Species Corallicola aquarius gen. nov. sp. nov. and Anthozoaphila gnarlus gen. nov. sp. nov. J Eukaryot Microbiol. 2021 Mar 25;e12852.

2. Morrison DA. Evolution of the Apicomplexa: where are we now? Trends in Parasitology. 2009 Aug 1;25(8):375–82.

3. Gould SB, Tham WH, Cowman AF, McFadden GI, Waller RF. Alveolins, a New Family of Cortical Proteins that Define the Protist Infrakingdom Alveolata. Molecular Biology and Evolution. 2008 Jun 1;25(6):1219–30.

4. Yoon HS, Grant J, Tekle YI, Wu M, Chaon BC, Cole JC, et al. Broadly sampled multigene trees of eukaryotes. BMC Evol Biol. 2008 Jan 18;8:14.

5. Arisue N, Hashimoto T. Phylogeny and evolution of apicoplasts and apicomplexan parasites. Parasitol Int. 2015 Jun;64(3):254–9.

6. Seeber F, Steinfelder S. Recent advances in understanding apicomplexan parasites. F1000Res. 2016 Jun 14;5:F1000 Faculty Rev-1369.

7. Adl SM, Simpson AGB, Farmer MA, Andersen RA, Anderson OR, Barta JR, et al. The New Higher Level Classification of Eukaryotes with Emphasis on the Taxonomy of Protists. Journal of Eukaryotic Microbiology. 2005;52(5):399–451.

8. Votýpka J, Modrý D, Oborník M, Šlapeta J, Lukeš J. Apicomplexa. In: Archibald JM, Simpson AGB, Slamovits CH, Margulis L, Melkonian M, Chapman DJ, et al., editors. Handbook of the Protists. Cham: Springer International Publishing; 2017. p. 1–58. Available from: https://doi.org/10.1007/978-3-319-32669-6_20-1

9. Wolf A, Cowen D, Paige BH. Toxoplasmic encephalomyelitis. Am J Pathol. 1939 Nov;15(6):657-694.11.

10. Beverley JKA. Congenital Transmission of Toxoplasmosis through Successive Generations of Mice. Nature. 1959 May;183(4671):1348–9.

11. Crutcher JM, Hoffman SL. Malaria. In: Baron S, editor. Medical Microbiology . 4th ed. Galveston (TX): University of Texas Medical Branch at Galveston; 1996 . Available from: http://www.ncbi.nlm.nih.gov/books/NBK8584/

12. Hunter CA, Sibley LD. Modulation of innate immunity by Toxoplasma gondii virulence effectors. Nat Rev Microbiol. 2012 Nov;10(11):766–78.

13. Phyo AP, Dahal P, Mayxay M, Ashley EA. Clinical impact of vivax malaria: A collection review. PLoS Med. 2022 Jan;19(1):e1003890.

14. Helmy YA, Hafez HM. Cryptosporidiosis: From Prevention to Treatment, a Narrative Review. Microorganisms. 2022 Dec 13;10(12):2456.

15. Khan SM, Witola WH. Past, current, and potential treatments for cryptosporidiosis in humans and farm animals: A comprehensive review. Front Cell Infect Microbiol. 2023 Jan 24];13. Available from: https://www.frontiersin.org/journals/cellular-and-infection-microbiology/articles/10.3389/fcimb.2023.1115522/full

16. Swei A, O'Connor KE, Couper LI, Thekkiniath J, Conrad PA, Padgett KA, et al. Evidence for transmission of the zoonotic apicomplexan parasite Babesia duncani by the tick Dermacentor albipictus. Int J Parasitol. 2019 Feb;49(2):95–103.

17. Wang C, Wang D, Nie J, Gao X, Yin J, Zhu G. Unique Tubulin-Based Structures in the Zoonotic Apicomplexan Parasite Cryptosporidium parvum. Microorganisms. 2021 Sep 10;9(9):1921.

18. Moore RB, Oborník M, Janouškovec J, Chrudimský T, Vancová M, Green DH, et al. A photosynthetic alveolate closely related to apicomplexan parasites. Nature. 2008 Feb;451(7181):959–63.

19. Francia ME, Striepen B. Cell division in apicomplexan parasites. Nat Rev Microbiol. 2014 Feb;12(2):125–36.

20. Sena F, Cancela S, Bollati-Fogolín M, Pagotto R, Francia ME. Exploring Toxoplasma gondii´s Biology within the Intestinal Epithelium: intestinal-derived models to unravel sexual differentiation. Front Cell Infect Microbiol. 2023 May 29;13:1134471.

21. Ferguson DJP. Toxoplasma gondii: Detailed Description of the Coccidian (Asexual and Sexual) Development and Oocyst Sporulation. In: de Souza W, editor. Lifecycles of Pathogenic Protists in Humans Cham: Springer International Publishing; 2022 p. 419–41. Available from: https://doi.org/10.1007/978-3-030-80682-8_9

22. Martorelli Di Genova B, Knoll LJ. Comparisons of the Sexual Cycles for the Coccidian Parasites Eimeria and Toxoplasma. Front Cell Infect Microbiol. 2020 Dec 14;10:604897.

23. Wiley.com The Biology of Parasites | Wiley. Available from: https://www.wiley.com/en-us/The+Biology+of+Parasites-p-9783527328482

24. Roos DS. Themes and Variations in Apicomplexan Parasite Biology. Science. 2005 Jul;309(5731):72–3.

25. Yu CP, Chen BC, Chou YC, Hsieh CJ, Lin FH. The epidemiology of patients with toxoplasmosis and its associated risk factors in Taiwan during the 2007–2020 period. PLoS One. 2023 Aug 25;18(8):e0290769.

26. Bisetegn H, Debash H, Ebrahim H, Mahmood N, Gedefie A, Tilahun M, et al. Global seroprevalence of Toxoplasma gondii infection among patients with mental and neurological disorders: A systematic review and meta-analysis. Health Science Reports. 2023 Jun 5;6(6):e1319.

27. Morisaki JH, Heuser JE, Sibley LD. Invasion of Toxoplasma gondii occurs by active penetration of the host cell. J Cell Sci. 1995 Jun;108 (Pt 6):2457–64.

28. Weiss LM, Dubey JitenderP. Toxoplasmosis: a history of clinical observations. Int J Parasitol. 2009 Jul 1;39(8):895–901.

29. Zahir F, Abdellaoui M, Younes S, Benatiya IA, Tahri H. Severe ocular sequelae of congenital toxoplasmosis: huge macular scar. Pan Afr Med J. 2015 Mar 12;20:233.

30. Konradt C, Ueno N, Christian DA, Delong JH, Pritchard GH, Herz J, et al. Endothelial cells are a replicative niche for entry of Toxoplasma gondii to the central nervous system. Nat Microbiol. 2016 Feb 15;1:16001.

31. Hadfield SJ, Guy EC. Toxoplasmosis. Medicine. 2021 Dec 1;49(12):770–3.

32. English ED, Striepen B. The cat is out of the bag: How parasites know their hosts. PLoS Biol. 2019 Sep 5;17(9):e3000446.

33. Angel SO, Vanagas L, Alonso AM. Mechanisms of adaptation and evolution in Toxoplasma gondii. Mol Biochem Parasitol. 2024 Jun;258:111615.

34. Steinfeldt T, Könen-Waisman S, Tong L, Pawlowski N, Lamkemeyer T, Sibley LD, et al. Phosphorylation of Mouse Immunity-Related GTPase (IRG) Resistance Proteins Is an Evasion Strategy for Virulent Toxoplasma gondii. PLoS Biol. 2010 Dec 21;8(12):e1000576.

35. Lilue J, Müller UB, Steinfeldt T, Howard JC. Reciprocal virulence and resistance polymorphism in the relationship between Toxoplasma gondii and the house mouse. Elife. 2013 Oct 29;2:e01298.

36. Khan A, Taylor S, Ajioka JW, Rosenthal BM, Sibley LD. Selection at a single locus leads to widespread expansion of Toxoplasma gondii lineages that are virulent in mice. PLoS Genet. 2009 Mar;5(3):e1000404.

37. Attias M, Teixeira DE, Benchimol M, Vommaro RC, Crepaldi PH, De Souza W. The life-cycle of Toxoplasma gondii reviewed using animations. Parasit Vectors. 2020 Nov 23;13(1):588.

38. Freppel W, Ferguson DJP, Shapiro K, Dubey JP, Puech PH, Dumètre A. Structure, composition, and roles of the *Toxoplasma gondii* oocyst and sporocyst walls. Cell Surf. 2019 Dec 1;5:100016.

39. Dubey JP, Lindsay DS, Speer CA. Structures of Toxoplasma gondii Tachyzoites, Bradyzoites, and Sporozoites and Biology and Development of Tissue Cysts. Clin Microbiol Rev. 1998 Apr;11(2):267–99.

40. May DG, Scott KL, Campos AR, Roux KJ. Comparative Application of BioID and TurboID for Protein-Proximity Biotinylation. Cells. 2020 Apr 25;9(5):1070.

41. DUBEY JP, FERREIRA LR, MARTINS J, MCLEOD R. Oral oocyst-induced mouse model of toxoplasmosis: Effect of infection with Toxoplasma gondii strains of different genotypes, dose, and mouse strains (transgenic, out-bred, in-bred) on pathogenesis and mortality. Parasitology. 2012 Jan;139(1):1–13.

42. Silveira C, Vallochi AL, Rodrigues da Silva U, Muccioli C, Holland GN, Nussenblatt RB, et al. Toxoplasma gondii in the peripheral blood of patients with acute and chronic toxoplasmosis. Br J Ophthalmol. 2011 Mar;95(3):396–400.

43. Robbins JR, Zeldovich VB, Poukchanski A, Boothroyd JC, Bakardjiev AI. Tissue Barriers of the Human Placenta to Infection with Toxoplasma gondii. Infect Immun. 2012 Jan;80(1):418–28.

44. Schneider CA, Figueroa Velez DX, Orchanian SB, Shallberg LA, Agalliu D, Hunter CA, et al. Toxoplasma gondii Dissemination in the Brain Is Facilitated by Infiltrating Peripheral Immune Cells. mBio. 2022 Nov 29;13(6):e02838-22.

45. Baum J, Papenfuss AT, Baum B, Speed TP, Cowman AF. Regulation of apicomplexan actin-based motility. Nat Rev Microbiol. 2006 Aug;4(8):621–8.

46. Tosetti N, Dos Santos Pacheco N, Bertiaux E, Maco B, Bournonville L, Hamel V, et al. Essential function of the alveolin network in the subpellicular microtubules and conoid assembly in Toxoplasma gondii. Silvie O, Akhmanova A, Tewari R, editors. eLife. 2020 May 7;9:e56635.

47. Hu K, Roos DS, Murray JM. A novel polymer of tubulin forms the conoid of Toxoplasma gondii. Journal of Cell Biology. 2002 Mar 18;156(6):1039–50.

48. Mital J, Ward GE. Current and Emerging Approaches to Studying Invasion in Apicomplexan Parasites. In: Madame Curie Bioscience Database Landes Bioscience; 2013 Available from: https://www.ncbi.nlm.nih.gov/books/NBK6505/

49. Dobrowolski J, Sibley LD. The role of the cytoskeleton in host cell invasion by Toxoplasma gondii. Behring Inst Mitt. 1997 Mar;(99):90–6.

50. Dobrowolski JM, Carruthers VB, Sibley LD. Participation of myosin in gliding motility and host cell invasion by Toxoplasma gondii. Mol Microbiol. 1997 Oct;26(1):163–73.

51. Whitelaw JA, Latorre-Barragan F, Gras S, Pall GS, Leung JM, Heaslip A, et al. Surface attachment, promoted by the actomyosin system of Toxoplasma gondii is important for efficient gliding motility and invasion. BMC Biol. 2017 Jan 18;15(1):1.

52. Del Rosario M, Periz J, Pavlou G, Lyth O, Latorre-Barragan F, Das S, et al. Apicomplexan F-actin is required for efficient nuclear entry during host cell invasion. EMBO Rep. 2019 Dec 5;20(12):e48896.

53. Chelaghma S, Ke H, Barylyuk K, Krueger T, Koreny L, Waller RF. Apical annuli are specialised sites of post-invasion secretion of dense granules in Toxoplasma. McConville MJ, editor. eLife. 2024 Jan 25;13:e94201.

54. Dubois DJ, Soldati-Favre D. Biogenesis and secretion of micronemes in Toxoplasma gondii. Cell Microbiol. 2019 May;21(5):e13018.

55. Mageswaran SK, Guérin A, Theveny LM, Chen WD, Martinez M, Lebrun M, et al. In situ ultrastructures of two evolutionarily distant apicomplexan rhoptry secretion systems. Nat Commun. 2021 Aug 17;12(1):4983.

56. Engelberg K, Chen CT, Bechtel T, Sánchez Guzmán V, Drozda AA, Chavan S, et al. The apical annuli of Toxoplasma gondii are composed of coiled-coil and signalling proteins embedded in the inner membrane complex sutures. Cellular Microbiology. 2020;22(1):e13112.

57. Fu J, Zhao L, Yang J, Chen H, Cao S, Jia H. An unconventional SNARE complex mediates exocytosis at the plasma membrane and vesicular fusion at the apical annuli in Toxoplasma gondii. PLOS Pathogens. 2023 Mar 27;19(3):e1011288.

58. McFadden GI, Yeh E. The apicoplast: now you see it, now you don't. Int J Parasitol. 2017 Feb;47(2–3):137–44.

59. Stasic AJ, Moreno SNJ, Carruthers VB, Dou Z. The Toxoplasma Plant-Like Vacuolar Compartment (PLVAC). J Eukaryot Microbiol. 2022 Nov;69(6):e12951.

60. Biogenesis of the Inner Membrane Complex Is Dependent on Vesicular Transport by the Alveolate Specific GTPase Rab11B | PLOS Pathogens Available from: https://journals.plos.org/plospathogens/article?id=10.1371/journal.ppat.1001029

61. Koreny L, Mercado-Saavedra BN, Klinger CM, Barylyuk K, Butterworth S, Hirst J, et al. Stable endocytic structures navigate the complex pellicle of apicomplexan parasites. Nat Commun. 2023 Apr 15;14(1):2167.

62. Wan W, Dong H, Lai DH, Yang J, He K, Tang X, et al. The Toxoplasma micropore mediates endocytosis for selective nutrient salvage from host cell compartments. Nat Commun. 2023 Feb 22;14(1):977.

63. Aguet F, Antonescu CN, Mettlen M, Schmid SL, Danuser G. Advances in Analysis of Low Signal-to-Noise Images Link Dynamin and AP2 to the Functions of an Endocytic Checkpoint. Dev Cell. 2013 Aug 12;26(3):279–91.

64. Antonny B, Burd C, De Camilli P, Chen E, Daumke O, Faelber K, et al. Membrane fission by dynamin: what we know and what we need to know. EMBO J. 2016 Nov 2;35(21):2270–84.

65. Jackson AJ, Clucas C, Mamczur NJ, Ferguson DJ, Meissner M. Toxoplasma gondii Syntaxin 6 Is Required for Vesicular Transport Between Endosomal-Like Compartments and the Golgi Complex. Traffic (Copenhagen, Denmark). 2013 Nov;14(11):1166.

66. Pieperhoff MS, Schmitt M, Ferguson DJP, Meissner M. The role of clathrin in post-Golgi trafficking in Toxoplasma gondii. PLoS One. 2013;8(10):e77620.

67. McGovern OL, Rivera-Cuevas Y, Kannan G, Narwold Jr AJ, Carruthers VB. Intersection of endocytic and exocytic systems in Toxoplasma gondii. Traffic. 2018;19(5):336–53.

68. Nagano M, Toshima JY, Siekhaus DE, Toshima J. Rab5-mediated endosome formation is regulated at the trans-Golgi network. Commun Biol. 2019 Nov 15;2(1):1–12.

69. Hao H, Niu J, Xue B, Su QP, Liu M, Yang J, et al. Golgi-associated microtubules are fast cargo tracks and required for persistent cell migration. EMBO reports. 2020 Mar 4;21(3):e48385.

70. Kitano M, Kizuka Y, Sobajima T, Nakano M, Nakajima K, Misaki R, et al. Rab11-mediated post-Golgi transport of the sialyltransferase ST3GAL4 suggests a new mechanism for regulating glycosylation. Journal of Biological Chemistry 2021 Jan 1 Available from: https://www.jbc.org/article/S0021-9258(21)00126-5/abstract

71. Njiri OA, Zhang X, Zhang Y, Wu B, Jiang L, Li Q, et al. CD209 C-Type Lectins Promote Host Invasion, Dissemination, and Infection of Toxoplasma gondii. Front Immunol. 2020;11:656.

72. He X lin, Grigg ME, Boothroyd JC, Garcia KC. Structure of the immunodominant surface antigen from the Toxoplasma gondii SRS superfamily. Nat Struct Biol. 2002 Aug;9(8):606–11.

73. Wang Y, Yin H. Research progress on surface antigen 1 (SAG1) of Toxoplasma gondii. Parasit Vectors. 2014 Apr 13;7:180.

74. Håkansson S, Morisaki H, Heuser J, Sibley LD. Time-lapse video microscopy of gliding motility in Toxoplasma gondii reveals a novel, biphasic mechanism of cell locomotion. Mol Biol Cell. 1999 Nov;10(11):3539–47.

75. Hortua Triana MA, Márquez-Nogueras KM, Vella SA, Moreno SNJ. Calcium signaling and the lytic cycle of the Apicomplexan parasite *Toxoplasma gondii*. Biochimica et Biophysica Acta (BBA) - Molecular Cell Research. 2018 Nov 1;1865(11, Part B):1846–56.

76. Soldati D, Dubremetz JF, Lebrun M. Microneme proteins: structural and functional requirements to promote adhesion and invasion by the apicomplexan parasite *Toxoplasma gondii*. International Journal for Parasitology. 2001 Oct 1;31(12):1293–302.

77. Mordue DG, Håkansson S, Niesman I, Sibley LD. Toxoplasma gondii resides in a vacuole that avoids fusion with host cell endocytic and exocytic vesicular trafficking pathways. Exp Parasitol. 1999 Jun;92(2):87–99.

78. Black MW, Boothroyd JC. Lytic Cycle of Toxoplasma gondii. Microbiol Mol Biol Rev. 2000 Sep;64(3):607–23.

79. Meissner M, Schlüter D, Soldati D. Role of Toxoplasma gondii myosin A in powering parasite gliding and host cell invasion. Science. 2002 Oct 25;298(5594):837–40.

80. Frénal K, Polonais V, Marq JB, Stratmann R, Limenitakis J, Soldati-Favre D. Functional dissection of the apicomplexan glideosome molecular architecture. Cell Host Microbe. 2010 Oct 21;8(4):343–57.

81. Meissner M, Ferguson DJP, Frischknecht F. Invasion factors of apicomplexan parasites: essential or redundant? Curr Opin Microbiol. 2013 Aug;16(4):438–44.

82. Blader IJ, Coleman BI, Chen CT, Gubbels MJ. Lytic Cycle of Toxoplasma gondii: 15 Years Later. Annual Review of Microbiology. 2015 Oct 15;69(Volume 69, 2015):463–85.

83. Shen B, Sibley LD. The moving junction, a key portal to host cell invasion by apicomplexan parasites. Current opinion in microbiology. 2012 Mar 23;15(4):449.

84. Clough B, Frickel EM. The Toxoplasma Parasitophorous Vacuole: An Evolving Host-Parasite Frontier. Trends Parasitol. 2017 Jun;33(6):473–88.

85. Striepen B, Jordan CN, Reiff S, van Dooren GG. Building the perfect parasite: cell division in apicomplexa. PLoS Pathog. 2007 Jun;3(6):e78.

86. Shen B, Sibley LD. Toxoplasma aldolase is required for metabolism but dispensable for host-cell invasion. Proc Natl Acad Sci U S A. 2014 Mar 4;111(9):3567–72.

87. Cell Membranes | Learn Science at Scitable Available from: https://www.nature.com/scitable/topicpage/cell-membranes-14052567/

88. Kulbacka J, Choromańska A, Rossowska J, Wężgowiec J, Saczko J, Rols MP. Cell Membrane Transport Mechanisms: Ion Channels and Electrical Properties of Cell Membranes. In: Kulbacka J, Satkauskas S, editors. Transport Across Natural and Modified Biological Membranes and its Implications in Physiology and Therapy Cham: Springer International Publishing; 2017 p. 39–58. Available from: https://doi.org/10.1007/978-3-319-56895-9_3

89. Doyen D, Poët M, Jarretou G, Pisani DF, Tauc M, Cougnon M, et al. Intracellular pH Control by Membrane Transport in Mammalian Cells. Insights Into the Selective Advantages of Functional Redundancy. Front Mol Biosci 2022 Feb 18 Available from: https://www.frontiersin.org/journals/molecular-biosciences/articles/10.3389/fmolb.2022.825028/full

90. Schwarz DS, Blower MD. The endoplasmic reticulum: structure, function and response to cellular signaling. Cell Mol Life Sci. 2016 Jan 1;73(1):79–94.

91. Pfeffer SR. How the Golgi works: a cisternal progenitor model. Proc Natl Acad Sci U S A. 2010 Nov 16;107(46):19614–8.

92. Nuclear Membrane Available from: https://www.genome.gov/genetics-glossary/Nuclear-Membrane

93. Alenghat FJ, Golan DE. Membrane Protein Dynamics and Functional Implications in Mammalian Cells. Current topics in membranes. 2013;72:89.

94. van Meer G, Voelker DR, Feigenson GW. Membrane lipids: where they are and how they behave. Nat Rev Mol Cell Biol. 2008 Feb;9(2):112–24.

95. Edidin M. Lipids on the frontier: a century of cell-membrane bilayers. Nat Rev Mol Cell Biol. 2003 May;4(5):414–8.

96. Kumar GA, Chattopadhyay A. Membrane cholesterol regulates endocytosis and trafficking of the serotonin1A receptor: Insights from acute cholesterol depletion. Biochimica et Biophysica Acta (BBA) - Molecular and Cell Biology of Lipids. 2021 Apr 1;1866(4):158882.

97. Helle SCJ, Kanfer G, Kolar K, Lang A, Michel AH, Kornmann B. Organization and function of membrane contact sites. Biochim Biophys Acta. 2013 Nov;1833(11):2526–41.

98. Lipids: Definition, Characteristics, Structure, Types, Functions, Examples - PhD Nest 2021 Available from: https://www.phdnest.com/lipids/

99. Watson H. Biological membranes. Essays in Biochemistry. 2015 Oct 26;59:43.

100. Turnover and flow of the cell membrane for cell migration | Scientific Reports Available from: https://www.nature.com/articles/s41598-017-13438-5

101. Ellgaard L, Helenius A. Quality control in the endoplasmic reticulum. Nat Rev Mol Cell Biol. 2003 Mar;4(3):181–91.

102. Emr S, Glick BS, Linstedt AD, Lippincott-Schwartz J, Luini A, Malhotra V, et al. Journeys through the Golgi—taking stock in a new era. The Journal of Cell Biology. 2009 Nov 16;187(4):449.

103. Contreras FX, Ernst AM, Haberkant P, Björkholm P, Lindahl E, Gönen B, et al. Molecular recognition of a single sphingolipid species by a protein's transmembrane domain. Nature. 2012 Jan;481(7382):525–9.

104. Park JW, Park WJ, Kuperman Y, Boura-Halfon S, Pewzner-Jung Y, Futerman AH. Ablation of very long acyl chain sphingolipids causes hepatic insulin resistance in mice due to altered detergent-resistant membranes. Hepatology. 2013 Feb;57(2):525–32.

105. Hashidate-Yoshida T, Harayama T, Hishikawa D, Morimoto R, Hamano F, Tokuoka SM, et al. Fatty acid remodeling by LPCAT3 enriches arachidonate in phospholipid membranes and regulates triglyceride transport. Cravatt B, editor. eLife. 2015 Apr 21;4:e06328.

106. Park JW, Park WJ, Futerman AH. Ceramide synthases as potential targets for therapeutic intervention in human diseases. Biochim Biophys Acta. 2014 May;1841(5):671–81.

107. Hankins HM, Baldridge RD, Xu P, Graham TR. Role of flippases, scramblases, and transfer proteins in phosphatidylserine subcellular distribution. Traffic. 2015 Jan;16(1):35–47.

108. Pomorski TG, Menon AK. LIPID SOMERSAULTS: UNCOVERING THE MECHANISMS OF PROTEIN-MEDIATED LIPID FLIPPING. Prog Lipid Res. 2016 Oct;64:69–84.

109. Bisio H, Krishnan A, Marq JB, Soldati-Favre D. Toxoplasma gondii phosphatidylserine flippase complex ATP2B-CDC50.4 critically participates in microneme exocytosis. PLOS Pathogens. 2022 Mar 24;18(3):e1010438.

110. Transmembrane Protein - an overview | ScienceDirect Topics Available from: https://www.sciencedirect.com/topics/biochemistry-genetics-and-molecular-biology/transmembrane-protein

111. Dimova R. Recent developments in the field of bending rigidity measurements on membranes. Advances in Colloid and Interface Science. 2014 Jun 1;208:225–34.

112. Das BB, Park SH, Opella SJ. Membrane protein structure from rotational diffusion. Biochim Biophys Acta. 2015 Jan;1848(0):229–45.

113. Devkota R, Pilon M. FRAP: A Powerful Method to Evaluate Membrane Fluidity in Caenorhabditis elegans. Bio Protoc. 2018 Jul 5;8(13):e2913.

114. Nissim-Rafinia M, Meshorer E. Photobleaching Assays (FRAP & FLIP) to Measure Chromatin Protein Dynamics in Living Embryonic Stem Cells. Journal of Visualized Experiments : JoVE. 2011 Jun 29;(52):2696.

115. Siletsky SA. Proton Pumps: Molecular Mechanisms, Inhibitors and Activators of Proton Pumping. Int J Mol Sci. 2023 May 22;24(10):9070.

116. Armstrong CM, Hollingworth S. Na+ and K+ channels: history and structure. Biophysical Journal. 2021 Jan 21;120(5):756.

117. Shintani T, Klionsky DJ. Cargo Proteins Facilitate the Formation of Transport Vesicles in the Cytoplasm to Vacuole Targeting Pathway. J Biol Chem. 2004 Jul 16;279(29):29889–94.

118. Ritter B, Murphy S, Dokainish H, Girard M, Gudheti MV, Kozlov G, et al. NECAP 1 Regulates AP-2 Interactions to Control Vesicle Size, Number, and Cargo During Clathrin-Mediated Endocytosis. PLoS Biol. 2013 Oct 1;11(10):e1001670.

119. Čopič A, Latham CF, Horlbeck MA, D'Arcangelo JG, Miller EA. ER Cargo Properties Specify A Requirement For COPII Coat Rigidity Mediated By Sec13p. Science. 2012 Mar 16;335(6074):1359–62.

120. Traub LM. Tickets to ride: selecting cargo for clathrin-regulated internalization. Nat Rev Mol Cell Biol. 2009 Sep;10(9):583–96.

121. Alberts B, Johnson A, Lewis J, Raff M, Roberts K, Walter P. Intracellular Vesicular Traffic. In: Molecular Biology of the Cell 4th edition Garland Science; 2002 Available from: https://www.ncbi.nlm.nih.gov/books/NBK21045/

122. Cabrera M, Muñiz M, Hidalgo J, Vega L, Martín ME, Velasco A. The Retrieval Function of the KDEL Receptor Requires PKA Phosphorylation of Its C-Terminus. Mol Biol Cell. 2003 Oct;14(10):4114–25.

123. Hammer JA, Sellers JR. Walking to work: roles for class V myosins as cargo transporters. Nat Rev Mol Cell Biol. 2012 Jan;13(1):13–26.

124. Tumbarello DA, Kendrick-Jones J, Buss F. Myosin VI and its cargo adaptors – linking endocytosis and autophagy. J Cell Sci. 2013 Jun 15;126(12):2561–70.

125. Nebenführ A. Vesicle traffic in the endomembrane system: a tale of COPs, Rabs and SNAREs. Current Opinion in Plant Biology. 2002 Dec 1;5(6):507–12.

126. Grosshans BL, Ortiz D, Novick P. Rabs and their effectors: Achieving specificity in membrane traffic. Proceedings of the National Academy of Sciences. 2006 Aug 8;103(32):11821–7.

127. Jahn R, Scheller RH. SNAREs — engines for membrane fusion. Nat Rev Mol Cell Biol. 2006 Sep;7(9):631–43.

128. Pfeffer SR. Rab GTPase regulation of membrane identity. Current Opinion in Cell Biology. 2013 Aug 1;25(4):414–9.

129. McNew JA, Parlati F, Fukuda R, Johnston RJ, Paz K, Paumet F, et al. Compartmental specificity of cellular membrane fusion encoded in SNARE proteins. Nature. 2000 Sep;407(6801):153–9.

130. Martens S, McMahon HT. Mechanisms of membrane fusion: disparate players and common principles. Nat Rev Mol Cell Biol. 2008 Jul;9(7):543–56.

131. Cao S, Yang J, Fu J, Chen H, Jia H. The Dissection of SNAREs Reveals Key Factors for Vesicular Trafficking to the Endosome-like Compartment and Apicoplast via the Secretory System in Toxoplasma gondii. mBio. 2021 Aug 3;12(4):e01380-21.

132. Harrison SC, Kirchhausen T. Conservation in vesicle coats. Nature. 2010 Aug;466(7310):1048–9.

133. Faini M, Beck R, Wieland FT, Briggs JAG. Vesicle coats: structure, function, and general principles of assembly. Trends Cell Biol. 2013 Jun;23(6):279–88.

134. Thor F, Gautschi M, Geiger R, Helenius A. Bulk Flow Revisited: Transport of a Soluble Protein in the Secretory Pathway. Traffic. 2009;10(12):1819–30.

135. Hernandez-Gonzalez M, Larocque G, Way M. Viral use and subversion of membrane organization and trafficking. J Cell Sci. 2021 Mar 4;134(5):jcs252676.

136. Elsevier Australia Bookstore Guyton and Hall Textbook of Medical Physiology: 14th edition | John E. Hall | ISBN: 9780323597128. Available from: https://www.elsevierhealth.com.au/guyton-and-hall-textbook-of-medical-physiology-9780323597128.html

137. Jackson LP, Kelly BT, McCoy AJ, Gaffry T, James LC, Collins BM, et al. A large-scale conformational change couples membrane recruitment to cargo binding in the AP2 clathrin adaptor complex. Cell. 2010 Jun 25;141(7):1220–9.

138. Antonny B. Mechanisms of membrane curvature sensing. Annu Rev Biochem. 2011;80:101–23.

139. Stachowiak JC, Brodsky FM, Miller EA. A cost-benefit analysis of the physical mechanisms of membrane curvature. Nat Cell Biol. 2013 Sep;15(9):1019–27.

140. Rivas RJ, Moore HP. Spatial segregation of the regulated and constitutive secretory pathways. J Cell Biol. 1989 Jul;109(1):51–60.

141. Martin TF. Stages of regulated exocytosis. Trends Cell Biol. 1997 Jul;7(7):271–6.

142. Svitkina T. The Actin Cytoskeleton and Actin-Based Motility. Cold Spring Harb Perspect Biol. 2018 Jan 2;10(1):a018267.

143. Rottner K, Schaks M. Assembling actin filaments for protrusion. Curr Opin Cell Biol. 2019 Feb;56:53–63.

144. Hill TL, Kirschner MW. Bioenergetics and kinetics of microtubule and actin filament assembly-disassembly. Int Rev Cytol. 1982;78:1–125.

145. Boulant S, Kural C, Zeeh JC, Ubelmann F, Kirchhausen T. Actin dynamics counteract membrane tension during clathrin-mediated endocytosis. Nat Cell Biol. 2011 Aug 14;13(9):1124–31.

146. Kaksonen M, Toret CP, Drubin DG. A Modular Design for the Clathrin- and Actin-Mediated Endocytosis Machinery. Cell. 2005 Oct 21;123(2):305–20.

147. Cooke R. The sliding filament model: 1972-2004. J Gen Physiol. 2004 Jun;123(6):643–56.

148. Cheng J, Grassart A, Drubin DG. Myosin 1E coordinates actin assembly and cargo trafficking during clathrin-mediated endocytosis. Mol Biol Cell. 2012 Aug 1;23(15):2891–904.

149. Leung JM, He Y, Zhang F, Hwang YC, Nagayasu E, Liu J, et al. Stability and function of a putative microtubule-organizing center in the human parasite Toxoplasma gondii. Mol Biol Cell. 2017 May 15;28(10):1361–78.

150. Kapitein LC, van Bergeijk P, Lipka J, Keijzer N, Wulf PS, Katrukha EA, et al. Myosin-V Opposes Microtubule-Based Cargo Transport and Drives Directional Motility on Cortical Actin. Current Biology. 2013 May 6;23(9):828–34.

151. Kirkbride KC, Sung BH, Sinha S, Weaver AM. Cortactin. Cell Adh Migr. 2011;5(2):187–98.

152. Zhang J, Yue J, Wu X. Spectraplakin family proteins – cytoskeletal crosslinkers with versatile roles. J Cell Sci. 2017 Aug 1;130(15):2447–57.

153. Alberts B, Johnson A, Lewis J, Raff M, Roberts K, Walter P. Transport into the Cell from the Plasma Membrane: Endocytosis. In: Molecular Biology of the Cell 4th edition Garland Science; 2002 Available from: https://www.ncbi.nlm.nih.gov/books/NBK26870/

154. Beenken A. Endocytosis Begins inside the Cell. Journal of the American Society of Nephrology. 2022 Apr;33(4):661.

155. Brown MS, Goldstein JL. Receptor-mediated endocytosis: insights from the lipoprotein receptor system. Proc Natl Acad Sci U S A. 1979 Jul;76(7):3330–7.

156. Pedrioli G, Paganetti P. Hijacking Endocytosis and Autophagy in Extracellular Vesicle Communication: Where the Inside Meets the Outside. Front Cell Dev Biol 2021 Jan 7 Available from: https://www.frontiersin.org/journals/cell-and-developmental-biology/articles/10.3389/fcell.2020.595515/full

157. Polyunsaturated phospholipids facilitate membrane deformation and fission by endocytic proteins | Science Available from: https://www.science.org/doi/10.1126/science.1255288?url_ver=Z39.88-2003&rfr_id=ori:rid:crossref.org&rfr_dat=cr_pub%20%200pubmed#core-collateral-purchase-access

158. Pfeffer SR. A prize for membrane magic. Cell. 2013 Dec 5;155(6):1203–6.

159. Batchelder EM, Yarar D. Differential Requirements for Clathrin-dependent Endocytosis at Sites of Cell–Substrate Adhesion. Mol Biol Cell. 2010 Sep 1;21(17):3070–9.

160. Antonescu CN, Aguet F, Danuser G, Schmid SL. Phosphatidylinositol-(4,5)-bisphosphate regulates clathrin-coated pit initiation, stabilization, and size. Mol Biol Cell. 2011 Jul 15;22(14):2588–600.

161. Haucke V, Kozlov MM. Membrane remodeling in clathrin-mediated endocytosis. Journal of Cell Science. 2018 Sep 3;131(17):jcs216812.

162. Kaksonen M, Roux A. Mechanisms of clathrin-mediated endocytosis. Nat Rev Mol Cell Biol. 2018 May;19(5):313–26.

163. Frost A, Unger VM, Camilli PD. The BAR Domain Superfamily: Membrane-Molding Macromolecules. Cell. 2009 Apr 17;137(2):191.

164. Stefano G, Renna L, Wormsbaecher C, Gamble J, Zienkiewicz K, Brandizzi F. Plant Endocytosis Requires the ER Membrane-Anchored Proteins VAP27-1 and VAP27-3. Cell Reports. 2018 May 22;23(8):2299–307.

165. Venugopal K, Werkmeister E, Barois N, Saliou JM, Poncet A, Huot L, et al. Dual role of the Toxoplasma gondii clathrin adaptor AP1 in the sorting of rhoptry and microneme proteins and in parasite division. PLoS Pathog. 2017 Apr;13(4):e1006331.

166. Ford MGJ, Mills IG, Peter BJ, Vallis Y, Praefcke GJK, Evans PR, et al. Curvature of clathrin-coated pits driven by epsin. Nature. 2002 Sep;419(6905):361–6.

167. Chen C, Zhuang X. Epsin 1 is a cargo-specific adaptor for the clathrin-mediated endocytosis of the influenza virus. Proc Natl Acad Sci U S A. 2008 Aug 1;105(33):11790–5.

168. Gleisner M, Kroppen B, Fricke C, Teske N, Kliesch TT, Janshoff A, et al. Epsin N-terminal Homology Domain (ENTH) Activity as a Function of Membrane Tension. J Biol Chem. 2016 Sep 16;291(38):19953–61.

169. Bucher D, Frey F, Sochacki KA, Kummer S, Bergeest JP, Godinez WJ, et al. Clathrin-adaptor ratio and membrane tension regulate the flat-to-curved transition of the clathrin coat during endocytosis. Nat Commun. 2018 Mar 16;9(1):1109.

170. Lewellyn EB, Pedersen RTA, Hong J, Lu R, Morrison HM, Drubin DG. An engineered minimal WASP-myosin fusion protein reveals essential functions for endocytosis. Dev Cell. 2015 Nov 9;35(3):281–94.

171. Xu J, Liang Y, Li N, Dang S, Jiang A, Liu Y, et al. Clathrin-associated carriers enable recycling through a kiss-and-run mechanism. Nat Cell Biol. 2024 Oct;26(10):1652–68.

172. Newmyer SL, Christensen A, Sever S. Auxilin-Dynamin Interactions Link the Uncoating ATPase Chaperone Machinery with Vesicle Formation. Developmental Cell. 2003 Jun 1;4(6):929–40.

173. Cremona O. Live stripping of clathrin-coated vesicles. Dev Cell. 2001 Nov;1(5):592–4.

174. de Carvalho TMU, Barrias ES, de Souza W. Macropinocytosis: a pathway to protozoan infection. Front Physiol. 2015 Apr 9;6:106.

175. Salloum G, Bresnick AR, Backer JM. Macropinocytosis: mechanisms and regulation. Biochem J. 2023 Mar 15;480(5):335–62.

176. Mayor S, Pagano RE. Pathways of clathrin-independent endocytosis. Nat Rev Mol Cell Biol. 2007 Aug;8(8):603–12.

177. del Pozo MA, Balasubramanian N, Alderson NB, Kiosses WB, Grande-García A, Anderson RGW, et al. Phospho-caveolin-1 mediates integrin-regulated membrane domain internalization. Nat Cell Biol. 2005 Sep;7(9):901–8.

178. Echarri A, Del Pozo MA. Caveolae – mechanosensitive membrane invaginations linked to actin filaments. Journal of Cell Science. 2015 Aug 1;128(15):2747–58.

179. Parton RG, Simons K. The multiple faces of caveolae. Nat Rev Mol Cell Biol. 2007 Mar;8(3):185–94.

180. Gervásio OL, Phillips WD, Cole L, Allen DG. Caveolae respond to cell stretch and contribute to stretch-induced signaling. Journal of Cell Science. 2011 Nov 1;124(21):3581–90.

181. Li R, Liu P, Wan Y, Chen T, Wang Q, Mettbach U, et al. A Membrane Microdomain-Associated Protein, Arabidopsis Flot1, Is Involved in a Clathrin-Independent Endocytic Pathway and Is Required for Seedling Development[C][W]. Plant Cell. 2012 May;24(5):2105–22.

182. Volonte D, Galbiati F, Li S, Nishiyama K, Okamoto T, Lisanti MP. Flotillins/cavatellins are differentially expressed in cells and tissues and form a hetero-oligomeric complex with caveolins in vivo. Characterization and epitope-mapping of a novel flotillin-1 monoclonal antibody probe. J Biol Chem. 1999 Apr 30;274(18):12702–9.

183. D'Souza-Schorey C, Chavrier P. ARF proteins: roles in membrane traffic and beyond. Nat Rev Mol Cell Biol. 2006 May;7(5):347–58.

184. Naslavsky N, Caplan S. EHD proteins: key conductors of endocytic transport. Trends Cell Biol. 2011 Feb;21(2):122–31.

185. Kalia M, Kumari S, Chadda R, Hill MM, Parton RG, Mayor S. Arf6-independent GPI-anchored protein-enriched early endosomal compartments fuse with sorting endosomes via a Rab5/phosphatidylinositol-3'-kinase-dependent machinery. Mol Biol Cell. 2006 Aug;17(8):3689–704.

186. Bitsikas V, Corrêa IR, Nichols BJ. Clathrin-independent pathways do not contribute significantly to endocytic flux. eLife. 2014 Sep 17;3:e03970.

187. Chadda R, Howes MT, Plowman SJ, Hancock JF, Parton RG, Mayor S. Cholesterol-sensitive Cdc42 activation regulates actin polymerization for endocytosis via the GEEC pathway. Traffic. 2007 Jun;8(6):702–17.

188. Sabharanjak S, Sharma P, Parton RG, Mayor S. GPI-anchored proteins are delivered to recycling endosomes via a distinct cdc42-regulated, clathrin-independent pinocytic pathway. Dev Cell. 2002 Apr;2(4):411–23.

189. Lai EC. Notch signaling: control of cell communication and cell fate. Development. 2004 Mar;131(5):965–73.

190. Ovcinnikovs V, Ross EM, Petersone L, Edner NM, Heuts F, Ntavli E, et al. CTLA-4-mediated transendocytosis of costimulatory molecules primarily targets migratory dendritic cells. Sci Immunol. 2019 May 31;4(35):eaaw0902.

191. Kennedy A, Waters E, Rowshanravan B, Hinze C, Williams C, Janman D, et al. Differences in CD80 and CD86 transendocytosis reveal CD86 as a key target for CTLA-4 immune regulation. Nat Immunol. 2022 Sep;23(9):1365–78.

192. Doherty GJ, McMahon HT. Mechanisms of endocytosis. Annu Rev Biochem. 2009;78:857–902.

193. Swanson JA. Shaping cups into phagosomes and macropinosomes. Nat Rev Mol Cell Biol. 2008 Aug;9(8):639–49.

194. Flannagan RS, Jaumouillé V, Grinstein S. The cell biology of phagocytosis. Annu Rev Pathol. 2012;7:61–98.

195. Underhill DM, Goodridge HS. Information processing during phagocytosis. Nat Rev Immunol. 2012 Jul;12(7):492–502.

196. The uniformity of phagosome maturation in macrophages - PMC [Internet]. [cited 2024 Dec 9]. Available from: https://pmc.ncbi.nlm.nih.gov/articles/PMC2172341/

197. Link F, Borges AR, Jones NG, Engstler M. To the Surface and Back: Exo- and Endocytic Pathways in Trypanosoma brucei. Frontiers in Cell and Developmental Biology. 2021 Aug 6;9:720521.

198. Allen CL, Goulding D, Field MC. Clathrin-mediated endocytosis is essential in Trypanosoma brucei. The EMBO Journal. 2003 Oct 1;22(19):4991.

199. Francis SE, David J. Sullivan Jr, Goldberg and DE. HEMOGLOBIN METABOLISM IN THE MALARIA PARASITE PLASMODIUM FALCIPARUM. Annual Review of Microbiology. 1997 Oct 1;51(Volume 51, 1997):97–123.

200. Lazarus MD, Schneider TG, Taraschi TF. A new model for hemoglobin ingestion and transport by the human malaria parasite Plasmodium falciparum. J Cell Sci. 2008 Jun 1;121(11):1937–49.

201. Howe R, Kelly M, Jimah J, Hodge D, Odom AR. Isoprenoid Biosynthesis Inhibition Disrupts Rab5 Localization and Food Vacuolar Integrity in Plasmodium falciparum. Eukaryotic Cell. 2013 Feb;12(2):215.

202. Jonscher E, Flemming S, Schmitt M, Sabitzki R, Reichard N, Birnbaum J, et al. PfVPS45 Is Required for Host Cell Cytosol Uptake by Malaria Blood Stage Parasites. Cell Host Microbe. 2019 Jan 9;25(1):166-173.e5.

203. Sabitzki R, Schmitt M, Flemming S, Jonscher E, Höhn K, Fröhlke U, et al. Identification of a Rabenosyn-5 like protein and Rab5b in host cell cytosol uptake reveals conservation of endosomal transport in malaria parasites bioRxiv; 2023 p. 2023.04.05.535711. Available from: https://www.biorxiv.org/content/10.1101/2023.04.05.535711v1

204. Spielmann T, Gras S, Sabitzki R, Meissner M. Endocytosis in Plasmodium and Toxoplasma Parasites. Trends Parasitol. 2020 Jun;36(6):520–32.

205. Milani KJ, Schneider TG, Taraschi TF. Defining the Morphology and Mechanism of the Hemoglobin Transport Pathway in Plasmodium falciparum-Infected Erythrocytes. Eukaryotic Cell. 2015 Apr 3;14(4):415.

206. Liu B, Blanch AJ, Namvar A, Carmo O, Tiash S, Andrew D, et al. Multimodal analysis of Plasmodium knowlesi-infected erythrocytes reveals large invaginations, swelling of the host cell, and rheological defects. Cell Microbiol. 2019 May;21(5):e13005.

207. Smythe WA, Joiner KA, Hoppe HC. Actin is required for endocytic trafficking in the malaria parasite Plasmodium falciparum. Cell Microbiol. 2008 Feb;10(2):452–64.

208. Dalal S, Klemba M. Amino acid efflux by asexual blood-stage Plasmodium falciparum and its utility in interrogating the kinetics of hemoglobin endocytosis and catabolism in vivo. Mol Biochem Parasitol. 2015 Jun;201(2):116–22.

209. Tutor MV, Shami GJ, Siddiqui G, Creek DJ, Tilley L, Ralph SA. The Plasmodium falciparum artemisinin resistance-associated protein Kelch 13 is required for formation of normal cytostomes. 2023 Aug 7 Available from: https://elifesciences.org/reviewed-preprints/90290

210. Gras S, Jimenez-Ruiz E, Klinger CM, Schneider K, Klingl A, Lemgruber L, et al. An endocytic-secretory cycle participates in Toxoplasma gondii in motility. PLoS Biol. 2019 Jun;17(6):e3000060.

211. Tanaka M, Kikuchi T, Uno H, Okita K, Kitanishi-Yumura T, Yumura S. Turnover and flow of the cell membrane for cell migration. Sci Rep. 2017 Oct 11;7(1):12970.

212. Periz J, Del Rosario M, McStea A, Gras S, Loney C, Wang L, et al. A highly dynamic F-actin network regulates transport and recycling of micronemes in Toxoplasma gondii vacuoles. Nat Commun. 2019 Sep 13;10(1):4183.

213. Koreny L, Mercado-Saavedra BN, Klinger CM, Barylyuk K, Butterworth S, Hirst J, et al. Stable and ancient endocytic structures navigate the complex pellicle of apicomplexan parasites. bioRxiv. 2022 Jan 1;2022.06.02.494549.

214. Harayama T, Riezman H. Understanding the diversity of membrane lipid composition. Nat Rev Mol Cell Biol. 2018 May;19(5):281–96.

215. Lamy A, Macarini-Bruzaferro E, Dieudonné T, Perálvarez-Marín A, Lenoir G, Montigny C, et al. ATP2, The essential P4-ATPase of malaria parasites, catalyzes lipid-stimulated ATP hydrolysis in complex with a Cdc50 β-subunit. Emerging Microbes & Infections. 2021 Jan 1;10(1):132–47.

216. Hankins HM, Sere YY, Diab NS, Menon AK, Graham TR. Phosphatidylserine translocation at the yeast trans-Golgi network regulates protein sorting into exocytic vesicles. MBoC. 2015 Dec 15;26(25):4674–85.

217. Arroyo-Olarte RD, Brouwers JF, Kuchipudi A, Helms JB, Biswas A, Dunay IR, et al. Phosphatidylthreonine and Lipid-Mediated Control of Parasite Virulence. PLOS Biology. 2015 Nov 13;13(11):e1002288.

218. Kissinger JC, Gajria B, Li L, Paulsen IT, Roos DS. ToxoDB: accessing the Toxoplasma gondii genome. Nucleic Acids Res. 2003 Jan 1;31(1):234–6.

219. Jiménez-Ruiz E, Wong EH, Pall GS, Meissner M. Advantages and disadvantages of conditional systems for characterization of essential genes in Toxoplasma gondii. Parasitology. 2014 Sep;141(11):1390–8.

220. Wang JL, Huang SY, Behnke MS, Chen K, Shen B, Zhu XQ. The Past, Present, and Future of Genetic Manipulation in *Toxoplasma gondii*. Trends in Parasitology. 2016 Jul 1;32(7):542–53.

221. Garneau JE, Dupuis MÈ, Villion M, Romero DA, Barrangou R, Boyaval P, et al. The CRISPR/Cas bacterial immune system cleaves bacteriophage and plasmid DNA. Nature. 2010 Nov;468(7320):67–71.

222. Jinek M, Chylinski K, Fonfara I, Hauer M, Doudna JA, Charpentier E. A programmable dual-RNA-guided DNA endonuclease in adaptive bacterial immunity. Science. 2012 Aug 17;337(6096):816–21.

223. Andenmatten N, Egarter S, Jackson AJ, Jullien N, Herman JP, Meissner M. Conditional genome engineering in Toxoplasma gondii uncovers alternative invasion mechanisms. Nat Methods. 2013 Feb;10(2):125–7.

224. Adhikari B, Narain A, Wolf E. Generation of auxin inducible degron (AID) knock-in cell lines for targeted protein degradation in mammalian cells. STAR Protocols. 2021 Dec 17;2(4):100949.

225. Yesbolatova A, Natsume T, Hayashi K ichiro, Kanemaki MT. Generation of conditional auxin-inducible degron (AID) cells and tight control of degron-fused proteins using the degradation inhibitor auxinole. Methods. 2019 Jul 15;164–165:73–80.

226. Mineo JR, McLeod R, Mack D, Smith J, Khan IA, Ely KH, et al. Antibodies to Toxoplasma gondii major surface protein (SAG-1, P30) inhibit infection of host cells and are produced in murine intestine after peroral infection. J Immunol. 1993 May 1;150(9):3951–64.

227. Wachter RM, Elsliger MA, Kallio K, Hanson GT, Remington SJ. Structural basis of spectral shifts in the yellow-emission variants of green fluorescent protein. Structure. 1998 Oct 15;6(10):1267–77.

228. Lee S, Lim WA, Thorn KS. Improved Blue, Green, and Red Fluorescent Protein Tagging Vectors for S. cerevisiae. PLoS One. 2013 Jul 2;8(7):e67902.

229. Keppler A, Gendreizig S, Gronemeyer T, Pick H, Vogel H, Johnsson K. A general method for the covalent labeling of fusion proteins with small molecules in vivo. Nat Biotechnol. 2003 Jan;21(1):86–9.

230. Los GV, Encell LP, McDougall MG, Hartzell DD, Karassina N, Zimprich C, et al. HaloTag: A Novel Protein Labeling Technology for Cell Imaging and Protein Analysis. ACS Chem Biol. 2008 Jun 1;3(6):373–82.

231. Nile Red - an overview | ScienceDirect Topics [Internet]. [cited 2024 Jun 6]. Available from: https://www.sciencedirect.com/topics/chemistry/nile-red

232. England CG, Luo H, Cai W. HaloTag technology: a versatile platform for biomedical applications. Bioconjug Chem. 2015 Jun 17;26(6):975–86.

233. Day CA, Kraft LJ, Kang M, Kenworthy AK. Analysis of protein and lipid dynamics using confocal fluorescence recovery after photobleaching (FRAP). Curr Protoc Cytom. 2012 Oct;CHAPTER:Unit2.19.

234. Mavrakis M, Rikhy R, Lippincott-Schwartz J. Plasma Membrane Polarity and Compartmentalization are Established Before Cellularization in the Fly Embryo. Dev Cell. 2009 Jan;16(1):93–104.

235. Roumégous C, Abou Hammoud A, Fuster D, Dupuy JW, Blancard C, Salin B, et al. Identification of new components of the basal pole of Toxoplasma gondii provides novel insights into its

molecular organization and functions. Front Cell Infect Microbiol 2022 Oct 13 Available from: https://www.frontiersin.org/journals/cellular-and-infection-microbiology/articles/10.3389/fcimb.2022.1010038/full

236. Francia ME, Dubremetz JF, Morrissette NS. Basal body structure and composition in the apicomplexans Toxoplasma and Plasmodium. Cilia. 2016 Feb 4;5(1):3.

237. Arias Padilla LF, Munera Lopez J, Shibata A, Murray JM, Hu K. The initiation and early development of apical–basal polarity in Toxoplasma gondii. Journal of Cell Science. 2024 Oct 7;137(19):jcs263436.

238. Periz J, Whitelaw J, Harding C, Gras S, Del Rosario Minina MI, Latorre-Barragan F, et al. Toxoplasma gondii F-actin forms an extensive filamentous network required for material exchange and parasite maturation. eLife. 2017 Mar 21;6:e24119.

239. Whitelaw JA. The dynamic nature and functions of actin in Toxoplasma gondii [PhD]. University of Glasgow; 2017 Available from: https://eleanor.lib.gla.ac.uk/record=b3269717

240. Day CA, Kang M. The Utility of Fluorescence Recovery after Photobleaching (FRAP) to Study the Plasma Membrane. Membranes (Basel). 2023 May 2;13(5):492.

241. Simpson RJ. Fragmentation of protein using trypsin. CSH Protoc. 2006 Oct 1;2006(5):pdb.prot4550.

242. Stasic AJ, Moreno SNJ, Carruthers VB, Dou Z. The Toxoplasma plant-like vacuolar compartment (PLVAC). J Eukaryot Microbiol. 2022 Nov;69(6):e12951.

243. Skjeldal FM, Haugen LH, Mateus D, Frei DM, Rødseth AV, Hu X, et al. De novo formation of early endosomes during Rab5-to-Rab7a transition. Journal of Cell Science. 2021 Apr 27;134(8):jcs254185.

244. Rahajeng J, Caplan S, Naslavsky N. Common and distinct roles for the binding partners Rabenosyn-5 and Vps45 in the regulation of endocytic trafficking in mammalian cells. Experimental Cell Research. 2010 Mar 10;316(5):859–74.

245. Heaslip AT, Nelson SR, Warshaw DM. Dense granule trafficking in Toxoplasma gondii requires a unique class 27 myosin and actin filaments. MBoC. 2016 Jul;27(13):2080–9.

246. Venugopal K, Chehade S, Werkmeister E, Barois N, Periz J, Lafont F, et al. Rab11A regulates dense granule transport and secretion during Toxoplasma gondii invasion of host cells and parasite replication. PLoS Pathog. 2020 May;16(5):e1008106.

247. Grech J. A splitCas9-based screen identifies an essential Actin-dependent Golgi protein in Toxoplasma gondii Ludwig-Maximilians-Universität München; 2023 Available from: https://edoc.ub.uni-muenchen.de/33245/

248. Koreny L, Mercado-Saavedra BN, Klinger CM, Barylyuk K, Butterworth S, Hirst J, et al. Stable endocytic structures navigate the complex pellicle of apicomplexan parasites. Nat Commun. 2023 Apr 15;14(1):2167.

249. Bisio H, Soldati-Favre D. Signaling Cascades Governing Entry into and Exit from Host Cells by Toxoplasma gondii. Annual Review of Microbiology. 2019;73(1):579–99.

250. Foth BJ, Goedecke MC, Soldati D. New insights into myosin evolution and classification. Proc Natl Acad Sci U S A. 2006 Mar 7;103(10):3681–6.

251. Carmeille R, Lomoriello PS, Devarakonda PM, Kellermeier JA, Heaslip AT. Actin and an unconventional myosin motor, TgMyoF, control the organization and dynamics of the endomembrane network in Toxoplasma gondii. PLOS Pathogens. 2021 Feb 2;17(2):e1008787.

252. Pomorski T, Lombardi R, Riezman H, Devaux PF, van Meer G, Holthuis JCM. Drs2p-related P-type ATPases Dnf1p and Dnf2p Are Required for Phospholipid Translocation across the Yeast Plasma Membrane and Serve a Role in Endocytosis. Mol Biol Cell. 2003 Mar;14(3):1240–54.

253. Lopez-Marques RL, Theorin L, Palmgren MG, Pomorski TG. P4-ATPases: lipid flippases in cell membranes. Pflugers Arch. 2014;466(7):1227–40.

254. Arabiotorre A, Formanowicz M, Bankaitis VA, Grabon A. Phosphatidylinositol-4-phosphate signaling regulates dense granule biogenesis and exocytosis in Toxoplasma gondii. bioRxiv. 2023 Jan 9;2023.01.09.523261.

255. Gauthier NC, Rossier OM, Mathur A, Hone JC, Sheetz MP. Plasma Membrane Area Increases with Spread Area by Exocytosis of a GPI-anchored Protein Compartment. Mol Biol Cell. 2009 Jul 15;20(14):3261–72.

256. Saha S, Anilkumar AA, Mayor S. GPI-anchored protein organization and dynamics at the cell surface. Journal of Lipid Research. 2016 Feb 1;57(2):159–75.

257. Burda PC, Schaffner M, Kaiser G, Roques M, Zuber B, Heussler VT. A Plasmodium plasma membrane reporter reveals membrane dynamics by live-cell microscopy. Sci Rep. 2017 Aug 29;7(1):9740.

258. Day CA, Kang M. The Utility of Fluorescence Recovery after Photobleaching (FRAP) to Study the Plasma Membrane. Membranes (Basel). 2023 May 2;13(5):492.

259. Ouologuem DT, Roos DS. Dynamics of the Toxoplasma gondii inner membrane complex. J Cell Sci. 2014 Aug 1;127(Pt 15):3320–30.

260. Tosetti N, Dos Santos Pacheco N, Soldati-Favre D, Jacot D. Three F-actin assembly centers regulate organelle inheritance, cell-cell communication and motility in Toxoplasma gondii. Elife. 2019 Feb 12;8:e42669.

261. Frénal K, Jacot D, Hammoudi PM, Graindorge A, Maco B, Soldati-Favre D. Myosin-dependent cell-cell communication controls synchronicity of division in acute and chronic stages of Toxoplasma gondii. Nat Commun. 2017 Jun 8;8:15710.

262. Bretscher MS. Membrane Structure: Some General Principles. Science. 1973 Aug 17;181(4100):622–9.

263. Shi Z, Graber ZT, Baumgart T, Stone HA, Cohen AE. Cell membranes resist flow. Cell. 2018 Dec 13;175(7):1769-1779.e13.

264. Varma R, Mayor S. GPI-anchored proteins are organized in submicron domains at the cell surface. Nature. 1998 Aug 20;394(6695):798–801.

265. Kusumi A, Suzuki KGN, Kasai RS, Ritchie K, Fujiwara TK. Hierarchical mesoscale domain organization of the plasma membrane. Trends Biochem Sci. 2011 Nov;36(11):604–15.

266. Kusumi A, Sako Y, Yamamoto M. Confined lateral diffusion of membrane receptors as studied by single particle tracking (nanovid microscopy). Effects of calcium-induced differentiation in cultured epithelial cells. Biophys J. 1993 Nov;65(5):2021–40.

267. Fujiwara T, Ritchie K, Murakoshi H, Jacobson K, Kusumi A. Phospholipids undergo hop diffusion in compartmentalized cell membrane. J Cell Biol. 2002 Jun 10;157(6):1071–81.

268. Murase K, Fujiwara T, Umemura Y, Suzuki K, Iino R, Yamashita H, et al. Ultrafine membrane compartments for molecular diffusion as revealed by single molecule techniques. Biophys J. 2004 Jun;86(6):4075–93.

269. Hannan LA, Lisanti MP, Rodriguez-Boulan E, Edidin M. Correctly sorted molecules of a GPI-anchored protein are clustered and immobile when they arrive at the apical surface of MDCK cells. J Cell Biol. 1993 Jan;120(2):353–8.

270. Ritchie K, Shan XY, Kondo J, Iwasawa K, Fujiwara T, Kusumi A. Detection of Non-Brownian Diffusion in the Cell Membrane in Single Molecule Tracking. Biophysical Journal. 2005 Mar 1;88(3):2266–77.

271. Keighron JD, Ewing AG, Cans AS. Analytical tools to monitor exocytosis: a focus on new fluorescent probes and methods. Analyst. 2012 Apr 21;137(8):1755–63.

272. Allersma MW, Wang L, Axelrod D, Holz RW. Visualization of regulated exocytosis with a granule-membrane probe using total internal reflection microscopy. Mol Biol Cell. 2004 Oct;15(10):4658–68.

273. Luo N, Yan A, Yang Z. Measuring Exocytosis Rate Using Corrected Fluorescence Recovery After Photoconversion. Traffic. 2016 May;17(5):554–64.

274. Bowen AB, Bourke AM, Hiester BG, Hanus C, Kennedy MJ. Golgi-independent secretory trafficking through recycling endosomes in neuronal dendrites and spines. eLife. 6:e27362.

275. Zheng Q, Ayala AX, Chung I, Weigel AV, Ranjan A, Falco N, et al. Rational Design of Fluorogenic and Spontaneously Blinking Labels for Super-Resolution Imaging. ACS Cent Sci. 2019 Sep 25;5(9):1602–13.

276. A photoactivatable GFP for selective photolabeling of proteins and cells - PubMed Available from: https://pubmed.ncbi.nlm.nih.gov/12228718/

277. Ando R, Mizuno H, Miyawaki A. Regulated Fast Nucleocytoplasmic Shuttling Observed by Reversible Protein Highlighting. Science. 2004 Nov 19;306(5700):1370–3.

278. Amrollahi P, Zheng W, Monk C, Li CZ, Hu TY. Nanoplasmonic Sensor Approaches for Sensitive Detection of Disease-Associated Exosomes. ACS Appl Bio Mater. 2021 Sep 20;4(9):6589–603.

279. Malli S, Bories C, Bourge M, Loiseau PhilippeM, Bouchemal K. Surface-dependent endocytosis of poly(isobutylcyanoacrylate) nanoparticles by Trichomonas vaginalis. International Journal of Pharmaceutics. 2018 Sep 5;548(1):276–87.

280. Llobet A, Beaumont V, Lagnado L. Real-Time Measurement of Exocytosis and Endocytosis Using Interference of Light. Neuron. 2003 Dec 18;40(6):1075–86.

281. Langsley G, van Noort V, Carret C, Meissner M, de Villiers EP, Bishop R, et al. Comparative genomics of the Rab protein family in Apicomplexan parasites. Microbes Infect. 2008 Apr;10(5):462–70.

282. Jékely G. Small GTPases and the evolution of the eukaryotic cell. Bioessays. 2003 Nov;25(11):1129–38.

283. Chen PI, Kong C, Su X, Stahl PD. Rab5 Isoforms Differentially Regulate the Trafficking and Degradation of Epidermal Growth Factor Receptors *. Journal of Biological Chemistry. 2009 Oct 30;284(44):30328–38.

284. Kremer K, Kamin D, Rittweger E, Wilkes J, Flammer H, Mahler S, et al. An overexpression screen of Toxoplasma gondii Rab-GTPases reveals distinct transport routes to the micronemes. PLoS Pathog. 2013 Mar;9(3):e1003213.

285. Sabitzki R, Roßmann AL, Schmitt M, Flemming S, Guillén-Samander A, Behrens HM, et al. Role of Rabenosyn-5 and Rab5b in host cell cytosol uptake reveals conservation of endosomal transport in malaria parasites. PLoS Biol. 2024 May;22(5):e3002639.

286. Bisio H, Chaabene RB, Sabitzki R, Maco B, Marq JB, Gilberger TW, et al. The ZIP Code of Vesicle Trafficking in Apicomplexa: SEC1/Munc18 and SNARE Proteins. mBio. 2020 Oct 20;11(5):e02092-20.

287. Pal A, Hall BS, Nesbeth DN, Field HI, Field MC. Differential endocytic functions of Trypanosoma brucei Rab5 isoforms reveal a glycosylphosphatidylinositol-specific endosomal pathway. J Biol Chem. 2002 Mar 15;277(11):9529–39.

288. Chavrier P, Gorvel JP, Stelzer E, Simons K, Gruenberg J, Zerial M. Hypervariable C-terminal domain of rab proteins acts as a targeting signal. Nature. 1991 Oct 24;353(6346):769–72.

289. Chavrier P, Parton RG, Hauri HP, Simons K, Zerial M. Localization of low molecular weight GTP binding proteins to exocytic and endocytic compartments. Cell. 1990 Jul 27;62(2):317–29.

290. Zerial M, McBride H. Rab proteins as membrane organizers. Nat Rev Mol Cell Biol. 2001 Feb;2(2):107–17.

291. Rastogi R, Verma JK, Kapoor A, Langsley G, Mukhopadhyay A. Rab5 Isoforms Specifically Regulate Different Modes of Endocytosis in Leishmania. J Biol Chem. 2016 Jul 8;291(28):14732–46.

292. Zheng H, Zheng W, Wu C, Yang J, Xi Y, Xie Q, et al. Rab GTPases are essential for membrane trafficking-dependent growth and pathogenicity in Fusarium graminearum. Environ Microbiol. 2015 Nov;17(11):4580–99.

293. Fukuda M, Satoh-Cruz M, Wen L, Crofts AJ, Sugino A, Washida H, et al. The Small GTPase Rab5a Is Essential for Intracellular Transport of Proglutelin from the Golgi Apparatus to the Protein Storage Vacuole and Endosomal Membrane Organization in Developing Rice Endosperm. Plant Physiology. 2011 Aug 8;157(2):632.

294. Lakhan SE, Sabharanjak S, De A. Endocytosis of glycosylphosphatidylinositol-anchored proteins. J Biomed Sci. 2009 Oct 15;16(1):93.

295. Zulkefli KL, Houghton FJ, Gosavi P, Gleeson PA. A role for Rab11 in the homeostasis of the endosome-lysosomal pathway. Experimental Cell Research. 2019 Jul 1;380(1):55–68.

296. Niyogi S, Mucci J, Campetella O, Docampo R. Rab11 Regulates Trafficking of Trans-sialidase to the Plasma Membrane through the Contractile Vacuole Complex of Trypanosoma cruzi. PLOS Pathogens. 2014 Jun 26;10(6):e1004224.

297. Jeffries TR, Morgan GW, Field MC. A developmentally regulated Rab11 homologue in Trypanosoma brucei is involved in recycling processes. Journal of Cell Science. 2001 Jul 15;114(14):2617–26.

298. He K, Wang Q, Gao X, Tang T, Ding H, Long S. Transcriptomic and metabolomic analyses reveal the essential nature of Rab1B in Toxoplasma gondii. Parasit Vectors. 2023 Nov 8;16:409.

299. Carruthers VB, Dou Z. Deciphering protein prenylation in endocytic trafficking in Toxoplasma gondii. mBio. 2024 Apr 10;15(4):e0028324.

300. Wallace NS, Gadbery JE, Cohen CI, Kendall AK, Jackson LP. Tepsin binds LC3B to promote ATG9A trafficking and delivery. MBoC. 2024 Apr;35(4):ar56.

301. Cheng X, Chen K, Dong B, Yang M, Filbrun SL, Myoung Y, et al. Dynamin-dependent Vesicle Twist at the Final Stage of Clathrin-mediated Endocytosis. Nature cell biology. 2021 Jul 12;23(8):859.

302. Miao J, Ning G, Xia X, Liang X, Lucky AB, Siddiqui F, et al. Clathrins are involved in the endocytosis of host cytosol in the malaria parasite. bioRxiv. 2024 Dec 18;2024.12.17.629030.

303. Travier L, Mondragon R, Dubremetz JF, Musset K, Mondragon M, Gonzalez S, et al. Functional domains of the *Toxoplasma* GRA2 protein in the formation of the membranous nanotubular network of the parasitophorous vacuole. International Journal for Parasitology. 2008 Jun 1;38(7):757–73.

304. Griffith MB, Pearce CS, Heaslip AT. Dense granule biogenesis, secretion, and function in Toxoplasma gondii. J Eukaryot Microbiol. 2022 Nov;69(6):e12904.

305. Dos Santos Pacheco N, Tell i Puig A, Guérin A, Martinez M, Maco B, Tosetti N, et al. Sustained rhoptry docking and discharge requires Toxoplasma gondii intraconoidal microtubule-associated proteins. Nat Commun. 2024 Jan 9;15(1):379.

306. Klyachko VA, Jackson MB. Capacitance steps and fusion pores of small and large-dense-core vesicles in nerve terminals. Nature. 2002 Jul 4;418(6893):89–92.

307. He L, Wu XS, Mohan R, Wu LG. Two modes of fusion pore opening revealed by cell-attached recordings at a synapse. Nature. 2006 Nov 2;444(7115):102–5.

308. Dunkley TPJ, Watson R, Griffin JL, Dupree P, Lilley KS. Localization of organelle proteins by isotope tagging (LOPIT). Mol Cell Proteomics. 2004 Nov;3(11):1128–34.

309. Imjeti NS, Lebreton S, Paladino S, de la Fuente E, Gonzalez A, Zurzolo C. N-Glycosylation instead of cholesterol mediates oligomerization and apical sorting of GPI-APs in FRT cells. Mol Biol Cell. 2011 Dec;22(23):4621–34.

310. Alves AA, Alcantara CL, Dantas-Jr MVA, Sunter JD, De Souza W, Cunha-E-Silva NL. Dynamics of the orphan myosin MyoF over Trypanosoma cruzi life cycle and along the endocytic pathway. Parasitol Int. 2022 Feb;86:102444.

311. Jacot D, Daher W, Soldati-Favre D. Toxoplasma gondii myosin F, an essential motor for centrosomes positioning and apicoplast inheritance. EMBO J. 2013 Jun 12;32(12):1702–16.

312. Evans LL, Lee AJ, Bridgman PC, Mooseker MS. Vesicle-associated brain myosin-V can be activated to catalyze actin-based transport. J Cell Sci. 1998 Jul 30;111 (Pt 14):2055–66.

313. Griffing LR, Gao HT, Sparkes I. ER network dynamics are differentially controlled by myosins XI-K, XI-C, XI-E, XI-I, XI-1, and XI-2. Front Plant Sci. 2014 May 21;5:218.

314. Espreafico EM, Cheney RE, Matteoli M, Nascimento AA, De Camilli PV, Larson RE, et al. Primary structure and cellular localization of chicken brain myosin-V (p190), an unconventional myosin with calmodulin light chains. Journal of Cell Biology. 1992 Dec 15;119(6):1541–57.

315. Watanabe M, Nomura K, Ohyama A, Ishikawa R, Komiya Y, Hosaka K, et al. Myosin-Va Regulates Exocytosis through the Submicromolar Ca2+-dependent Binding of Syntaxin-1A. MBoC. 2005 Oct;16(10):4519–30.

316. Yoshimura A, Fujii R, Watanabe Y, Okabe S, Fukui K, Takumi T. Myosin-Va facilitates the accumulation of mRNA/protein complex in dendritic spines. Curr Biol. 2006 Dec 5;16(23):2345–51.

317. Rudolf R, Bittins CM, Gerdes HH. The role of myosin V in exocytosis and synaptic plasticity. J Neurochem. 2011 Jan;116(2):177–91.

318. Gautam G, Ali MS, Bhattacharya A, Gourinath S. EhFP10: A FYVE family GEF interacts with myosin IB to regulate cytoskeletal dynamics during endocytosis in Entamoeba histolytica. PLOS Pathogens. 2019 Feb 19;15(2):e1007573.

319. Manenschijn HE, Picco A, Mund M, Rivier-Cordey AS, Ries J, Kaksonen M. Type-I myosins promote actin polymerization to drive membrane bending in endocytosis. eLife. 8:e44215.

320. Wayt J, Cartagena-Rivera A, Dutta D, Donaldson JG, Waterman CM. Myosin II isoforms promote internalization of spatially distinct clathrin-independent endocytosis cargoes through modulation of cortical tension downstream of ROCK2. Mol Biol Cell. 2021 Feb 1;32(3):226–36.

321. Buss F, Luzio JP, Kendrick-Jones J. Myosin VI, an actin motor for membrane traffic and cell migration. Traffic. 2002 Dec;3(12):851–8.

322. Wang Z, Edwards JG, Riley N, Provance DW, Karcher R, Li XD, et al. Myosin Vb mobilizes recycling endosomes and AMPA receptors for postsynaptic plasticity. Cell. 2008 Oct 31;135(3):535–48.

323. Goode BL, Eskin J, Shekhar S. Mechanisms of actin disassembly and turnover. Journal of Cell Biology. 2023 Nov 10;222(12):e202309021.

324. Cooper JA. Effects of cytochalasin and phalloidin on actin. J Cell Biol. 1987 Oct;105(4):1473–8.

325. Brown JR, Peacock-Villada EM, Langford GM. Globular tail fragment of myosin-V displaces vesicle-associated motor and blocks vesicle transport in squid nerve cell extracts. Biol Bull. 2002 Oct;203(2):210–1.

326. Graindorge A, Frénal K, Jacot D, Salamun J, Marq JB, Soldati-Favre D. The Conoid Associated Motor MyoH Is Indispensable for Toxoplasma gondii Entry and Exit from Host Cells. PLoS Pathog. 2016 Jan 13;12(1):e1005388.

327. Lentini G, Dubois DJ, Maco B, Soldati-Favre D, Frénal K. The roles of Centrin 2 and Dynein Light Chain 8a in apical secretory organelles discharge of Toxoplasma gondii. Traffic. 2019;20(8):583–600.

328. Gicking AM, Ma TC, Feng Q, Jiang R, Badieyan S, Cianfrocco MA, et al. Kinesin-1, -2, and -3 motors use family-specific mechanochemical strategies to effectively compete with dynein during bidirectional transport. Ori-McKenney KM, Akhmanova A, Reinemann DN, editors. eLife. 2022 Sep 20;11:e82228.

329. Park JJ, Loh YP. Minireview: How Peptide Hormone Vesicles Are Transported to the Secretion Site for Exocytosis. Molecular Endocrinology. 2008 Dec 1;22(12):2583–95.

330. Vale RD. The molecular motor toolbox for intracellular transport. Cell. 2003 Feb 21;112(4):467–80.

331. Zhang R, Xu Y, Yi R, Shen J, Huang S. Actin cytoskeleton in the control of vesicle transport, cytoplasmic organization, and pollen tube tip growth. Plant Physiol. 2023 Aug 31;193(1):9–25.

332. Lu W, Gelfand VI. Go with the flow – bulk transport by molecular motors. Journal of Cell Science. 2022 Oct 17;136(5):jcs260300.

333. Myosin-Vb functions as a dynamic tether for peripheral endocytic compartments during transferrin trafficking | BMC Molecular and Cell Biology Available from: https://link.springer.com/article/10.1186/1471-2121-9-44

334. Visualization of Melanosome Dynamics within Wild-Type and Dilute Melanocytes Suggests a Paradigm for Myosin V Function In Vivo | Journal of Cell Biology | Rockefeller University Press Available from: https://rupress.org/jcb/article-abstract/143/7/1899/16006/Visualization-of-Melanosome-Dynamics-within-Wild

335. Sloves PJ, Delhaye S, Mouveaux T, Werkmeister E, Slomianny C, Hovasse A, et al. Toxoplasma sortilin-like receptor regulates protein transport and is essential for apical secretory organelle biogenesis and host infection. Cell Host Microbe. 2012 May 17;11(5):515–27.

336. Botella C, Sautron E, Boudiere L, Michaud M, Dubots E, Yamaryo-Botté Y, et al. ALA10, a Phospholipid Flippase, Controls FAD2/FAD3 Desaturation of Phosphatidylcholine in the ER and Affects Chloroplast Lipid Composition in Arabidopsis thaliana. Plant Physiol. 2016 Mar;170(3):1300–14.

337. Palmgren M, Østerberg JT, Nintemann SJ, Poulsen LR, López-Marqués RL. Evolution and a revised nomenclature of P4 ATPases, a eukaryotic family of lipid flippases. Biochim Biophys Acta Biomembr. 2019 Jun 1;1861(6):1135–51.

338. Bryde S, Hennrich H, Verhulst PM, Devaux PF, Lenoir G, Holthuis JCM. CDC50 proteins are critical components of the human class-1 P4-ATPase transport machinery. J Biol Chem. 2010 Dec 24;285(52):40562–72.

339. Palmgren MG, Nissen P. P-Type ATPases. Annual Review of Biophysics. 2011 Jun 9;40(Volume 40, 2011):243–66.

340. Andersen JP, Vestergaard AL, Mikkelsen SA, Mogensen LS, Chalat M, Molday RS. P4-ATPases as Phospholipid Flippases—Structure, Function, and Enigmas. Front Physiol Available from: https://www.frontiersin.org/journals/physiology/articles/10.3389/fphys.2016.00275/full

341. Segawa K, Kurata S, Yanagihashi Y, Brummelkamp TR, Matsuda F, Nagata S. Caspase-mediated cleavage of phospholipid flippase for apoptotic phosphatidylserine exposure. Science. 2014 Jun 6;344(6188):1164–8.

342. Lee S, Uchida Y, Wang J, Matsudaira T, Nakagawa T, Kishimoto T, et al. Transport through recycling endosomes requires EHD1 recruitment by a phosphatidylserine translocase. The EMBO Journal. 2015 Mar 4;34(5):669–88.

343. Chen B, Jiang Y, Zeng S, Yan J, Li X, Zhang Y, et al. Endocytic sorting and recycling require membrane phosphatidylserine asymmetry maintained by TAT-1/CHAT-1. PLoS Genet. 2010 Dec 9;6(12):e1001235.

344. Qiu D, England E, Lehane AM. PfATP2 is an essential flippase on the Plasmodium falciparum surface that influences parasite sensitivity to antiplasmodial compounds [Internet]. bioRxiv; 2024 [cited 2025 Jan 13]. p. 2024.12.23.630022. Available from: https://www.biorxiv.org/content/10.1101/2024.12.23.630022v1

345. Uncovering the essential genes of the human malaria parasite Plasmodium falciparum by saturation mutagenesis | Science Available from: https://www.science.org/doi/abs/10.1126/science.aap7847

346. Chen K, Günay-Esiyok Ö, Klingeberg M, Marquardt S, Pomorski TG, Gupta N. Aminoglycerophospholipid flipping and P4-ATPases in Toxoplasma gondii. J Biol Chem. 2021;296:100315.

347. Roles for the Drs2p–Cdc50p Complex in Protein Transport and Phosphatidylserine Asymmetry of the Yeast Plasma Membrane - Chen - 2006 - Traffic - Wiley Online Library Available from: https://onlinelibrary.wiley.com/doi/10.1111/j.1600-0854.2006.00485.x

348. Wicky S, Schwarz H, Singer-Krüger B. Molecular interactions of yeast Neo1p, an essential member of the Drs2 family of aminophospholipid translocases, and its role in membrane trafficking within the endomembrane system. Mol Cell Biol. 2004 Sep;24(17):7402–18.

349. Gilbert MJ, Thornton CR, Wakley GE, Talbot NJ. A P-type ATPase required for rice blast disease and induction of host resistance. Nature. 2006 Mar 23;440(7083):535–9.

350. Poulsen LR, López-Marqués RL, McDowell SC, Okkeri J, Licht D, Schulz A, et al. The Arabidopsis P4-ATPase ALA3 localizes to the golgi and requires a beta-subunit to function in lipid translocation and secretory vesicle formation. Plant Cell. 2008 Mar;20(3):658–76.

351. Pomorski T, Lombardi R, Riezman H, Devaux PF, van Meer G, Holthuis JCM. Drs2p-related P-type ATPases Dnf1p and Dnf2p are required for phospholipid translocation across the yeast plasma membrane and serve a role in endocytosis. Mol Biol Cell. 2003 Mar;14(3):1240–54.

352. Nir S, Bentz J, Wilschut J, Duzgunes N. Aggregation and fusion of phospholipid vesicles. Progress in Surface Science. 1983 Jan 1;13(1):1–124.

353. Yoshimura T, Maezawa S, Kameyama K, Takagi T. Fusion of phospholipid vesicles induced by clathrin: modulation of fused liposome size. J Biochem. 1994 Apr;115(4):715–23.

354. Seigneuret M, Devaux PF. ATP-dependent asymmetric distribution of spin-labeled phospholipids in the erythrocyte membrane: relation to shape changes. Proc Natl Acad Sci U S A. 1984 Jun;81(12):3751–5.

355. Daleke DL, Huestis WH. Incorporation and translocation of aminophospholipids in human erythrocytes. Biochemistry. 1985 Sep 24;24(20):5406–16.

356. Saito K, Fujimura-Kamada K, Hanamatsu H, Kato U, Umeda M, Kozminski KG, et al. Transbilayer phospholipid flipping regulates Cdc42p signaling during polarized cell growth via Rga GTPase-activating proteins. Dev Cell. 2007 Nov;13(5):743–51.

357. Das A, Slaughter BD, Unruh JR, Bradford WD, Alexander R, Rubinstein B, et al. Flippase-mediated phospholipid asymmetry promotes fast Cdc42 recycling in dynamic maintenance of cell polarity. Nat Cell Biol. 2012 Feb 19;14(3):304–10.

358. Farge E, Ojcius DM, Subtil A, Dautry-Varsat A. Enhancement of endocytosis due to aminophospholipid transport across the plasma membrane of living cells. Am J Physiol. 1999 Mar;276(3):C725-733.

359. Müller P, Pomorski T, Herrmann A. Incorporation of phospholipid analogues into the plasma membrane affects ATP-induced vesiculation of human erythrocyte ghosts. Biochem Biophys Res Commun. 1994 Mar 15;199(2):881–7.

360. Delbac F, Sänger A, Neuhaus EM, Stratmann R, Ajioka JW, Toursel C, et al. Toxoplasma gondii myosins B/C. J Cell Biol. 2001 Nov 12;155(4):613–24.

361. Figard L, Sokac AM. A membrane reservoir at the cell surface. Bioarchitecture. 2014;4(2):39–46.

362. Aguet F, Upadhyayula S, Gaudin R, Chou Y ying, Cocucci E, He K, et al. Membrane dynamics of dividing cells imaged by lattice light-sheet microscopy. Mol Biol Cell. 2016 Nov 7;27(22):3418–35.

363. Tanaka M, Fujimoto K, Yumura S. Regulation of the Total Cell Surface Area in Dividing Dictyostelium Cells. Front Cell Dev Biol. 2020 Apr 8

364. Sinha B, Köster D, Ruez R, Gonnord P, Bastiani M, Abankwa D, et al. Cells Respond to Mechanical Stress by Rapid Disassembly of Caveolae. Cell. 2011 Feb 4;144(3):402–13.

365. McNeil PL, Steinhardt RA. Plasma membrane disruption: repair, prevention, adaptation. Annu Rev Cell Dev Biol. 2003;19:697–731.

366. Kozlov MM, Chernomordik LV. Membrane tension and membrane fusion. Curr Opin Struct Biol. 2015 Aug;33:61–7.

367. Charras G, Paluch E. Blebs lead the way: how to migrate without lamellipodia. Nat Rev Mol Cell Biol. 2008 Sep;9(9):730–6.

368. Cao XJ, Zee BM, Garcia BA. Heavy methyl-SILAC labeling coupled with liquid chromatography and high-resolution mass spectrometry to study the dynamics of site -specific histone methylation. Methods Mol Biol. 2013;977:299–313.

369. Rivera-Cuevas Y, Mayoral J, Di Cristina M, Lawrence ALE, Olafsson EB, Patel RK, et al. Toxoplasma gondii exploits the host ESCRT machinery for parasite uptake of host cytosolic proteins. PLoS Pathog. 2021 Dec;17(12):e1010138.

370. Marotta DE, Gerald N, Dwyer DM. Rab5b localization to early endosomes in the protozoan human pathogen Leishmania donovani. Mol Cell Biochem. 2006 Nov;292(1–2):107–17.

371. Li W, Grech J, Stortz JF, Gow M, Periz J, Meissner M, et al. A splitCas9 phenotypic screen in Toxoplasma gondii identifies proteins involved in host cell egress and invasion. Nat Microbiol. 2022 Jun;7(6):882–95.

372. Peng D, Tarleton R. EuPaGDT: a web tool tailored to design CRISPR guide RNAs for eukaryotic pathogens. Microb Genom. 2015 Oct;1(4):e000033.

Acknowledgements

I would like to express my deepest gratitude to my first supervisor, Prof. Markus Meißner, for giving me the opportunity to pursue a PhD in his lab and for his kind guidance on research topics and challenges. Thank you for your constant support, valuable advice, and for always being willing to listen to the problems that arose during this journey.

My thanks also go to my direct lab supervisor, Dr. Simon Gras, for providing me with such an exciting research topic, for his guidance, and for offering great insights throughout my work. I am especially grateful for the fun and collaborative environment, particularly at 6 am in TC with loud music.

I would also like to thank Prof. Michael Boshart for generously agreeing to be my Doktorvater, for his invaluable advice during every TAC meeting, and for his support beyond those meetings.

A big thank you to Prof. Nicolai Siegel and Prof. Tobias Spielmann for being part of my TAC committee and for their excellent feedback, suggestions, and ideas, which greatly enriched my work.

To all the members of the Meißner Lab, both past and present, I am incredibly grateful. Mriko, thank you for teaching me everything I needed to know about Toxoplasma. Matthew, Janessa, and Wei, we started this journey together, and I am so thankful for your friendship, for being such wonderful fellow PhD students, and for all the fun we had in the office. Even after you completed your PhDs, you continued to support and listen to me, and for that, I am deeply grateful.

Miriam, Ella, PeiPei, Thrishla, Yuan, and Victoria, thank you for being amazing lab mates, for your constant willingness to help, and for creating an office environment that I genuinely enjoyed coming to every day. I would also like to thank the postdocs Elena and Javier for their endless supply of tips, knowledge, and support. A special thank you to Marzena, the "fairy godmother" of the lab, for always caring, listening, and looking out for everyone, as well as to the entire diagnostics team.

To my family and friends, the biggest thanks goes to you. For always listening to my complaints about life and the PhD, for letting me vent, and for sharing in my frustrations.

To my parents, thank you for your unwavering belief in me and for reminding me that I could achieve anything I set my mind to. Your constant support, no matter how small my problems seemed, has meant the world to me. To my boyfriend, thank you for always being by my side, for never tiring of listening to me, when things didn't work out, and for supporting me through it all. Without all of you, I wouldn't have come this far, I might have given up a long time ago. This thesis is for you.

Thank you.